School of Chemical Engineering and Advanced Materials

Characterisation of a Nanoporous Polymers for Water Treatment

~ By ~

Mohammed Salman Kadhim

Supervisors:

Dr. A. Oila & Prof. S.J. Bull

November 2017

Disclaimer

This thesis is submitted for the degree of PhD in nanoscience and technology nanomaterials from Newcastle University, in the school of Chemical Engineering and Advance Materials. All my work was done under supervision from Dr Adrian Oila and Professor Steve Bull.

Neither the author nor the Newcastle University at Newcastle upon Tyne accepts any liability for the contents of this document. The novelty in this work, is using the PolyHIPE after sulphonation as an ion exchanger to remove heavy metals from waste water which no one has used before. The reason for using this material is its low weight and its highly porous structure which means high efficiency, and it could be put under a regeneration process to be reused again. In addition to the cost of the material and its processing is relatively low. Its results show good performance for this material to remove the heavy metals from water to low levels meeting WHO values.

Abstract

Materials which have structural dimensions between 1 nm and 100 nm are called nanomaterials. These materials have unique geometric, physicochemical and mechanical properties. As a result of their properties, nanomaterials can be tailored for specific applications. Polymers Synthesized from High Internal Phase Emulsions (PolyHIPEs) are a type of porous material with high specific surface area due to their nanoscale structure which have the ability to function as ion exchange media that can remove contaminants from water. PolyHIPEs can therefore be used in ion exchange modules to remove metals from wastewater. The advantage of using PolyHIPEs is that fewer steps are necessary compared with traditional filtration methods, and they are more economic and more selective than the traditional materials.

A high internal-phase emulsion (HIPE) contains both oil and aqueous or dispersed phases. The oil phase has monomers such as styrene, a cross-linker such as Divinylbenzene (DVB), and non-ionic surfactants while the aqueous phase consists of deionized water and polymerisation initiators such as potassium pyrosulphate. The emulsion is subjected to the polymerization process, usually at 60˚C and pores are produced within the polymer due to the presence of the aqueous phase. The polyHIPE is then washed with propanol to release the residual surfactant and unreacted monomer. In this work, we used different HIPE mixing times (10, 15, 20, 25, and 30 minutes, respectively) in order to change the pore size distribution. After synthesis the PolyHIPEs are subjected to a sulphonation process which changes the PolyHIPE character from hydrophobic to hydrophilic. Finally, ion exchange experiments have been conducted by using sulphonated PolyHIPE beads as is and coated with iron oxide. As simulated contaminated water nickel and copper solutions were used during this process. The results show the removal efficiency of the metal ion from solution was much higher with sulphonated beads at range of pH (6, 7, 8 and 9). Changing the pH allowed the metals to be removed from the PolyHIPE for recovery and filter regeneration but the amount of metals after the regeneration process is low compared with initial concentration.

Dedication

Thank you may Allah I could not have done anything in my life without you!

The thesis is especially dedicated to my country ministry of higher education and scientific research, Iraq, Iraqi Cultural Attaché - UK!

This thesis is dedicated to my family!

This thesis is dedicated to my friends!

Publications

Acknowledgements

I would like to thank my sponsor Ministry of Higher Education in Iraq, Iraqi Cultural Attaché - UK for all their support.

Contents

List of Figures

List of Tables

Nomenclature

DVB	Divinylbenzene
FT-IR	Fourier transform infrared spectroscopy
HIPE	High Internal Phase Emulsion
PVC	Polyvinyl chloride
SEM	Scanning electron microscope
Span 80	Span 80, sorbitan monolete, emulsifier S80
VBC	Vinyl benzyl Chloride
W/O	Water/oil phase ratio
NF	Nano filtration
$KMnO_4$	Potassium permanganate
NaClO	Sodium hypochlorite
MWCNTs	Carbon Nanotubes
Pb (II)	Lead (II)
Ca^{2+}	Calcium ion
Mg^{2+}	Magnesium ion
Fe_2O_3	Iron (III) oxide
PEGDMA	polyethylene glycol dimethacrylate
HPO_4^{2-}	Hypohosphate ion
$PO4^{3-}$	Phosphate ion
HLB	hydrophilic-lipophilic balance

1. General Background and Motivation

In this chapter an introduction to the traditional methods for waste water treatment is given, and this is compared with the novel method which is used in this work. Then an explanation for the effect of heavy metals in waste water and its influence on human health is given, including the effect of nickel and copper metal ions which are used in the current experiments. Moreover, the availability of these heavy metal around the world in different places is discussed. The advantages for using these heavy metals in different application depends on their properties and price and the cost of removal of such metals from wastewater may be mitigated by income from selling the metals recovered if the quality is suitable. Different techniques that have been used to remove these heavy metals from waste water are discussed such as the adsorption, chemical precipitation and ion exchange etc. to give clear idea about the differences between these methods and the advantages and disadvantages for each. The adsorption process and ion exchange process are used in this work when we use the PolyHIPE after coating with iron oxide and after sulphonation during the filtration process. Thus the advantages for using the PolyHIPE as a media for water treatment will be identified and what are the specific properties for this material which make it preferable to use it in waste water treatment. Iron oxide, which is used in the coating process to enable the adsorption process, is discussed in addition to the use of styrene-based polymers rather than other polymers systems as the basis for the filter material. Finally, a thesis structure completes this chapter.

1.1. Introduction

Wastewater treatment is used to remove toxic metals and bacteria that are present in groundwater sources because these impurities have an adverse effect on human health (Lettinga, 1995) due to accumulation inside the body cells, (Boujelben et al., 2009). Generally, the treatment is divided in primary and secondary steps as shown Figure 1-1. In the primary treatment, screens with different pore size supported by iron or steel bars are used over settling tanks to release the solid material which is available inside the wastewater. The diameter of the screen holes is relatively large, in the order of 10 millimetres. Ninety percent of the solid material may be removed by the primary treatment but not all the waste can be removed during this stage (Lettinga, 1995, Karvelas et al., 2003, Brix, 1993).

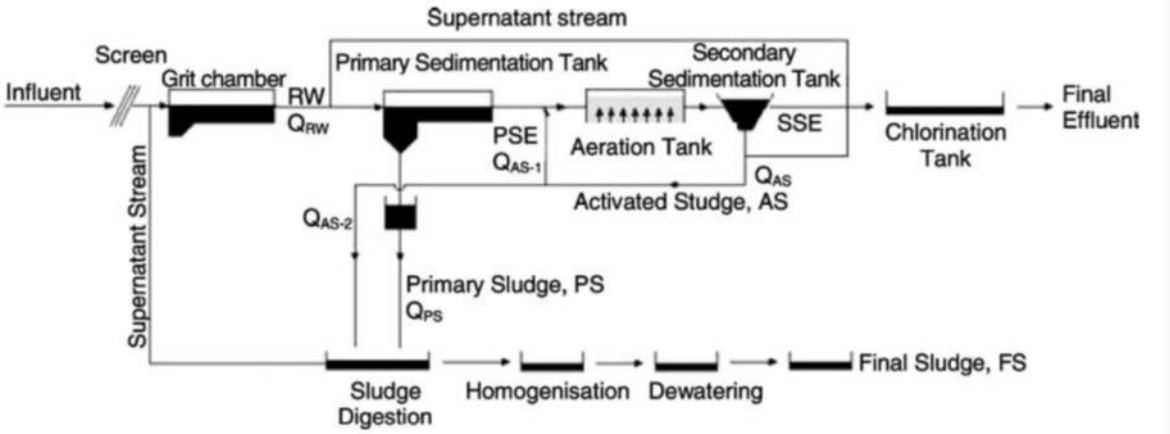

Figure 1-1. Diagram showing the steps of normal type of water treatment mechanism, screening, Primary Sedimentation and secondary Sedimentation (Karvelas, Katsoyiannis, & Samara, 2003)

In the secondary step of wastewater treatment, bacteria are used to remove the pollutants which remain from the primary step. Finally, fast spinning centrifuges are used to separate solids from the liquid. The resulting water is disinfected by using chlorine, ozone, or ultraviolet light (Cheremisinoff, 2002a). In the tertiary step the dissolved materials such as organic chemicals, nutrients, phosphorus and nitrogen are removed by using physical, chemical and biological processes (Karvelas et al., 2003, Lettinga et al., 1980, Cheremisinoff, 2002c).

During the chemical methods chemical components like iron salts are added to the water to make large size complexes (i.e., iron may be added to the wastewater to react with specific ions such as phosphate). Another method for the purification of water is called the attached growth process and it takes place at the surface of the filtration media stone or plastic filters for instance allowing microbial growth inside the waste water. These bacteria can consume the organic material that is available in wastewater before they are removed by physical filtration. Similarly, the suspended growth methods are used to release biodegradable organic material by microbial growth in suspension. This process allows the microbes to consume the organic matter which is removed with them by further filtration (Cheremisinoff, 2002b, Karvelas et al., 2003, Loukidou and Zouboulis, 2001, Lee et al., 2001).

There are some contaminants, such as dissolved metal ions, in the water which must be removed by other methods to meet water purity targets as shown in Table 2-1. Such other methods include ion exchange columns. PolyHIPEs can be used as ion exchange modules to remove metals from wastewater in the second step because, due to their structure with small size of

pores, they could be completely closed by large particles and are unsuitable for the first stage. The advantage of using PolyHIPEs is the more efficient removal of selected species compared to the traditional materials (Katsoyiannis and Zouboulis, 2002). PolyHIPEs are porous materials with micro and nano-pores generated in the internal structure after the polymerisation process (Krajnc et al., 2005a). In the preparation step the material consists of a dispersed phase (internal phase) and a continuous phase (external phase) and the ratio of oil to aqueous phase should be at least 76% , more than this ratio the droplets generate in polyhedral and non-uniform shape (Busby et al., 2001, Cameron, 2005b, Busby et al., 2002); (Hayman et al., 2004).

In this study PolyHIPEs prepared using different mixing times have subsequently been exposed to sulphonation using sulphuric acid and then coated with iron oxide. The procedure of PolyHIPE preparation consists in the gradual addition of the aqueous phase by means of a pump to the stirred reactor which contains the oil phase. The mixing continues while the droplet size reduces. The aqueous phase consists of distilled water, an initiator, and certain additives (Krajnc et al., 2005b, Calkan, 2007). The oil phase consists of a monomer, surfactant, and a cross linker (Tai et al., 2001).

Supplementary pores between the neighbouring pores can be generated in the PolyHIPEs after the washing process which removes the aqueous phase, the surfactant and the unreacted monomer following the polymerization process as show in Figure 1-2. In addition, the mixing processes helps to put the continuous phase, which is located between the droplets, in a low energy state creating a thin film between these droplets. During the polymerization process, the contraction that takes place in the oil phase leads to the formation of interconnecting pores, the final film structure contains the styrene monomer and divinylbenzene cross-linker (see Figure 1-3) (Jimat, 2011). This is subsequently polymerised.

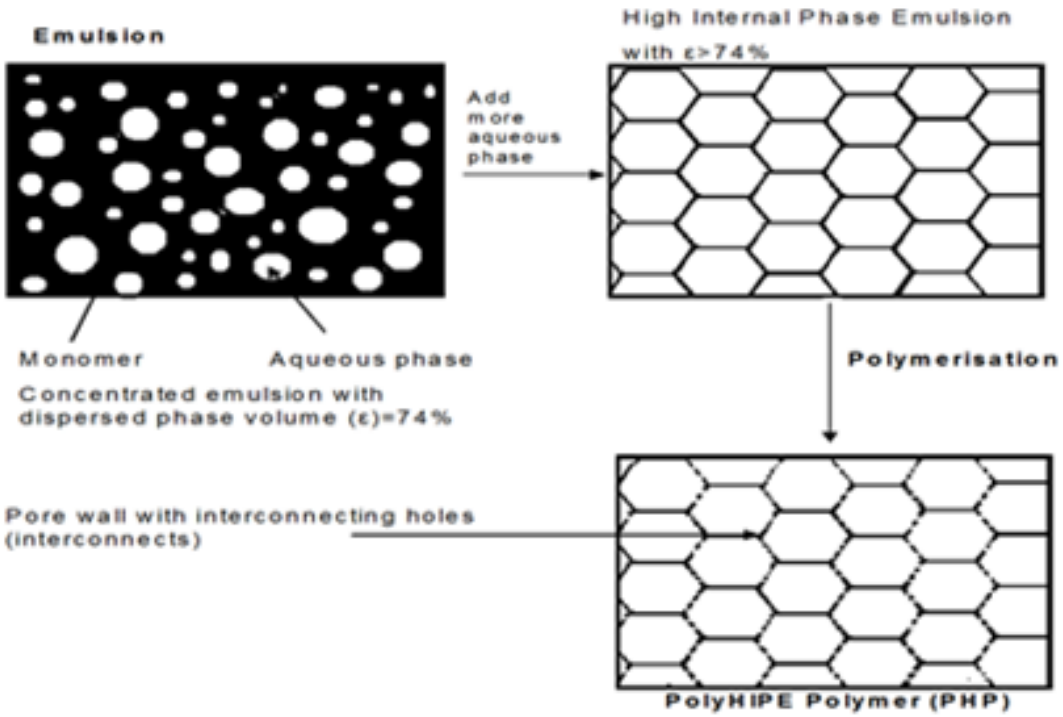

Figure 1-2. Diagram showing the preparation PolyHIPEs: (Emulsion, polymerization and solidification ,(Byron, 2000).

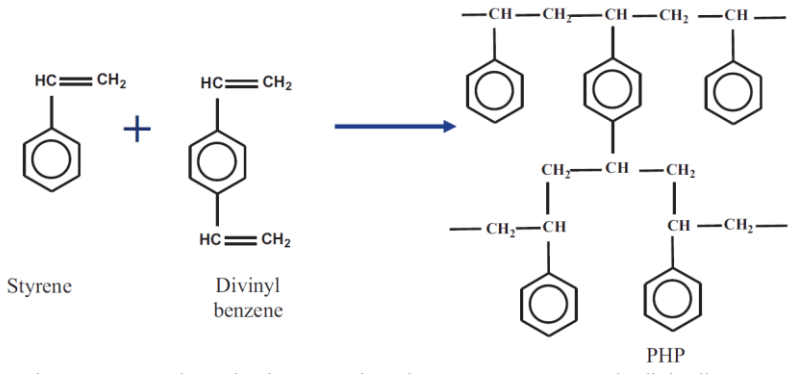

Figure 1-3. The chemical interaction between the styrene/DVB chains to form the PolyHIPE(Jimat, 2011).

Generally, a PolyHIPEs structure is considered an open structure with different small pores inside windows of interconnected larger pores. The pore size depends on the emulsion stability. Increased stability leads to small droplet size due to large interfacial area while in low stability emulsions, the droplets tend to coalesce therefore large pores will form (Hasan, 2013). The stability of the emulsion also has a strong influence on the structure of the PolyHIPE. For example, it was found that for an oil phase consisting of styrene monomer and divinylbenzene

(DVB) as cross-linker which has high hydrophobicity, the stability of the emulsion is increased so the PolyHIPE structure has smaller pore dimeter (Barbetta et al., 2000, Williams et al., 1990) (Cameron, 2005b).

The structure of the resulting PolyHIPE also has an effect on the washing process which is used to remove the surfactant and the residual monomer from the internal structure. It was observed that 20% shrinkage occurs during the drying process compared with the original volume. This is attributed to the presence of closed pores inside the structure which prevent the removal of the residual monomer and surfactant, because the solvent used in washing process cannot reach the entire structure due to these closed pores compared with the open structure (Wu et al., 2013). It was suggested that, the shrinkage process did not occur during the polymerization process because the polymer network prevents the collapse of the PolyHIPE structure (Menner and Bismarck, 2006).

The solvent which is used for the washing process has an important effect on the stability of the PolyHIPE. It was found that when using swelling solvents (such as tetra hydro furan (THF)) some pores were destroyed due to capillary forces arising from the solvent filling these pores. Therefore, a solution was suggested to solve this problem by putting the PolyHIPE in non-swelling solvents (ethanol) (Jerábek et al., 2008).

According to Boujelben et al. (2009) the following requirements must be met in the preparation and modification of PolyHIPEs:

1. PolyHIPEs should have suitable internal structure and morphology, such as the size of the pores and the degree of interconnection between them.
2. The PolyhHIPEs should have the ability to form a monolithic structure.
3. The PolyHIPE chemistry should be sustainable as should the modifications to the PolyHIPE structure to promote the required performance.

1.2 Heavy Metals in waste water

There are many heavy metals which may be present in waste water such as nickel, cadmium and arsenic with different concentrations which are naturally available or which come from industry processes(Kadirvelu et al., 2001b) . The atomic weight of these heavy metals is between 63.5 and 200.6 (Srivastava and Majumder, 2008) and their concentrations can be above the acceptable limit which determined by the World Health Organization Guideline. The concentration of nickel originally from industry may reach 800mg/l (Rajic et al., 2010) while the acceptable limit for the nickel in waste water is approximately 5mg/l (Ismail et al., 2012, Barakat, 2011) and its concentration in drinking water should be not more than 0.07mg/l (Edition, 2011). When the concentration of heavy metals in drinking water is more than the concentration limit determined by the World Health Organization Guidelines, it will affect human health (Molinari et al., 2008). Therefore, many different methods were developed to remove heavy metals such as arsenic, barium, cobalt, cadmium, chromium, copper, lead, manganese, mercury, nickel, selenium, silver, and tin from waste water (Periasamy and Namasivayam, 1995).

The importance of the development of a new methods to supply clean and safe water for people is justified by the large number of people dying each year due to polluted water (El-Dessouky and Ettouney, 2002). It estimated that nearly 5,000 to 6,000 children die every day due to contaminated drinking water (Ashbolt, 2004, Hutton et al., 2007). It has been estimated that 0.78 billion people in the world do not have safe water (Unicef and World Health, 2014). It is also estimated that in a few decades the amount of safe water will reduce by one-third (Amin et al., 2014). Thus there is a driving force to develop new methods to improve the quality and safety of drinking water.

The mechanism of the interaction between heavy metals and body cells has been explained by many researchers. Heavy metals have the ability to bond with cells in the human body by electrophilic attraction. This process is approximately similar to the bond between heavy metals and functional groups (carboxylic acids, amines, thiols etc.) which are at the surface of many materials. The interaction between heavy metals and functional groups come from the tendency of these heavy metals to attract toward functional groups with high electron density to make chemical bonds. Additionally, bonding between the strong positive ionic charge and multiples functional group may occur at the same time (Rivas et al., 2003).

In addition to that, they have high ionic radius and average charge more than +1, therefore making bonds with from 4-10 coordinated ligand groups. The size and the charge of the metal plays an important role in determination of the number and the strength of these bonds, and there can be differences in toxicity and chemistry between these metals which are significant.

The influence of heavy metals becomes significant at higher concentrations in the human body because of the electrophilic behaviour, so bonding with the functional groups in the body cells occurs more readily which may destroy these cells and cause many diseases as shown in Table 1-1. Some functional groups such as carboxylic acids (-COOH), amines ($-NH_2$), thiols (-SH) have high electron density, and they have the same effect as heavy metals by bonding with proteins and destroying them (Järup, 2003, Davidson, 2010, Kurniawan et al., 2006).

Table 1-1: Different Heavy Metal Toxicities (Kurniawan et al., 2006, Davidson, 2010, Järup, 2003).

Heavy Metal	Toxicities
Arsenic	Gastrointestinal, cardiovascular, nervous system disruption, bone marrow, depression, haemolysis, hepatomegaly, melanosis, polyneuropathy and encephalopathy, death
Cadmium	Kidney damage, renal disorder, carcinogenic
Chromium	Headache, nausea, diarrheal, vomiting, carcinogenic
Copper	Liver damage, Wilson disease, insomnia
Gold	Autoimmunity
Lead	Autoimmunity, headache, irritability, abdominal pain, various nervous system and psychological disturbances, retardation
Mercury	Tremors, changes in personality, restlessness, anxiety, sleep disturbance, depression, autoimmunity, death
Nickel	Dermatitis, nausea, chronic asthma, coughing, Carcinogenic
Zinc	Depression, lethargy, seizures, ataxia, thirst

The concentration limits of heavy metals in potable water are specified by the World Health Organization Guidelines as given in Table 1-2 (Pergolizzi et al., 2008).

Table 1-2:- World Health Organization's Guideline values for heavy metals (Edition, 2011).

Heavy Metal	Guideline Value (mg/l)
Arsenic	0.01
Barium	0.7
Cadmium	0.003
Copper	2
Manganese	0.4

The methods used for heavy metal removal from waste water depend on their concentration. The origin of the heavy metal contamination is also important and also the location where the contamination is generated. For instance, Table 1-3 gives the definition for discharge and effluent discharge (Furse et al., 2006) in the USA and China. Somewhat surprisingly the maximum discharge limits are lower in China but those limits are better policed in the USA where water quality prosecutions are much more common.

Table 1-3:- show Maximum Effluent Discharges for the Electroplating Industry in the USA and PRC. Where EPAa Environmental Protection Agency, USA, b Ministry of Environmental Protection, PRC.

Heavy Metal	EPAa Max. Effluent Discharge (mg/l)	MEPb Max. Effluent Discharge (mg/l)
Silver	0.7	0.3
Copper	2.7	0.5
Nickel	2.6	0.5
Chromium	4.0	1.0

1.2.1 Copper in wastewater

Copper is widely used in different applications such as in water pipes but still has an effect on human health as shown in Table 1-1. Copper ions (Cu^{2+}) in waste water can have a significant effect on the human health after ingestion because it can cause different health problems such as impairments, carcinogenicity and mutagenesis in many parts in the body. Therefore different technologies, such as activated carbon, are used to remove it to reach the limit specified by the World Health Organization which is 2mg/l (Edition, 2011). Agricultural waste was used as the best adsorbate for this ion due to its high uptake and low cost as well as flexibility of usage enabling it to remove single and multi-metals at the same time (Bilal et al., 2013).

An increase in the amount of copper in drinking water also leads to mutagenesis in humans when its concentration is above the permissible limit of 1.3 mg/l in industry effluents, a value determined by the United States Environmental Protection Agency (Shawabkeh et al., 2004). In addition to all the problems which heavy metals may cause when entering the human body by ingestion, skin contact can occur and this might cause skin cancer (Vieira et al., 2010).

1.2.2 Nickel in wastewater

Nickel is one the most widely used in industry for design products because it have many properties as listed below.

- Its melting point is high (1453 °C)
- It has good resistance to Corrosion
- Because the internal structure face-centred cubic so it consider as a ductile material and it could be used as catalyst

Nickel is used in synthesis of non-ferrous alloys and super alloys; electroplating processes, catalysts; nickel–cadmium batteries; coins, welding, pigments and electronic products (Cavallo et al., 2003). Household applications use nickel in about 8% (Nieboer et al., 1999). Food supplements can also contain of nickel (Ruhrberg, 2006).

Nickel can be easily deposited on a reuse of substrates, so it can be used in different applications such as computer hard disks, kitchen utensils, medical devices, automobile trim, and bathroom fixtures (Davidson, 2010). Nickel can be recovered by using it and it can be used again in last applications due to its physicochemical properties as listed below (World Health, 2005).

Nickel has two electrons in the valence band, and +1, +3, or +4 oxidation states may be available. Metallic nickel does not react with water, but it has the ability to react with hydrochloric, sulfuric or nitric acid. While nickel salts such as acetate, chloride, nitrate, and sulphate are soluble in water, carbonates and hydroxides have lower solubility in water. Sulfides, disulphides, sub sulfides, and oxides are insoluble in water (Haudrech et al., 1994, Morgan and Flint, 1989).

Natural water commonly contains a nickel component $[Ni(H_2O)_6]^{2+}$ at the pH range between 5 and 9. Nickel can form complexes with many chemical components such as OH^-, SO_4^{2-}, HCO_3^-, Cl^-, and NH_3 at different pH values (Nieboer et al., 1999). Nickel can enter water via metallurgical (Rule et al., 2006), electronic industries (Veglio et al., 2003), and electroplating (Castelblanque and Salimbeni, 2004).

The concentration of nickel in groundwater depends on parameters such as the depth of the water, the pH and the kind of soil. Therefore, its concentration varies from area to area around the world. For instance, the concentration of nickel in the Netherlands is between 7.9 μg/litre in urban areas to 16.6 μg/litre in rural areas. Additionally, it was reported that acid rain (low pH) increases nickel mobility in the soil which might lead to an increase in its concentration as well (Nieboer et al., 1999). Smoking is another source of nickel because cigarettes give between 0.04–0.58 μg of nickel to the atmosphere per cigarette (Nieboer et al., 1999).

This removal of copper and nickel ions from wastewater is a significant requirement and it is a challenge to reduce concentrations down to Wold Health Organization Guideline limits.

Heavy metals such as nickel can be adsorbed by intestines a mechanism of adsorption which is not clear right now. It was estimated that, reducing iron in the intestines lead to increasing nickel adsorption, while intestinal mucosal cells absorbed nickel partially with the transfer system of iron (Tallkvist et al., 1994).

1.3 Wastewater Treatment Techniques

Among many industry processes that take place across the world each day, some products like algal blooms, detergents, fertilizers, pesticides, and chemicals generate many heavy metal compounds with different chemical structures. New technologies and new materials with low cost and high efficiency to remove these heavy metals from waste water are widely investigated (Boujelben et al., 2009). For instance, metal oxides show better performance in adsorption processes than other materials such activated carbon, magnetite, fly ash, or calcined phosphates, because they have higher affinity towards metal cations (Varma et al., 2013).

Heavy metals from different industry processes can have a significant effect on human health (Inglezakis et al., 2003), because they are toxic materials which can accumulate (Seiler et al., 1988). Therefore, methods such us ion exchange, membrane technology, precipitation/coagulation and adsorption are used to remove these metals from waste water (O'Connell et al., 2008). In the following sections the technologies most widely used to remove heavy metals from waste water are briefly discussed.

1.3.1 Adsorption

Adsorption processes have many advantages compared with other methods in terms of simplicity, efficiency and convenience (Stafiej and Pyrzynska, 2007, Afkhami et al., 2007, Yabe and de Oliveira, 2003, Cervera et al., 2003). In these processes the contaminant is adsorbed from solution onto the surface of a suitable material where it remains trapped until the material is removed from the process stream or the surface is regenerated. Most adsorption processes involve the use of polymers coated with different materials (Gupta et al., 2009). The filtration process efficiency using this techniques depends on many parameters such as pH; the amount of adsorbate; the contact time between the adsorbate and the heavy metal ion, and the concentration of the material used in the coating. These parameters also have an influence on the regeneration processes which are used after filtration to regenerate the adsorbate surface in order to reuse it (Adeli et al., 2012).

Different materials have been used as adsorbants in filtration processes. It was found that low cost fly ash materials which came from the sugar industry in Egypt were effective to adsorb many heavy metals such as Cu^{2+}, Zn^{2+} and Cr^{3+} which are found in waste waters from industry. The results showed that it was an active material to remove approximately 95% of these ions after changing different parameters such as pH, adsorbant dose, metal ion concentration, and shaking time. Activated carbon is an expensive adsorbant with high efficiency in removing

heavy metals (Gupta et al., 1998a, Gupta and Ali, 2000, Gupta et al., 1998b, Gupta et al., 1997a, Gupta et al., 1997b).

Clinoptilolite powders (natural zeolite containing silica and alumina), activated alumina, silica gel, and activated carbon are effective in removing different heavy metals like nickel from waste water. All these adsorbants can be made more efficient by increasing their surface area (Ismail et al., 2012). Iron oxides are also considered as important adsorbant materials which have been studied for removing the heavy metals (Lo and Chen, 1997, Diz and Novak, 1999).

Generally, the adsorption process consists of two steps (1) a transfer process for heavy metal ions from the solution to the adsorbant surface (2) adsorption at active sites on the surface of the adsorbant, (Barakat, 2011). The demand for using natural materials as adsorbants to remove heavy metals from waste water has recently increased since it is sustainable alterative to synthetic materials. For instance, chitosan was used to remove Cu (II) (Ngah et al., 2002), and cross-linked starch gel (Zhang and Chen, 2002), to remove Pb (II) ions. Polysaccharides showed excellent performance during filtration compared to activated Carbon (Crini, 2005). Additionally, it was reported that, the chemical structure and complexing group was the most important factor to determine the removal efficiency for polysaccharides (O'Connell et al., 2008).

1.3.2 Ozonation, Reverse Osmosis and Nanomaterials Techniques

In ozone treatment, ozone from a generator is bubbled through the contaminated water and oxidises organic chemicals within it. There may be some oxidation of metal ions as well. Ozonation has two disadvantages which are high cost and short life of the ozone generator (von Gunten, 2003). Although this method does not have sufficient efficiency to remove high concentrations of micro pollutants it is still considered as an advanced method to remove heavy metals at low concentration. In contrast, Reverse Osmosis (RO) is considered better than other techniques to remove low concentrations of contaminants but it needs more energy (Braeken et al., 2006). Adsorbant nanomaterials technology needs lower energy than RO and it has many advantages such as good reactivity, high adsorption due to high surface area (Qu et al., 2013, Alivisatos, 1996, Rosenthal, 2001).

1.3.3 Chemical Precipitation

Trapping contaminants in insoluble precipitates can be used when concentrations are high enough. The mechanism of this technology depends on the interaction between a chemical and heavy metals ions to produce an insoluble complex, according to reaction Eq 1-1.It is complex will fall to the bottom of the container then it can be separated from the water by filtration or sedimentation.

$$M^{2+} + 2(OH)^{-} \leftrightarrow M(OH)_2 \downarrow \quad \text{Eq 1-1}$$

Here M^{2+} represents the heavy metal in ion form, while $M(OH)_2$ refers to the hydroxide in insoluble form.

A compound that forms a soluble hydroxide on addition to water is required to start the interaction such as calcium and iron hydroxide. There are many advantages for using this process such as simplicity, safety during operation and low cost (Kurniawan et al., 2006). Sulphides are widely used in this technology to form hydroxide precipitation (Fu and Wang, 2011).

1.3.4 Activated Carbon and carbon-based Adsorbants

Activated carbon adsorbants have been used many times in filtration processes for removing heavy metals from waste water, because their structure consists of both micropores and mesopores which results in high surface area (Jusoh et al., 2007, Kang et al., 2004). Many additives such as alginate (Park et al., 2007), tannic acid (Üçer et al., 2006), magnesium (Yanagisawa et al., 2010), surfactants (Ahn et al., 2009), were added to activated carbon to improve its performance toward adsorbing the heavy metals from waste water. However, it is still considered as high cost adsorbant (Fu and Wang, 2011).

According to (Iijima, 1991), since 1991 carbon nanotubes (CNTs) have been used in many trials and they showed very good properties which make them suitable for different applications. One of these application was removing heavy metals from waste water e.g removing lead (Wang et al., 2007, Kabbashi et al., 2009), and cadmium (Kuo and Lin, 2009).

The results from the last few decades have shown that, the CNTs have good efficiency to remove heavy metals. CNTs are divided into two kinds, (1) single-walled carbon nanotubes (SWCNTs) and (2) multi-walled carbon nanotubes (MWCNTs) (Odom et al., 1998). Both types

of CNTs attract the heavy metals from waste water by different mechanism such as electrostatic attraction, adsorption precipitation and interaction with functional groups which attract metal ions (Rao et al., 2007). CNTs were used to remove heavy metals from waste water but they showed low adsorption capacities. After oxidation by different solutions such as HNO_3, NaClO and $KMnO_4$ their performance increased (Fu and Wang, 2011). Wang et al. (2007) have used MWCNTs to remove Pb (II) from waste water, with an adsorption capacity of approximately 75.3% (Fu and Wang, 2011).

In another study Li et al. (2010), used three adsorbents (activated Carbon (AC), unfunctionalised (MWCNTs) and functionalised (MWCNTs)) to remove Cr (VI) from waste water. It was reported that, unfunctionalised MWCNTs had the highest removal efficiency of 98% for a 100 ppb Cr (VI) solution. While AC shows less removal efficiency than non-functionalised and functionalised MWCNTs. Li et al. (2010) reported that, CNTs immobilized by calcium alginate (CNTs/CA) were used to reach 67.9% mg/g adsorption capacity (Fu and Wang, 2011).

Multi-walled carbon nanotubes (MWCNTs) were also used to remove nickel from waste water before and after the oxidation process with nitric acid at 150 ◦C. The filtration process was done by changing many parameters such as pH and initial concentration and contact time at room temperature. The results showed that, oxidized CNTs have better removal efficiency than non-oxidized CNTs; the removal capacity was 18 and 49mg/g, respectively. The adsorption process for the oxidized CNTs was complete at a shorter time than non-oxidized CNTs (Kandah and Meunier, 2007).

1.3.5 Low-Cost Adsorbents

The most important factors in choosing between different adsorbants is the cost of the adsorbant, the type of the adsorbant how many processes are required before the adsorbant filtration process and material availability. Thus, low cost adsorbants which require few preparation processes and are available naturally or from industry processes are favoured (Bailey et al., 1999). It was reported that, agricultural wastes, kaolinite and montmorillonite all have good performance to remove the heavy metals from waste water (Sud et al., 2008).

1.3.6 Chemical Modification of Adsorbants

Chemical modification by an acid is considered as an effective method to remove heavy metals from waste water. For instance, montmorillonite clay was subjected to acidic treatment to decompose its structure; hydrochloric acid was used for this process (Vengris et al., 2001). The results showed an increase in the capacity to remove many heavy metals such as nickel, copper and zinc to concentrations which are admissible by the Wold Health Organization Guideline (Vengris et al., 2001). The filtration process was done by using solutions with different pH values (between 6.2 and 6.8) since copper hydroxide $Cu(OH)_2$ precipitates at higher pH. The acceptable limit of theses metals in pure water (Ni=0.5mg/l, Cu=1mg/l, Zn=1mg/l) could be achieved (Vengris et al., 2001).

In another study, Orange peel was modified with sodium hydroxide and calcium chloride, which resulted in increased the adsorption capacity towards many metals ion such as Cu (II), Pb (II) and Zn (II) with an increase of up to 59.7%, 84.8% and 164% respectively (Feng and Guo, 2012). There are many disadvantages in using this technology, because of the huge amount of chemicals required to remove the heavy metals from the waste water and a large amount of sludge is produced during this process. Further processes are needed to remove this and this increases the cost of this method. Furthermore, the metal precipitation mechanism is slow, and the precipitates are small leading to poor settling (Aziz et al., 2008) and limited metal recovery.

Thus, it is clear that chemical treatments may improve the adsorption capacity of a particular adsorbant but the cost can be high and the ease of recovery of the metals may be compromised if the polymer substrate is unsuitable.

1.4 PolyHIPEs as Filtration Media

It has previously been shown that PolyHIPE can used as a filter material either as a physical filter or a substrate for an ion exchanger. PolyHIPEs have nano and micro pores and they can be functionalised by coating with suitable material to enhance this. PolyHIPEs contain a Nano–structured surface that reacts with contaminants and can be considered as nanomaterials which have different physical properties compared conventional materials. Nanostructured materials have new properties such us high surface area, antifouling surfaces, strong adsorption and easy fictionalisation which could be used to remove range of metals from waste water (Qu et al., 2013, Rickerby and Morrison, 2007, Vaseashta et al., 2007).

Traditional methods for waste water treatment do not have the same removal efficiency as nanomaterials (Amin et al., 2014). For example the biological methods cannot be used to remove certain contaminants because many of them are soluble in the solution (Ozaki, 2004, Urase and Kikuta, 2005). The ozonation method is considered expensive and it is effective only for short times (Adams et al., 2002, Boujelben et al., 2009).

Functionalised nanostructured materials have been shown to be more efficient in removal of heavy metals (Vörösmarty et al., 2000). It was also found a polymer adsorbant (the main structure for the PolyHIPE) was effective for removing heavy metals when it was combined with ultrafiltration (Bodzek et al., 1999, Rivas et al., 2003). Therefore PolyHIPE coated with a specific adsorbant could be used in an ion–exchange process as an effective method for removing heavy metals from waste water when its concentration is low (Bilal et al., 2013).

1.4.1 Polymer Selection

Many researchers have used polymers as a host for different adsorbants to remove heavy metals from waste water because both polymers and the metals could be reused after removing the heavy metals in a regeneration process. The polymer provides a physically robust substrate for the adsorbant layer which is stable during both filtrations and regeneration. This regeneration is economically desirable to reduce the cost of the purification processes. The regeneration process could be achieved by changing the pH or use of electrochemical or thermal pathways (Molinari et al., 2008, Geckeler and Volchek, 1996, Molinari et al., 2004, Tavares et al., 2002).

Polymers can be the substrate the adsorbant or may directly attract contaminates to their surface functional groups. Polymeric chains contain charged functional groups, which allow heavy metals to penetrate deeply inside their structure according to the Donnan membrane principle (Cumbal and SenGupta, 2005, Pan et al., 2010, Su et al., 2009, Pan et al., 2009b, Zhang et al., 2009). For instance hydrous manganese dioxide was used as hybrid adsorbent after deposition onto a porous polystyrene substrate to use it as a cation exchanger (Su et al., 2009). The polymer could be used as a host for different oxides such as ferric oxides, manganese oxides, aluminium oxides, titanium oxides, magnesium oxides and cerium oxides, and it was used to remove lead from a standard solution showing good performance with a removal capacity of 395 mg/g. These results were obtained in the presence of other metals such as Ca^{2+} , Mg^{2+} , and Na^{+} and the concentration of lead was reduced from 1 mg/l to less than 0.01 mg/l which is below the acceptable limit according to the drinking water standard recommended by WHO (Hua et al., 2012).

Thus, polystyrene is a suitable filter substrate polymer as it is relatively cheap and easy to process and has therefore been used as filter substrate but other polymer systems could also be used.

1.4.2 Metal Oxide Nanoparticles

Metal oxides such as nano-sized ferric oxides, manganese oxides, aluminium oxides, titanium oxides, magnesium oxides and cerium oxides have good performance when used to remove heavy metals from aqueous systems due to their high surface area and they have good adsorption efficiency toward the heavy metals (Hua et al., 2012). It was reported that, they could be used with another material as a host. For instance, PolyHIPE as a porous host which support the metal oxide (Hua et al., 2012) especially when the metal oxides show high sorption because of their high capacity and selectivity, which leads to higher removal efficiency (Deliyanni et al., 2009).

Iron oxides with nanostructure have high surface energy which makes them active towards the adsorption of heavy metals but it makes them less stable, and they can agglomerate due to van der Waals forces (Pradeep, 2009). Due to its weak mechanical strength, iron oxide has to be supported on different materials with a porous structure such as activated carbon, natural materials, and synthetic polymers (Pan et al., 2009a).

Factors such as, size, stability and shape of the particles have a huge effect on the adsorption process. Therefore, the morphology, size, crystal structure, surface area and the pH of zero point of charge (pH pzc) have been studied to improve the adsorption performance of metal oxides. Regardless of its structure, there are two methods to produce metal oxide with nanostructure and high stability (1) physical methods which include inert gas condensation, severe plastic deformation, high-energy ball milling, ultrasound shot peening, and (2) chemical method such as reverse micelle (or micro emulsion) controlled chemical co-precipitation, chemical vapour condensation, pulse electrode deposition, liquid flame spray, liquid-phase reduction, and gas-phase reduction (Li et al., 2006).

Iron oxide is considered friendly to the environment, so it has been widely used to remove secondary contaminants (Deliyanni et al., 2004). Many studies were done to remove heavy metals from waste water by using nanosized iron oxide in different forms such as goethite (FeOOH), haematite (Fe_2O_3) (Grossl et al., 1994, Chen and Li, 2010), amorphous hydrous Fe oxides (Fan et al., 2005), maghemite (Fe_2O_3) (Hu et al., 2006), magnetite (Fe_3O_4) (Mahdavian and Mirrahimi, 2010, Wang et al., 2010, Badruddoza et al., 2011) and iron/iron oxide (Macdonald and Veinot, 2008, Guan et al., 2007).

This project will assess the effect of the PolyHIPE supported iron oxide nanoparticles as an adsorption filter based on these results.

1.5 Aims and Objectives

The aim of this work is to synthesis PolyHIPE with a defined structure (nano and micro pores with interconnect between them) by controlling the preparation conditions (mixing time) and then assess its performance as an ion exchanger and adsorbant after sulphonation with sulphuric acid and a coating process with iron oxide. The resulting structure will be used to remove nickel and copper ions from simulated waste water.

The objectives s of this study were to identify the polyHIPE parameters which we could change to improve the filtration process to reach the discharge limit for nickel and copper in water. PolyHIPE materials were used because they have a porous structure with different pore size and this porous structure gives iron oxide nanoparticles the opportunity to enter to the entire structure; therefore more iron oxide will loaded in the water coating layer of the material and this means increasing the number of active sites which are used in the filtration processes. Thus the removal efficiency will increase (Katsoyiannis and Zouboulis, 2002). An additional objective was to find cheap materials for use in the filtration processes rather than using high cost adsorbant (Kratochvil and Volesky, 1998, Bailey et al., 1999).

1.6 Structure of the thesis

Chapter 1 introduces the project and gives general information about reasons for using PolyHIPEs as filtration media and the most important methods that are used to remove heavy metals from waste water.

Chapter 2 contains the literature review and discusses the parameters which can be changed to produce a suitable PolyHIPE for filtration studies.

Chapter 3 gives the experimental methodology for the work undertaken, including the PolyHIPE preparation, filtration studies and the equipment which was used for characterization of the materials and filtration solutions during the project.

Chapter 4 details results of the PolyHIPE polymer (PHP) synthesis and how the sample structure depends on processing using the results from a range of test methods including SEM, BET and FTIR.

Chapter 5 discusses the filtration performance of post sulphonated PolyHIPE as an ion exchanger to remove nickel and copper from wastewater.

Chapter 6 discusses improvements to the use of the PolyHIPE after sulphonation in order to remove more nickel and copper from the standard solutions.
Chapter 7 give the results for using PolyHIPE after coating with iron oxide as an adsorbant filter.
Chapter 9 investigates the regeneration processes that might be used to recover the heavy metals from the PolyHIPE after the filtration process.

Finally Chapter 10 summarises the work undertaken and suggests the future work which might be done to increase the removal efficiency of polyHIPE-based adsorbants for heavy metal contamination in wastewater.

1.7 Summary

This chapter has summarised the background material and justification for the choice of functionalised PolyHIPE as a new material for removing the heavy metals from waste water based on its unique properties such as high surface area and porosity and the ability to tailor its performance by controlling the functionalisation process. Therefore it has the potential to be more efficient that the traditional methods and more selective due to the fact that it can be fictionalised with different specific materials to be suitable for removing different heavy metals. Both industrial and natural weathering processes can lead to water contamination with heavy metals and these can have a significant effect on human health. Thus further work is needed to develop improved technologies for use in waste water treatment preferably by using cheap material with high performance. In this thesis the use of polyHIPE will be investigated for such application and its processing and how it might be optimised to improve performance is discussed in the next chapter.

2. Structure and Chemistry of PolyHIPE

In this chapter the most important factors such as cross linker, surfactant etc. which can be changed to produce PolyHIPE with better mechanical and physical properties like surface area and pore size are introduced. These processing changes can have a huge effect on the resulting structure of the PolyHIPE which influences its properties, therefore the performance of this material in an application can be optimised by changing these parameters. Functionalisation can further improve properties and the sulphonation process is explain in more details due to its priority in this work where it was used it to change the PolyHIPE from hydrophobic to hydrophilic by addition of SO_3H groups to the PolyHIPE structure. This functional group can be used as strong cation exchanger with the heavy metals such as nickel and copper. The ion exchange mechanism is explained in this chapter. In addition, the parameters used to increase the removal efficiency for heavy metals from waste water are explained such as pH, temperature the amount of adsorbant. The use of PolyHIPE as an ion exchanger is analysed to estimate the benefit of using it in the filtration process. Finally the mechanism of regeneration and measuring zero of point charge is explained. The first is used in this work to recover the heavy metals from PolyHIPE after the filtration process and the second is to determine the value of pH in which the iron oxide should be used in the coating process to give zero surface charge which is important if the material is to be used to adsorb heavy metals from wastewater without ion exchange.

2.1. Factors Affecting PolyHIPE Structure

There are many factors which determine the final structure of the PolyHIPEs such as the pore size, the ratio of interconnections between pores and the total surface area (Zhou et al., 2007). At the same time, these factors can be changed by changing the ratio of the materials through the preparation step or by changing the preparation conditions such as mixing time and mixing speed (Walsh et al., 1996). Below the most important factors are briefly discussed.

2.1.1. Cross-Linker

Williams et al. (1990) Considered the cross-linker as one of the most important parameters which influences the morphology of the PolyHIPE. They discovered that the emulsion became more stable by using Divinylbenzene (DVB) rather than using styrene alone. This is because it is difficult to create open cell pores inside the PolyHIPE structure without a cross-linker.

The cross linker is added to the emulsion as a stabilizer, therefore if the amount of the cross linker is insufficient the PolyHIPE product may appear as powder (Normatov and Silverstein, 2007b, Akay et al., 2005a). The cross linker forms a network inside the polymers which prevents the collapse of the PolyHIPE structure (Barbetta et al., 2000).

The ratio of cross-linker in the oil phase also has significant effect on the pore size of the resulting PolyHIPE (Williams et al., 1990). It was found that, the average pore size was reduced from 15 to 5 μm by increasing the styrene/DVB ratio. As a result, the stability of the structure increases by reducing the pore size.

2.1.2. Surfactant

A surfactant contains both, polar and non-polar groups which interact at the interface between the oil and aqueous phases and this leads to the formation of a interfacial film which increases the stability of the emulsion (Hauthal, 1990). Adding the surfactant to the oil phase has an effect on the morphology of the resulting PolyHIPE as well. It was found by Williams et al. (1990) that when the ratio of the surfactant was 4% the PolyHIPE produced consisted of large pores, whereas when the ratio increased up to 5% smaller pores appeared on the surface, and when the ratio increased up to 8% the resulting surface had fine pores. At 30% surfactant the surface was very smooth (Williams et al., 1990).

In a study conducted by Williams and Wrobleski (1988) it was found that when the surfactant is low (i.e. <5% related to the oil phase) closed pores will be formed in the PolyHIPE structure

but when the concentration of the surfactant is high (i.e. >7%) open cells were generated. This is because the thickness of the monomer film located between the droplets increases when the surfactant concentration increases and a window appears in the cell walls during polymerization. At low concentration the droplet may shrink to give a closed structure(Hasan, 2013). It was also observed that, increasing the surfactant concentration compared with the monomer leads to the reduction of the pore size due to reduced interfacial tension between these two phases.

The surfactant may help in creating new pores inside the PolyHIPE structure therefore the morphology might be changed by increasing the surfactant ratio in the oil phase. It was suggested that the surfactant tail group may be attracted by another group which is located in the same region and agglomerate to form a new phase, and after removing the surfactant through the washing process a new pore might be generated (Bhumgara, 1995). Some polymers can act as co-surfactants. Vinyl benzyl chloride (VBC) which has polar and non-polar groups can be absorbed at the interface of the emulsion increasing the stability of the emulsion by reducing the tension at the interface area (Barbetta et al., 2000).

2.1.3. Mixing Time/Dosing Time

The emulsion which results from mixing the oil and the aqueous phase is less stable because of the high interfacial tension. The droplets tend to accumulate and coalesce and this produces large pores inside the structure. This can be controlled to a certain extent by putting energy into the system from the mixing process. This depends on the time for which mixing occurs. The total mixing time is calculated from..Eq 2-1 .In general an increased mixing time will reduce the droplets to a smaller size therefore the pore size will decrease. As a result, the emulsion will be more stable (Walsh et al., 1996). The mixing process supplies the energy to the droplets so when the energy is high the droplet can be broken into smaller droplets (Jimat, 2011).

$$T_t = t_D + t_M \quad \text{..Eq 2-1}$$

where t_D is the dosing time and t_M is mixing time.

2.1.4. Moulding Type

The type and shape of the material which is used as a container for the emulsion has a strong influence on the morphology of the PolyHIPE (Cameron, 2005a). It was observed that when a glass mould was used, a weak physical bonding between the sample surface and the container surface takes place. It was also observed that a polyvinyl chloride (PVC) mould has a negative effect on the stability of the PolyHIPE because the HIPE reacts with the container (Cameron, 2005a).

2.2. PolyHIPEs Surface Area

PolyHIPEs can be tailored for many applications (Wakeman et al., 1998) because it is relatively easy to control the pore size range (Zheng et al., 2014). The surface area depends on the pore size. For instance, PolyHIPEs with a surface area of 10 m^2/g have been obtained when the pore size range was between 3-7 µm (Krajnc et al., 2005b). A significant number of published studies have been carried out with the aim to increase the surface area by changing process parameters or by adding new materials. A porogenic solvent was found to produce small pores inside the walls which separate the larger pores and this leads to an increase in surface area (Hainey et al., 1991). The addition of toluene resulted in PolyHIPEs with a considerable increase in surface area (from 3 to 350 m^2/g according to (Williams et al., 1990)).

2.3. Mechanical Properties

Generally, PolyHIPEs have poor mechanical properties being brittle. It was suggested (Wu et al., 2013) that increasing the organic phase is one of the solutions to improve the mechanical performance of the these materials. Certain additives may be used to change the mechanical properties and make PolyHIPEs suitable for specific applications (Zheng et al., 2014). Cameron (2005b) showed that by adding Kevlar fibres to a styrene/DVB PolyHIPE significantly influenced both the morphology and the mechanical properties increasing the compressive and flexural modulus and also the toughness (Hayward et al., 2013). Silica added to the emulsion leads to an increased Young's modulus by up to 280% (Haibach et al., 2006). The type of cross linker also has an effect on the mechanical properties. It was found that the PolyhHIPE brittleness was reduced when using polyethylene glycol dimethacrylate (PEGDMA) as the cross-linker (Menner et al., 2006).

2.4. Chemical Modification of PolyHIPEs by Sulphonation

The PolyHIPE prepared with polystyrene contains phenyl groups which are classified as active sites. This allows for additional reactions with various chemical components to produce PolyHIPEs with specific reactive sites for a given application. The hydrophilic properties of PolyHIPEs can be controlled through the sulphonation process which takes place on these groups (Cameron, 2005b).

The sulphonation process is considered as one of the most important chemical treatments applied to PolyHIPEs in order to increase the capacity of PolyHIPE to absorb water. The hydrophobic character can be changed to hydrophilic by adding the sulphonate group (SO_3H) as shows in Figure 2-1 and Figure 2-2 (Yee et al., 2013). The PolyHIPEs can be functionalized with specific ions that can be used in ion exchange removing processes for wastewater treatment (Wakeman et al., 1998). The process of sulphonation consists in heating the PolyHIPEs with concentrated sulphuric acid at a temperature of 40 °C, for 24 to 112 hours or by using microwave radiation to drive the chemical reaction (Yee et al., 2013).

Because the most reactive sites are available inside the structure of the PolyHIPE, the following factors contribute to the degree of sulphonation: the solvent; the swelling process; and the compatibility of the solvent. The solvent used should swell the PolyHIPE structure to give the ability to the solvent to enter into the structure and to attach to the active sites. The swelling process should continue for the entire time of sulphonation. The solvent should be compatible with the polymer considering the hydrophobic character of the polymer (Cameron et al., 1996). This chemical process can be modified by controlling some factors through the preparation steps. For example, a high degree of sulphonation and better control on the porosity may be obtained through synthesis of PolyHIPEs from styrene/DVB, by increasing the ratio of the cross-linker up to 20%. As a result, the degree of sulphonation increases due to an increase of the active sites inside the PolyHIPE, whereas, swelling processes during the sulphonation reduce with increasing the pore volume. This affects the amount of sulphuric acid that reaches the reactive sites inside the structure of the PolyHIPE hence the degree of sulphonation will reduce (Ahmed et al., 2004, Wakeman et al., 1998).

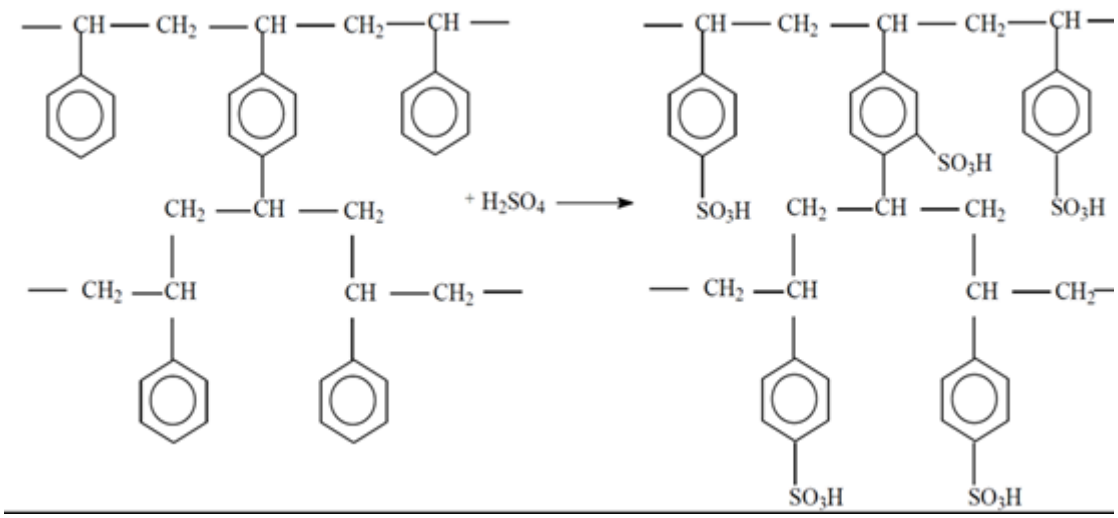

Figure 2-1. The chemical interaction between the (styrene/DVB) chains and sulphuric acid through the sulphonation process for PolyHIPEs (Jimat, 2011).

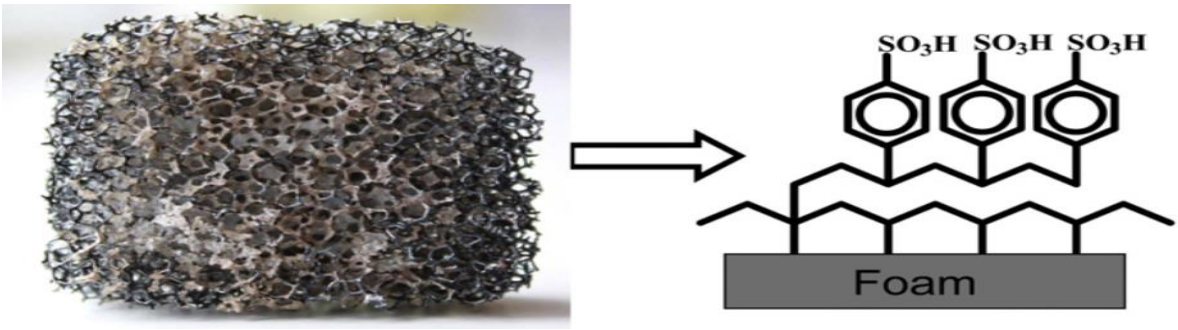

Figure 2-2. The internal chains and the shape of external structure of PolyHIPE after the sulphonation process,(Ordomsky et al., 2012).

After the sulphonation process the PolyHIPE becomes acidic due to the SO_3H in its structure. The SO_3H group joins the benzene ring of the styrene and the degree of sulphonation depends on how many sulphuric groups will attach to the ring (Bhumgara, 1995). Because of the high concentration of the sulphuric acid it is difficult to obtain uniform swelling. In order to remove the air from the structure the PolyHIPEs are treated in vacuum before the sulphonation (Wakeman et al., 1998). It was reported that the adsorption capacity of a carbonaceous material was increased after the sulphonation process (Adams et al., 1988).

2.5. Ion Exchange and Adsorption Filtration Mechanisms

2.5.1 Mechanism of ion exchange

Ion exchange processes occur in natural and in manufactured materials. These materials consist of a negative or positive charge group surrounded by ions with a different charge. These ions could be replaced with similarly charged ions from other materials. Organic materials are widely used as ion exchange media (Wakeman et al., 1998).

The mechanism of the ion exchange process depends on replacement between the heavy metal ion and an ion (from the resin) with the same charge, and these processes could be designed to be selective for a specific metal by adding ligands. Although these advantages in ion exchange processes have been demonstrated, it is still not a favourite way to remove the heavy metals from waste water, because it requires pre-treat processes to prevent resin contamination and not all the heavy metals could be removed by this method (Tan et al., 1985). However, there are many advantages which make this method widely used in purification processes, such as its high capacity, quick kinetics and high removal efficiency (Kang et al., 2004). So, it is considered an effective method to remove heavy metals from waste water (Alyüz and Veli, 2009). For instance, acidic resin with sulphonate groups (e- SO_3H) or carboxylic acids (eCOOH) could be used as an exchanger to remove cations from aqueous solution after exchange with hydrogen ions, when the solution was passed through a column containing this exchanger in the form of beads according to the chemical reaction in Eq 2-2 below (Fu and Wang, 2011).

$$NR - SO_3H + M^{n+} \rightarrow (R - SO_3)n\, M^{n+} + nH^+ \qquad \text{Eq 2-2}$$

It was reported by these researchers that, in addition to the influence of these functional groups in the removing process, there are many factors that should be taken into account to get better removal such as (1) active site numbers, (2) chemical situation of these sites (3) if there is affinity between the heavy metal and the active sites (Park et al., 2010). More control of all these parameters may lead to high removal efficiency. For instance, Dowex HCR S/S was used as a cation exchanger, and it shows high removal efficiency for many metals such as nickel and zinc at about 98 % (Alyüz and Veli, 2009)

Generally, There are many parameters which determine the ion exchange efficiency of any resins such as pH, temperature , the concentration of initial metals and the contact time between heavy metals and the exchanger (Gode and Pehlivan, 2006). In addition to that, many natural materials such as zeolites and silicate minerals, are considered low cost exchangers and could

be used after changing these parameters. It was found by different researchers that, zeolites have good capacities with different conditions and show selectively for heavy metals (Motsi et al., 2009, Ostroski et al., 2009, Taffarel and Rubio, 2009). While others reported that, clinoptilolite shows better performance when it is loaded with Fe-oxide; the exchange capacity to remove Cu, Mn and Zn was increased (Dimirkou and Doula, 2008, Doula, 2009). Potato peeling were used to remove the heavy metals from waste water after treat it with nitric acid, when the shaking technique was increased contact between heavy metals and the exchanger. A decrease in pH value after filtration was reduced which was attributed to an increase in the concentration of hydrogen ions which came from the ion exchange process (Panda et al., 2008, Aman et al., 2008). Ion exchange was used as the removing process for Cu (II) and Pb (II) from waste water by using pine cone powder after treating it with KOH (Ofomaja et al., 2010).

2.5.2 Mechanism of Adsorption filtration

Adsorption is the retention of gas, liquid or solid on a surface due to positive interaction (attraction) between the surface and the atoms or molecules of the adsorbed material. Adsorption filters have a high surface area able to adsorb a large amount of substances. The adsorbed substances can be removed from the adsorption filter by a subsequent desorption process. In adsorption filtration the species to be filtered is just adsorbed onto the surface of a filtration material and there is no exchange of ions. The surface chemistry can be tuned to remove selected contaminants from wastewater.

The number of surface active functional groups is critical to the performance of an adsorption (or ion exchange) filter material. For instance, it was estimated that the increase in removal efficiency for oxidized CNTs was due to CNTs containing many functional groups over their surface resulting from oxidation, and this enhanced its hydrophilic properties and exchange capability (Li et al., 2002). Furthermore, the surface area of the adsorbate increased during the oxidation process, hence the number of active site increase, so the adsorption capacity increased (Dabrowski and Curie, 1999). In the oxidation process done by soaking CNTs in nitric acid for 2 hours , to release Carbon and iron, the samples was washed many times until the pH showed no differences so ion exchange is not a major contributor to the process (Kandah and Meunier, 2007).

Surface area can be increased by breaking down a material structure by chemical treatment as in the case of the acid treatment of clays. For instance, exfoliation (breaking up of the material into individual silicate layers) of the montmorillonite structure occurs after acid treatment,

therefore its uptake capacity increases. Thus acid-modified clay was used to remove copper, nickel and zinc from waste water (Vengris et al., 2001).

2.5.3 PolyHIPEs in Ion Exchange

The PolyHIPEs structure consists of large porosity with interconnected pores. This micro-nano open structure makes the PolyHIPE suitable for certain applications such as filtration (Normatov and Silverstein, 2007a, Cameron, 2005b, Cameron and Sherrington, 1997)). PolyHIPE combined with a suitable ion exchanger could be used for selective ion exchange applications because they have a three dimensional network and an irregular high surface area structure after the sulphonation process and it gave better contact area between the solution and resin (Wakeman et al., 1998).

There are many factors which influence the efficiency of the ion exchange capacity when using a polymer as an exchanger media. The amount of cross-linker determines the distance between the chains (a few Angstrom for high ratio cross- linker and hundreds of Angstroms for low ratios). The cross-linker also determines the mobility of the counter ions inside the PolyHIPE structure (Wakeman et al., 1998). The pore volume has a significant effect on the ion exchange capacity per unit volume. It was found that it decreases when the pore volume increases up to pore volume 0.14 ml (Malik et al., 2010). The initial concentration of the metal which is intended to be removed from the wastewater is also important, as well as the contact time between the wastewater and the filtration media (Alikhani and Moghbeli, 2014).

In addition for all these parameters which could be changed to improve the removal efficiency for an ion exchanger, many additives could be used to enhance its ability to remove the heavy metals. For instance, Polyvinyl-alcohol has been used to remove fluoride and arsenic from a standard solution after the application of a coating containing Fe and Al (Alexandratos, 2009). Another example was a PolyHIPE material which contain a porous structure, so it widely use as the ion exchange media for removing heavy metals from waste water. For instance, Piperzine moieties generated by the polymerization of 4-nitrophenylacrylate have been used to remove atrazine (class of nitrogen-containing heterocycles) from waste water. The same amount of atrazine was removed from an aqueous solution at room temperature after 24 hours by a highly porous PolyHIPE and after 72 hours by a low porosity PolyHIPE (Pulko et al., 2007).

2.5.4 PolyHIPEs as adsorbants

Additionally, PolyHIPEs are considered as potential adsorbents due to their high surface area about $10m^2/g$ (Hasan, 2013), which provides better contact area with the wastewater. This gives PolyHIPEs the ability to treat a large amount of liquid as it penetrates through the internal structure, in addition to the interaction with the reactive groups which are available inside its structure (Pulko et al., 2007, Moine et al., 2003). Furthermore, using PolyHIPEs in filtration processes has many advantages compared with the traditional methods: no toxic sludge generated, higher efficiency and selectively (Katsoyiannis and Zouboulis, 2002).

2.6. Factors Affecting Adsorption Filtration Processes

To remove metals from the waste water generally requires ‘‘adsorptive filtration’’. The mechanism of this technique depends on the attachment processes between a heavy metals and absorber materials which are used to coat a porous sorbant such as PolyHIPE. This modification layer gives a chance to remove the cation or anion from the liquid depending on type of absorbed materials (Benjamin et al., 1996, Lo et al., 1997, Huang and Liu, 1997, Lo and Chen, 1997). There are many parameters that have effect on this process as listed below.

2.6.1. Contact Time

Normally, with an increase in the contact time between heavy metals and the absorber, the removal efficiency would be increased. It was observed that, the removal of nickel from waste water increases with an increase in the contact time up to 60min. With increasing contact time above this a dynamic equilibrium process occurred, so the removal then goes very slowly (Varma et al., 2013).

In addition to that, it was reported that the removal processes do not necessarily need a long contact time if the adsorbant has enough reaction efficiency. For instance, by using microalgae the concentration of the nickel decreased from 30 to 0.9 mg/l in only 5min contact time which represented approximately 97% Ni removal efficiency and after 90 min the remaining concentration was reduced to 0.4 mg/l(Roy et al., 1993). With another competitive metal like zinc in the water the ratio of removal was at 98% for Ni and Zn. High removal efficiency might be attributed to high surface area for this adsorbate and high binding ability with these heavy metals (Roy et al., 1993). But, after continuing to increase the contact time from 90 up to 300 min there were no changes in the amount of nickel which was removed from the waste water (Chong et al., 2000). This suggests saturation of all the available removal sites.

The removal efficiency changes with changing the metals, so not all the heavy metals have the same removal efficiency at the same contact time for a given adsorbant. For instance, it was found by supplying different metals to the filtration process that, after 50min the adsorption capacities were 2.35 mg/g (94.0%), 2.41 mg/g (96.41%), and 2.39 mg/g (95.6%), respectively for Ni^{2+} , Cu^{2+} , and Zn^{2+} while in the case of Cr^{3+} the adsorption capacity was (2.38 mg/g; 95.2%) after 70-min (Taha, 2006).

2.6.2. The influence of the pH

The pH is considered one of the most important factors which influences the removal processes for heavy metals from waste water. For instance, the removal processes of cadmium and nickel were better at pH > 6 than pH <4 because after pH 6 hydrolysis of nickel and cadmium happen (Gupta et al., 2003). Furthermore, changing the pH of the solution may lead to the creation of new compounds such as nickel hydroxide at pH 8.2, which leads to a reduction in removal efficiency (Gupta et al., 2003). In addition to that, changing the pH of the solution changes the surface charges of the adsorbant and determines the point of zero charge (PZC). For instance, pure iron oxide, whether crystalline or not, has PZC between pH7 and pH9 (Benjamin et al., 1996). At a higher pH than this value, iron oxides are anionic [$Fe(OH)_4^-$] and can be used for adsorbing cationic metals, while below that value it present as cationic ($Fe(OH)^{2+}$). The pH value not only has effect on the material which is used in the removing process, but also it has influence on the behaviour of the heavy metal itself in the solution, because heavy metals can have a different charge with different pH range. For example, arsenate As (V) at pH 3 it is available in anionic forms, while after pH 7 it is cationic (Katsoyiannis and Zouboulis, 2002)

Furthermore, the removal efficiency changes with changing the pH. It was found that, nickel can be removed by iron oxide at pH 7 (Malandrino et al., 2006), but it was also reported that, nickel removal from waste water increases with increasing the pH of the solution (Rajapaksha et al., 2012). Also, gibbsite, laterite and goethite showed an increase in nickel adsorption with increasing the pH from 4.0 to 6.8 and the increase was by 4-5 times when the pH increased from 6 to 8 (Rajapaksha et al., 2012).

Additionally, it was reported that the removal efficiency depends on the structure of the material used as adsorbant in addition to the pH value. For instance, at pH range from 1-8 the adsorption for many heavy metals such as As, Cd, Cr, Co, Cu, Fe, Pb, Mn, Ni and Zn by montmorillonite was better than kaolinite (Bhattacharyya and Gupta, 2008). And the same behaviour was shown with goethite and hematite (Beukes et al., 2000). Additionally, Basaldella et al. (2007), found that the pH has influence on the adsorption process for many heavy metals. For instance Cr (III)

was removed by using NaA zeolite at neutral pH, while Barakat (2008) used 4A zeolite to remove Cu (II) and Zn (II) at neutral and alkaline pH . In another study Nah et al. (2006) modified zeolite with iron oxide to remove Pb (II) ion from waste water and it showed excellent adsorption capacity at the pH range between 5 and 11. Pb(II), Cu(II), and Zn(II) can be removed by calcined phosphate at pH5 (Aklil et al., 2004).

Adsorption and precipitation processes may happen at high pH at the same time. For nickel in high pH solution it was found that there may be the formation of nickel hydroxide ($Ni(OH)_2$). But it was reported for nickel removal that, at very high pH close to 9.5, the amount of nickel in a very dilute solution was not enough for the precipitation process, because the precipitation process required a certain concentration of metal (Arai, 2008, Eick and Fendorf, 1998, Rajapaksha et al., 2012). It was reported that copper at pH between 6.2–6.8 forms copper hydroxide $Cu(OH)_2$, when potato peels were used to remove Cu (II) from waste water, therefore the results showed a reduction in removal efficiency at a pH value more than 6.0 due to the this (Nguyen et al., 2013).

Before the precipitation process, it was found that the removal efficacy increases with increasing the pH. The reason for this increase in the removal of nickel at a high pH was due to reducing the competition between H^+ and the active sites, which have negative or neutral charge, when using clinoptilolite to remove nickel. The removal efficiency increased with increasing the pH from 6 to 8 (Ismail et al., 2012). It was also found that the surface at pH 6 was full of H^+ ions which participate in the ion exchange process between the active site and the Ni^{2+}. Basically increasing the pH leads to an increase in the surface acidification, as a result of proton release from available active sites (Adams et al.).

In addition to that, the pH could determine the mobility of the heavy metals in the solution. For example, nickel that came from ground water after rain was more soluble because this heavy metal normally has more mobility at low pH (less than 6.5 (Prows et al., 2003)). Other heavy metals like iron, copper, zinc, manganese, and cobalt behave similarly at low pH (Dean et al., 1972). Furthermore it was argued that, sometimes many parameters could be changed with pH such as contact time and solution composition to reach the better adsorption conditions. For instance, when grape residue was used as an adsorbant for nickel and copper from waste water which came from wine production the results after 60 min contact time showed that the pH between 5.5–6.0 was effective and gave the best adsorption behaviour (Villaescusa et al., 2004).

In the binary system when more than one metal needs to be removed from waste water, the removal efficiency will change approximately in the same way as with a single metal system.

It was reported that, the absorption of both nickel and copper (the concentration was 10mg/l) changed with changing the value of pH, when the uptake was zero at pH 1 and then increased up to 78% at pH 5.5. It was estimated that, this increment comes from reducing the concentration of H^+ with increasing the pH which basically means less competition between the these metals and the hydrogen ions (Villaescusa et al., 2004). When membrane technology was used for water purification, pH had no effect on the membrane removal efficiency until nickel hydroxide was formed at pH 9 (Davidson, 2010).

2.6.3. Effect of Agitation Speed

In order to get good contact between the adsorbant and the liquid and ensure that the mass transport from the liquid to the surface is optimised it can be necessary to agitate the system to mix the adsorbant particles in the solution. This can be achieved by stirring or shaking or other mechanical methods or controlling slow in the filter system. The Agitation speed has huge effect on the contact time between the adsorbent and the heavy metals in solution, so the removal efficiency increases with increasing rate. For instance, it was found that, the removal efficiency was increased by 10% when the agitation (stirring) speed increased from 250 to 500rpm, when the concentration of nickel was 25mg/l and the contact time was 60 min. This increase was attributed to an increase in the collision between the adsorbant and the Ni (II) ions. After filtration reaches saturation the removal rate became constant because of steady-state movement of the heavy metal (Ni^{++}) between the solution and the active sites (Ismail et al., 2012). In the same study, it was reported that flow rate is another factor which is important to determine the removal capacity, where it was reported that increasing flow rate increased the time to treat the standard solution to the same extent. This decrease was attributed to decreasing the time of contact between the adsorbant and the ions in the solution. For instance, it was reported that increasing flow rate from 240 ml/h to 500 ml/h leads to a decrease in the removal efficiency from 80 to 60% (Ismail et al., 2014).

2.2.4. Shaking Time

In some adsorption filtration studies a fixed amount of asdorbant is added to a flask with a fixed amount of standard solution to be treated and the closed flask is then shaken to enhance contact. Sometimes the effect of the shaking time and the pH is studied together and it gives better results when both are considered. It was found that, the shaking process helped to remove 1.42 mg/g (97.7%), 1.40 mg/g (93.0%), 1.41 mg/g (94.0%), and 1.43 mg/g (95.3%), of Ni^{2+}, Cr^{3+}, Cu^{2+}, and Zn^{2+} from solution respectively by using fly ash (Taha, 2006).The efficiency was larger than in the absence of shaking in all cases.

2.4.5. Initial Concentration and Competitive Adsorption Reactions

The initial concentration of the metal in the waste water may determine the removal efficiency for a heavy ions. It was found that the arsenic removal process was faster when its concentration was less than 50 mg/l compared with higher concentrations (200 mg/l), when the experiment was done at pH 5.0. In addition, many anionic and cationic metals may exist in the waste water with heavy metals, which may reduce the effectiveness of the adsorption process by interaction with available adsorption sites. For instance, many anionic and cationic species such as phosphates, carbonates, chlorides and nitrates are present in waste water which interact with adsorption sites and reduce the removal efficiency.

Initial concentration is considered as the driving force for the transportation of the heavy metals from the standard solution to the active sites (Sahmoune et al., 2011, Taha et al., 2011). It was found that, the adsorption capacity increased with an increase in initial concentration (Kumar et al., 2012). But, in some cases the removal efficiency decreases with increasing the initial concentration, because the active sites of the adsorbant saturated quickly. Additionally, it was reported that the decrease of removal efficiency was because the transport process of heavy metals to the surface from the solution was slow (Kumar et al., 2012).

It was found that a concentration of phosphates in the range 20–50 mg/l has huge effect on the removal processes for As (V) from ground water when iron hydroxides were used as the adsorbant, due to making surface complexes with the hydroxyl groups (Meng et al., 2001). Phosphate concentrations at more than 200 μg/l show a negative effect on the removal efficiency for arsenic from waste water, but when their concentration was low, the removal efficiency was not changed. Carbonates, chlorides and nitrates showed a strong competition with arsenic toward the active site (Katsoyiannis and Zouboulis, 2002). Furthermore organic materials such as humic substances (the major organic components of soils) may also exist in waste water and are considered a challenge for the removal process. It was found that the influence of humic substances was high at the pH range of 4-6, while at pH over 8 it was negligible (Boujelben et al., 2009).

In another study the effect of competitive metals on removal efficiency of nickel has been studied by using range of heavy metal ions (chromium, mercury and lead) in the form of sulphates, fluorides and arsenates with different concentration in the range 5 to 500 mg/l. It was reported that, the removal efficiency decreased with increasing the sulphate concentration up to 20 mg/l, after that concentration the increase does not show any effect on the removal

process. Until the availability of fluoride ions with 200mg/l concentration the nickel removal efficiency remains the same at about 93%.

In nickel removal from a mixed ion contaminated water increasing the concentration of lead from 5 to 100mg/l lead to a decreasing of the removal efficiency. The removal processes totally stopped when the concentration of lead was 100 mg/l (Pandey et al., 2007). It was also reported that the removal efficiency was higher when using a single metal than when using many metals together; using a standard solution containing nickel and zinc gave less removal efficiency than single ion systems at the same concentration. However, the overall removal efficiency for all these metals together was higher than the single metal alone; also in comparison the removal efficiency for nickel was higher than for zinc and copper. It was found that copper hydroxide generation was the reason for poor copper removal (Vengris et al., 2001).

Table 2-1. Physical and chemical properties of well water, (Meng et al., 2001)

	Well water	Filtered water
As (µg/L)	158	12
pH	7.4	6.9
Turbidity (ntu)	0.6	0.15
Total alkalinity (mg CaCO3/L)	234	135
Total hardness (mg CaCO3/L)	210	207
Electrical conductivity (µs)	496	531
Residual chlorine (mg/L)	0	0.5
Fe (mg/L)	4.1	0.13
Mn (mg/L)	0.26	0.25
Mg (mg/L)	34.8	34.7
Ca (mg/L)	26.6	25.6
Na (mg/L)	14.5	13.7
K (mg/L)	26.5	20.6
Cl (mg/L)	30	30
I (mg/L)	0.68	0.11
SO4 (mg/L)	12	60
PO4 (mg-P/L)	2.7	0.04
SiO2 (mg-Si/L)	14.5	13.1
F (mg/L)	<0.1	<0.1

These competitive metals may interact with the adsorbant in different ways. For instance, many researchers reported that there are complexes that form between Fe (III) and phosphates (PO_4^{-3} or HPO_4^{-2}) depending on the ratio [OH^-]/ [PO_4^{-3}] or [HPO_4^{-2}] when iron oxide was used to remove arsenate and phosphates in a competitive manner. It was reported that removal efficiency was reduced by decreasing the pH due to increasing the possibility for phosphate entering in the sheath of the Fe(III) ion (Stumm and Morgan, 1981). Bicarbonates also had adverse effects on the removal processes by reducing the adsorption process when iron oxide was used as adsorbant (Pirnie, 1999). Since phosphates, carbonates, chlorides and nitrates are normally available in ground water, together with the nickel, they may also have the effect on the removal efficiency, however, the concentration of these compounds in drinking water should be not more than the concentrations shown in Table 2-1. (Meng et al., 2001).

The concentrations of these metals are not the same in different places around the world. For instance nickel concentration is different between different places, groundwater, seawater and surface water (Andersen et al., 1996). With change of pH the concentration of nickel changes as well, at pH < 6.2, but the nickel concentration was higher in groundwater at ~980μg /l in most cases. However, less than 1 to 87 μg /l nickel concentration was found in urban storm water (Tchounwou et al., 2012).

Changing the removal efficiency sometimes comes from chemical blocking by some competitive chemical groups. For example, it was reported that the reduction in the removal efficiency for many metals such as Cd (II), Cu (II), and Zn (II) by 32.8%, 58.5% and 65.3% respectively occurs because of chemical blocking after pre-treatment by carboxyl groups. The reduction was attributed to OH groups which came from alkaline pre-treatments (Nguyen et al., 2013). This adverse effect of OH groups is because they also participate in the removal process by making bonds with the heavy metals but do not trap them on the surface dues to the solubility of metal hydroxides at the operating pH. It was reported by Kumar et al. (2012) that carboxyl and hydroxyl groups which are available in cashew nut shells play an important role in removing Cd (II) from waste water. Also, it was reported by (Lasheen et al., 2012) that, carboxylic groups participated in removing Pb (II) using orange peel after a chemical modification process. Furthermore, FTIR results indicated the involvement of functional groups such as hydroxyl, amine, carboxyl, and carbonyl in the removal process for nickel Ni (II) using Caesalpinia bonducella seed powder (Gutha et al., 2011). Orange peel after grafted polymerization was used as an adsorbant to remove heavy metals by chemical groups such as carboxyl and hydroxyl in the removal process (Feng et al., 2011).

The behaviour of the heavy metal itself has an effect on the removal efficiency. For instance, at pH between 4-8 the removal capacity for solutions containing the same concentrations of nickel, copper and zinc was about 75, 150 and 300 mg/l respectively, and the results show that these metals are completely removed after 20, 40 and 50 minutes, whilst chromium removal takes a longer time which was about 80 min. Other metals reached an acceptable limit after 60 min (Dermentzis et al., 2011). Eventually, the initial metal concentration determines the speed of uptake which is necessary to deliver discharge concentration. For instance, it was reported that 40 min was enough to remove Cu (II) ions while removing Ni (II) ions takes 400 minutes when the pH of the solution was between (4 -5.5) (O'Connell et al., 2008).

2.6.4. Effect of Adsorbant Mass

Another factor which has significant effect on the filtration processes is the amount of adsorbant which is used during the filtration process, also called the adsorption mass. Normally the removal efficiency increases with increasing the adsorption mass. This is because there is an excess of easily accessible adsorption sites when the adsorbant mass is high. For instance, it was found that, the nickel removal efficiency increases with increasing the mass of the adsorbate from 68 to 72% at constant pH. Removal efficiency increases when the concentration of adsorbant poly(acrylic acid sodium salt) (PAANa) is high and the concentration of nickel is low, which may be attributed to increasing the number of active sites for adsorption compared to the amount of material to be removed (Davidson, 2010). The same behaviour was shown when cashew nut shell was used to remove coper from waste water. Increasing the amount of the adsorbant leads to a rapid increase in the removal efficiency of Cd (II); maximum removal percentage was at 3 g/ l, and it was reported this increase may be due to a high number of active sites achieved at a high amount of adsorbant. In contrast Boota et al. (2009) observed a decrease in the removal efficiency of Cu(II) and Zn(II) with increasing the amount of Lignocellulosic fibre, which may be attributed to decreasing the surface area and reducing the number of active adsorbant sites.

2.6.5. Effect of Temperature

The temperature of the solution which is used during the filtration process plays a significant role in determining the amount of the heavy metals which are removed from waste water, because it determines many parameters such as the diffusion rate for metal ions in the solution and also the solubility of these ions (Park et al., 2010). In addition Sahmoune et al. (2011) found that, the functional group activity of the adsorbant depends on the temperature. For instance,

when (Zea mays) stalk sponge was used as an adsorbant to remove Pb (II) and Cd (II) from waste water, the removal efficiency increased by 1.1 to 1.8 times when the temperature increased by from 20 ^{o}C to 40 ^{o}C (García-Rosales and Colín-Cruz, 2010). The same behaviour was observed by using watermelon shell to remove Cu (II) from waste water (Banerjee et al., 2012). This increase was attributed to a reduced thickness of boundary layer which surrounds the absorbant (Nguyen et al., 2013). Also, it was reported that when the adsorption capacity increases with increasing temperature, this may be attributed to the endothermic behaviour of the adsorption process (Gupta et al., 2003).

2.6.6. The Amount of Iron Hydroxides Coated on the Surface

Iron oxide is considered as one of the most important materials that is used as an adsorbant for removing heavy metals (Boujelben et al., 2009). Its concentration when used through the coating method is considered an important factor which has influence on heavy metal removal efficiency. It was found that the removal efficiency increases by increasing the amount of iron oxides in the coating layer (Meng et al., 2001). PolyHIPE was used as a host for iron oxide due to its highly connected porous structure, so iron oxide has the opportunity to enter to the internal structure. As a result of the coating thickness increase the removal efficiency increased (Hering et al., 1997).

2.6.7. Effect of Surface Area

Increasing the surface area of the adsorbant leads to enhanced adsorption efficiency due to reducing the competition between heavy metals towards the active sites by increasing surface site numbers. For instance, by using natural clay to remove many heavy metals such as copper, nickel and zinc, using a hydrochloric acid exfoliation treatment increased the uptake capacity of the adsorbant for nickel, copper due to an increase in the surface area (Vengris et al., 2001).

2.7. Regeneration

Regeneration is the reverse process in which the heavy metals are removed from an adsorbant after use. This is often achieved by changing the pH of the solution flowing past the adsorbant (Brown et al., 2000). The reusability test gives an estimation for how much metal was removed and how much can be reclaimed. This process takes place after the solution concentration has been reduced to the breakthrough limit (acceptable limit by the World Health Organization). For instance a strongly alkaline solution (pH>10) was used in the regeneration process for arsenic from iron oxide which does not dissolve at that pH but its surface charge is changed. In

this situation, the arsenic could separate from the iron oxides. This process had to be repeated five times before the regeneration process was completely finished. In addition to that, different solutions like HCl, HNO_3, CH_3COOH, NaOH were used for regeneration processes. HCl and HNO_3 were more efficient than the other solvents such as acetic acid and sodium hydroxide (Katsoyiannis and Zouboulis, 2002).

It was found that the value of pH which should be used for the regeneration process depends on the chemical composition of the adsorbant. For instance, it was reported that pH1 was enough to regenerate the cellulose-g-GMA-imidazole from different ions with 100% recovery. Increasing the pH up to 2 reduced the recovery of these metals to near 30%, and this behaviour continued with increasing the pH value. Furthermore, the adsorbant could be reused but it showed lower removal efficiency to re-adsorb the metal ions from waste water (O'Connell et al., 2008). It is clear that removing all metal from the adsobant after regeneration is difficult and re-used material is not as effective at metal ion removal.

Summarizing, there are two reasons for the regeneration processes, firstly to reuse the adsorbant and secondly to extract the heavy metal after a purification processes for use in different applications, for instance nickel could be used in electroplating and storage batteries (Kadirvelu et al., 2001a, Meena et al., 2005).

2.8. Point of Zero Charge (PZC)

The Point Zero charge determines the surface adsorption behaviour of materials. For instance, pure iron oxide, whether crystalline or non-crystalline, has zero surface charge at pH around 7 to 9 (Wilkie and Hering, 1996, Benjamin et al., 1996). Over these PZC values, iron oxides are present in the singly-charged anionic form ($Fe(OH)_4^-$) and hence inappropriate for adsorbing anionic components but attractive to cations (Katsoyiannis and Zouboulis, 2002). It was reported that iron oxide surface complexes could make bonds with arsenic at high pH (Edwards, 1994, Dzombak and Morel, 1990). Furthermore, it was observed that precipitation interaction takes place between the iron(III) and nickel(Il) hydroxides to produce nickel ferrite $NiFe_2O_4$ at high pH, when iron oxide was in the anionic form (Pandey et al., 2007).

2.9. Summary

Absorbant materials can remove heavy metals by direct adsorption or ion exchange and can be considered as cheap, high capacity adsorbants if based on a cheap substrate material. PolyHIPEs have open structure and high surface area and can be processed relatively inexpensively and could therefore be good candidate adsorbant materials. They can also be functionalized for good removal for the heavy metals from waste water. There are many parameters like pH and temperature that can be changed to enhance the removal process. Additionally, regeneration processes can be applied to the adsorbant after the filtration process to recover the metal for reuse and regenerate the filter so it can be used it again. Changing the processing of the material to produce a polyHIPE with better properties and morphology for filtration is thus the goal of this project. The experimental approaches used to achieve this are presented in the next chapter.

3. Experimental Methods

In this chapter the methods which were used to prepare the PolyHIPE samples and the processes take place using theses sample such as sulphonation with sulphuric acid and coating with iron oxide are explained. Techniques that were used to determine the PolyHIPE surface morphology and composition are then introduced. The filtration test procedures and the techniques used to measure the concentration of heavy metals which were used for the filtration process are then introduced. Finally, how to make the regeneration process and measure the zero of point charge iron oxide to assess its suitability as an adsorbant is explained.

3.1. Sample Preparation

PolyHIPEs have been prepared using a method described in a previous publication (Akay et al., 2005b). The PolyHIPE were prepared by mixing an aqueous phase and an oil phase each with several constituents (Figure 3-1):

•Aqueous phase: 1% potassium persulphate as free radical initiator and 5% sulphuric acid for in situ sulphonation.

• Oil phase: 76w/w% styrene, 14w/w% divinylbenzene (DVB) crosslinker, 10w/w% sorbitan monolete (Span 80) non-ionic surfactant with low HLB (hydrophilic-lipophilic balance). This is used to prevent the phase separation process between the oil and aqueous phases (Hayward et al., 2013).

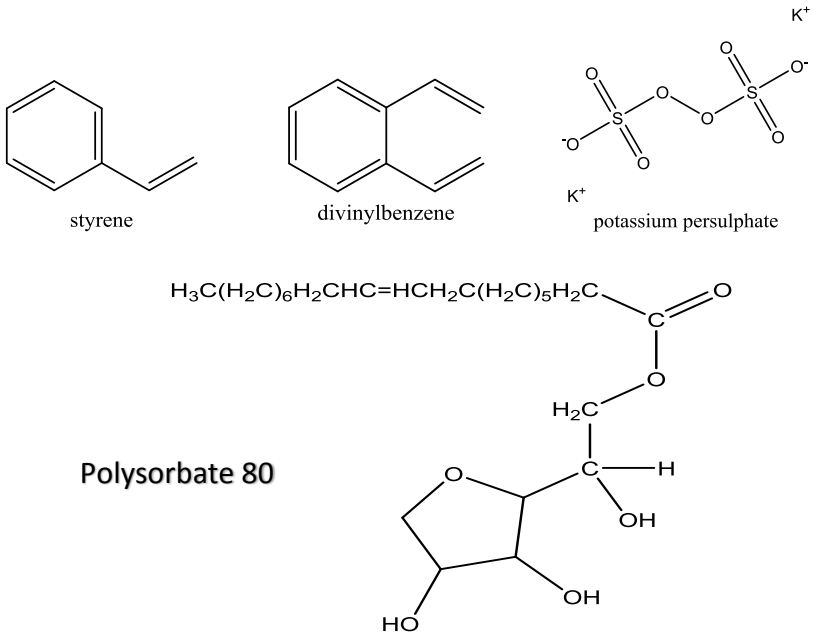

Figure 3-1. The chemical structure of the PolyHIPE components.

To make the HIP the oil phase was added to the tank of a stirred tank reactor as shown in Figure 3-2 and the stirrer was started at a stirrer speed of 300 rpm. The aqueous phase was then slowly added to the oil phase using a peristaltic pump under continuous stirring. After this dosing was complete the HIPE was subjected to various mixing times (10, 15, 20, 25, 30 minutes. Then the emulsion was transferred to a container (a falcon tube) of 50 ml capacity with a diameter of 2.6 cm. Subsequently, the container was placed inside an oven and the temperature was increased to 60 °C. The polymerization of the oil phase then took place overnight. Samples of 5-7 mm thickness as shown in Figure 3-3, were cut out of the monolith removed from the tube and they were dried resting on a paper towel overnight in a fume cupboard.

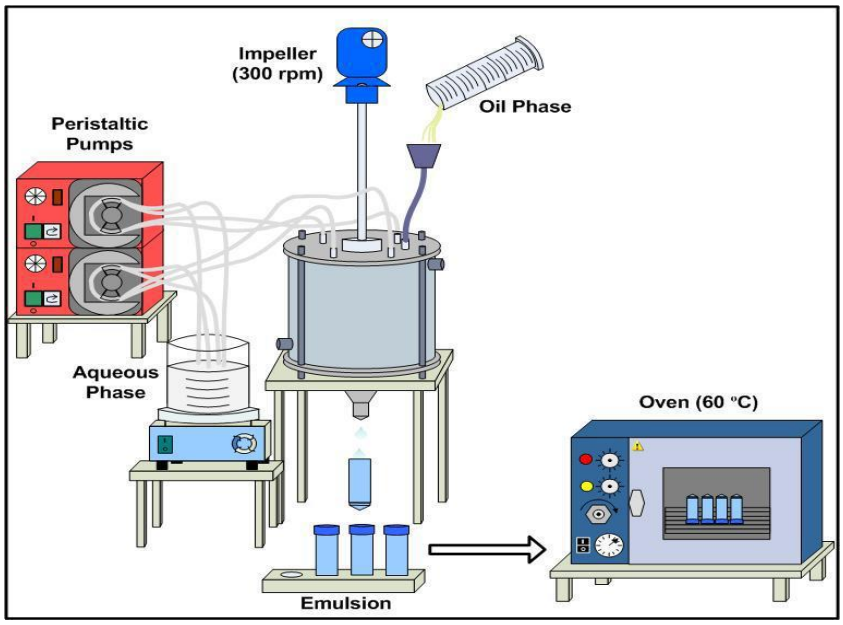

Figure 3-2. Schematic diagram of the apparatus used for PHP preparation.

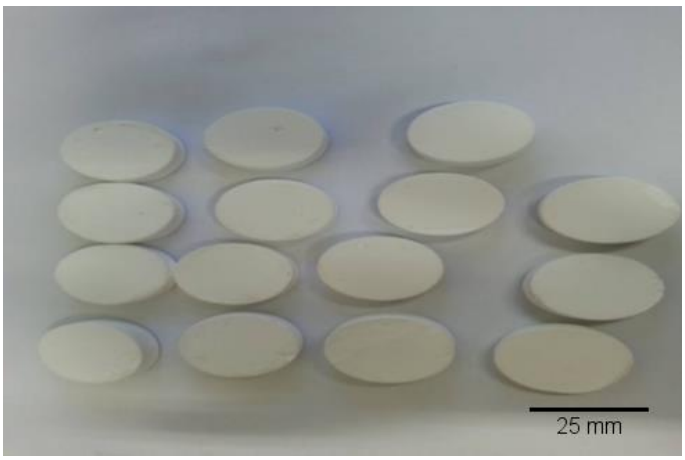

Figure 3-3. Disc samples after polymerization

3.2. Washing Process

The final step in the preparation of the PolyHIPEs was washing in order to release the surfactant and residual aqueous phase. This is necessary because they have a negative effect on the windows available in the PolyHIPEs reducing the interconnecting pores. The samples were washed using a soxhlet as shown in Figure 3-4, with 2-propanol solvent and distilled water for 3 hours. After that the samples were placed in a fume cupboard overnight to dry. After drying the samples were placed inside an oven at 60 °C to drive off any remaining water or solvent (Hasan, 2013).

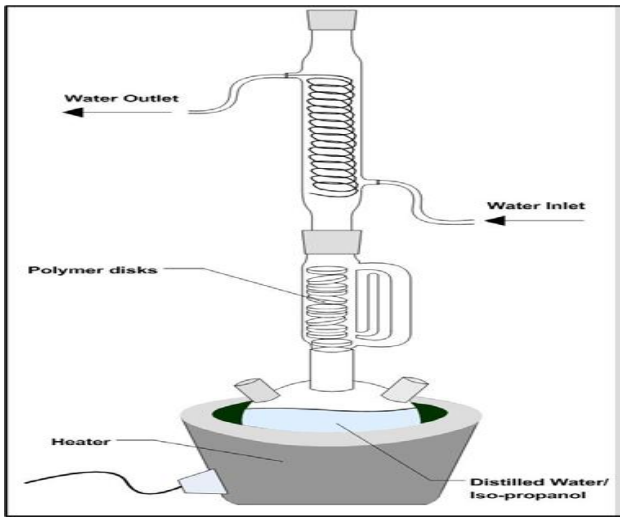

Figure 3-4. Schematic diagram of the socxhlet used for polymer washing process.

3.3. The Sulphonation Process

The sulphonation process includes in soaking the samples in concentrated sulphuric acid (H_2SO_4 from Sigma Aldrich), for three hours followed by treatment of the soaked samples in a microwave oven for 60 seconds as shown in Figure 3-5. The samples were placed on the microwave platen and subjected to 15s bursts of microwave energy before being turned over and the process repeated. This was done four times. The samples were then washed with deionized water by using the soxhlet as shown in Figure 3-4 then dried in oven at 60 °C, Figure 3-6 show the PolyHIPE beads after sulphonation which were used during the filtration process

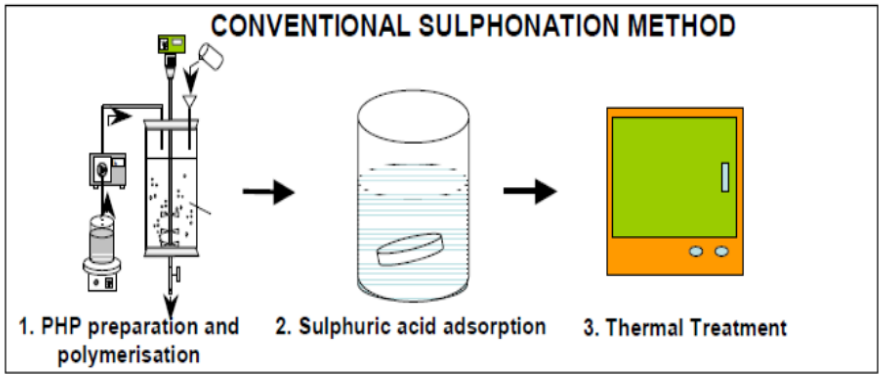

Figure 3-5. The mechanism of sulphonation process

Figure 3-6. The PolyHIPE beads after sulphonation process

3.4. Coated PolyHIPEs and Standard Solution Preparation

For pure adsorption studies poly HIPE was coated with iron oxide nanoparticles. The suspension of iron hydroxides (hydrous ferric oxides (HFO)) for the coating process was prepared by using Fe $(NO_3)_3.9H_2O$ (Merck) dissolved in diluted de-ionized water. The pH was adjusted to 5.0 by adding Na OH (1N) because ferric oxides were practically insoluble at this pH value (Hering et al., 1997, Katsoyiannis and Zouboulis, 2002) with continuous stirring to get a homogenous solution as shown in Figure 3-7(a). PolyHIPE was added to the solution in the form of beads which have diameters between 3-5mm. An overhead stirrer was used in order to avoid settling of the particles during the coating process (Figure 3-7(b)) which lasted for three hours to get a uniform coating layer. Then, these beads were washed with deionized water several times, to remove unattached iron oxide, then dried in an oven at 80°C for 6 hours. Figure 3-8 shows the PolyHIPE beads after the coating process with iron oxide.

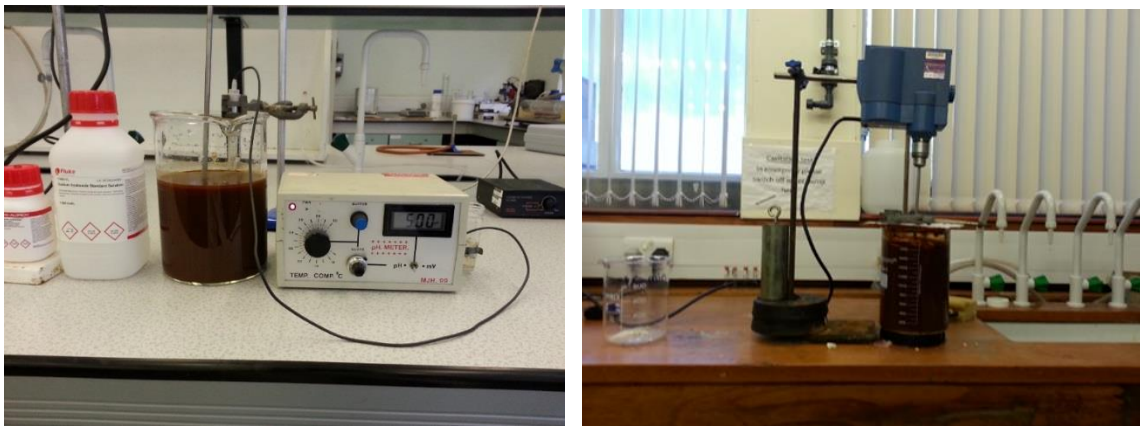

(a) *(b)*

Figure 3-7. Figures (a) refer to preparation the stock solution (b) refer to the coating processes

Figure 3-8. PolyHIPE beads after coating with iron oxide

3.5. Filtration

The filtration process (Figure 3-22) was done by passing a standard nickel solution through a plastic column which contains the PolyHIPE beads after coating with iron oxide or after sulphonation. The stock solutions of nickel used in the filtration processes had different concentration, (16, 100, 20 mg/l) after dissolving Ni $(NO_3)_2$. $2H_2O$ from Sigma Aldrich in doubly distilled water, while the copper chloride standard solution with 20 mg/l concentration was prepared by using copper sulphate. The pH of the solutions was adjusted by dropwise addition of sodium hydroxide (NaOH (1N)), or hydrochloric acid (HCl (1M)) solutions (Adeli et al., 2012).

3.3. Analytical Methods

3.3.1. Scanning Electron Microscopy (SEM)

Scanning electron microscopy (SEM) was used to investigate the morphology of the PolyHIPEs. The samples were coated with gold by using a Polaron e1500 Sputter Coater and then examined using a Philips Field Emission Gun (FEG) electron microscope. The SEM image is produced as a result for the interaction between an electron beam and the sample as shown in Figure 3-9. There are two kinds of interaction elastic and inelastic interactions. Elastic interaction takes place when electrons emitted by the electron gun are defected by the sample surface, as result of this process backscattered electrons (BSE) are generated. Inelastic interactions occur between the incident electrons and the sample electrons and atoms, when some of the incident electron energy transfers to sample electrons causing excitation of these electrons which form secondary electrons (SE). X-rays, Auger electrons, and cathodluminescence can also be generated by these interactions. (Zhou et al., 2006). The secondary signal was used to determine surface topography and quantitative compositional information was obtained from the x-rays generated. Schematic of the SEM structure Figure 3-9, when in the first part in the top there is electron gun which is used to generate the electrons and accelerate it to 0.1-0.3 keV by using Alignment coil. Then this electron beam is directed to the sample by electromagnetic lenses and apertures. High-vacuum is used to avoid any scattering for the electron beam by the air. The specimen stage, electron beam scanning coils, signal detection, and processing system are used to form the image for the sample.

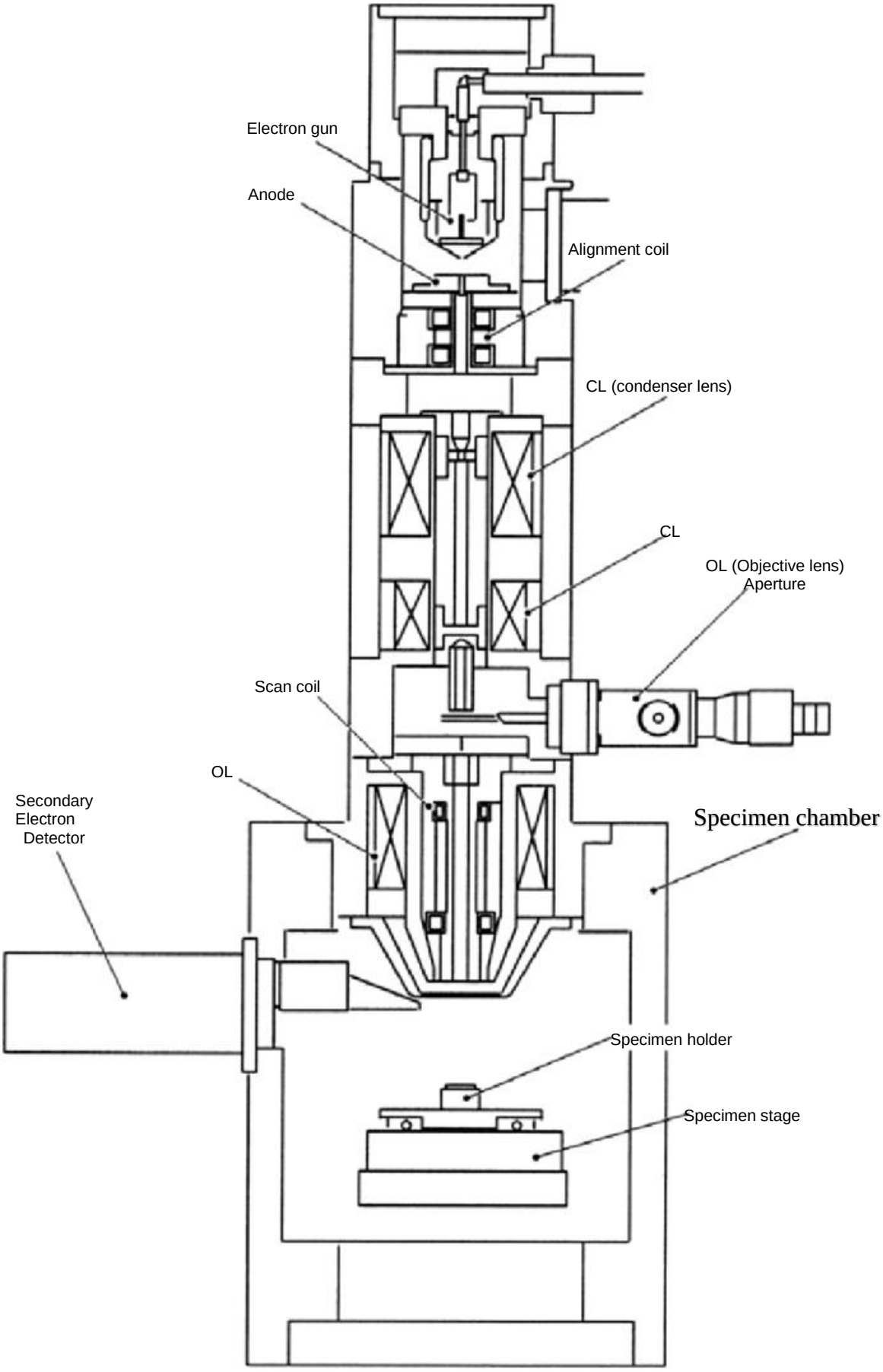

Figure 3-9. FEG-Philips electron microscope schematic (Zhou et al., 2006).

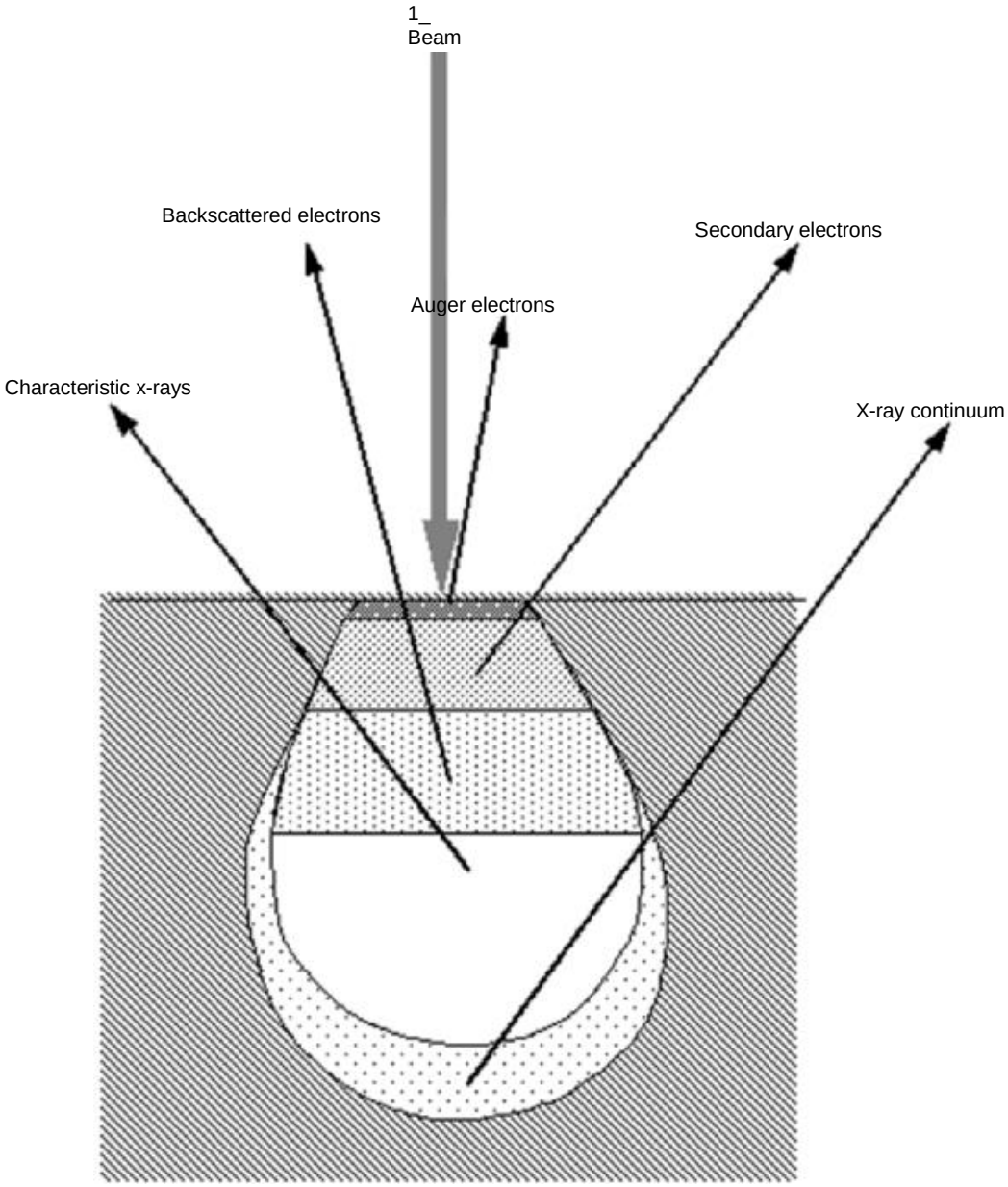

Figure 3-10: Diagram for scanning electron microscope (Zhou et al., 2006)

3.3.2. Fourier Transform Infrared Spectroscopy (FTIR)

The polymer materials and any contamination phases were identified by using FTIR spectroscopy. In this method infrared radiation penetrates the sample and part of the radiation will be adsorbed by the sample. FTIR gives information about the functional groups present in the structure. A Varian 800 FT-IR spectrometer system was used to analyse the samples Figure 3-11. The machine produces spectra between 4000 cm^{-1} and 400 cm^{-1} from solid, liquid and oil samples. In conventional IR spectroscopy a monochromatic radiation penetrates the sample through a slit which collects and focuses the light towards the sample. Fourier transform spectroscopy is a less intuitive way to obtain the same information. Rather than shining a monochromatic beam of light at the sample, this technique shines a beam containing many frequencies of light at once, and measures how much of that beam is absorbed by the sample. Next, the beam is modified to contain a different combination of frequencies, giving a second data point. This process is repeated many times. Afterward, a computer takes all this data and works backward to infer what the absorption is at each wavelength.

Polymers contain many functional groups, each infrared absorption bands correspond to a functional group, for instance different chemical bonds in a molecule have different vibrational states and each motion absorbs infrared light at a certain wavelength. This selectivity allows this technique to detect different chemical components in one sample. Groups with a strong dipole (i.e. with polar bonds) have strong IR absorption. With IR range between 4,000–1,000 cm^{-1}, there are two kinds of vibrations that can be detected, stretching vibration which depend on bond length and bending which depend on bond angles changing (Berthomieu and Hienerwadel, 2009).

Unknown samples can be identified by using FTIR, to measure the quantity of different components of their structure. This test can also generate a fingerprint on the sample and each fingerprint corresponding to a molecular structure. For thin layers an attenuated total reflectance (ATR) detector may be used - A Pike Technologies diamond crystal plate ATR detector is used in this machine. The ATR crystal reflects the IR beam to the sample many times to maximise the signal for analysis.

Figure 3-11. TIR which used in Fourier Transform Infrared Spectroscopy equipment,(Sarojam, 2010).

3.3.3. Compression Test

Compression tests were performed with a Tinius-Olsen mechanical testing machine (see Figure 3-12). Different tests for the materials could be done by using this machine such as tension, compression, flexure and shear but in this work compression tests have been used to assess the mechanical properties of the PolyHIPE materials. Parallel-sided disc shape samples (Figure 3-3) were cut from the monoliths polymerized in the falcon tubes and compressed between two steel plates. A 5kN load cell was used to measure compressive force which was converted to engineering stress by dividing by the original cross-sectional area of the sample. The displacement of the cross head was divided by the original sample thickness to determine engineering strain. This was done using the Tinius Olsen Horizon software. All tests were done at room temperature at a cross head displacement rate of 1mm/minute. Tests were stopped when the PolyHIPE had been compressed to about less than half its original thickness.

Figure 3-12. Tinius-Olsen mechanical testing equipment.

3.3.4. Surface Area and Pore Size

The surface area was determined using a Brunauer-Emmet-Teller (BET) machine (see Figure 3-13). This machine uses the gas adsorption technique to measure the surface area and the pore size distribution. Nitrogen gas is used as the adsorbate. The pore size distribution calculated from the adsorption or desorption data depends on the amount of the gas adsorbed. The machine measurement depends on the different Gas Sorption processes occurring and can determine the surface area and pore size in the range 0.4 to 200 nm. The BET machine makes a physical measurement for the sample surface structure by using nitrogen gas with known size that is adsorbed at constant temperature on the sample surface. Different amounts of nitrogen are added and an isotherm is formed from the amount of adsorbed gas and the sample pressure. This adsorption isotherm can be used to determine different surface properties by applying well-known standard analysis techniques – this is done in the control computer and in this study the BET analysis method was adopted throughout. Generally adsorbate molecules cover the sample surface during the adsorption process. These may be retained by physisorption or chemisorption processes and this leads to desorption at different pressures and hysteresis in the adsorption/desorption isotherm. Since nitrogen is inert to the surfaces tests here the analysis is based on the physisorption process having taken place in the calculation for the pore size and surface area.

Figure 3-13. BET machine used to measure the surface area and pore size.

3.3.5. Adsorption and Desorption Isotherm

The results obtained from the BET machine consist of adsorption and desorption isotherms. The adsorption data gives information about the surface area, while the pore size can be measured using adsorption or desorption data or both of them. At constant temperature the amount of nitrogen gas adsorbed increases with an increase in pressure of nitrogen and this determines the adsorption isotherm. Figure 3-14 shows the different types of isotherms that can be observed depending on the structure of the material; the isotherm is determined by plotting the volume adsorbed (cc/g) against relative pressure, where the relative pressure is determined by dividing the measured sample pressure by the saturation vapour pressure. The saturation vapour pressure is calculated from the boiling pressure of the adsorbing gas in the liquid form. The pressure in a closed sample vial was measured for each data point and this was used to determine the volume of gas adsorbed by the surface of the sample. The amount of adsorbed gas is calculated by subtracting the free space of the tube from the volume of gas which was dosed to the sample. The sample pressure divided by the saturation vapour pressure determines the relative pressure which is plotted on the x-axis (Hasan, 2013).

Pore size was calculated using the method BET as classified by the International Union of Pure and Applied Chemistry (IUPAC) (Sing, 1985):

(i.) Pores with dimeter up to 50 nm (0.05 μm) are called macropores;

(ii.) Pores with dimeter between 2 nm and 50 nm are called mesoporous;

(iii.) Pores with dimeter less than 2 nm are called micropores.

According to (Brunauer et al., 1940), there are five different types of isotherm for different solids depending on the van der Waals adsorption of gases Figure 3-14.

1. Oxygen on charcoal at -183 °C for Type I (Langmuir adsorption),
2. Nitrogen on iron catalysts at -195 °C for Type II (S-shaped/sigmoidal),
3. Bromine on silica gel at 79 °C for Type III,
4. Benzene on ferric oxide gel at 50 °C for Type IV,
5. And water vapour on charcoal at 100 °C for Type V.

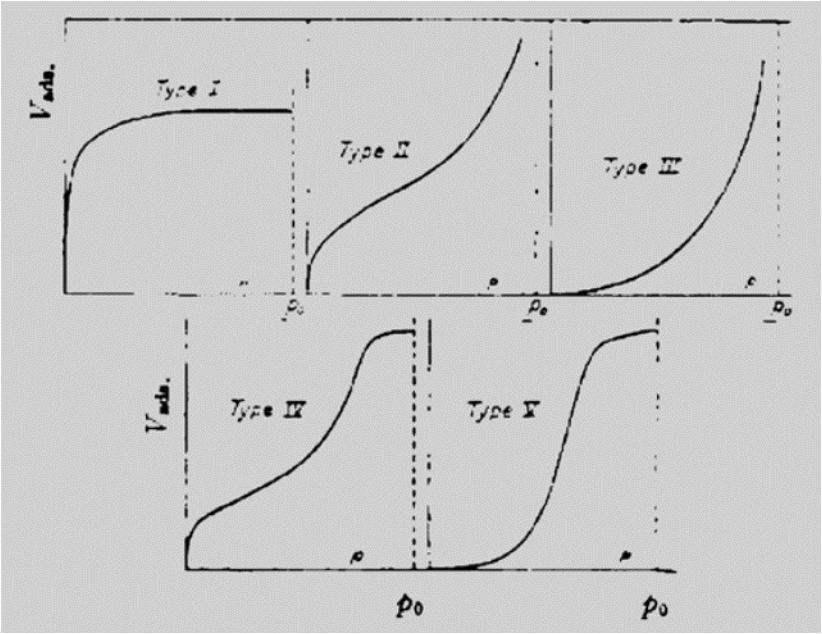

Figure 3-14. The isotherms are categorised into six different types, (Sing, 1985).

From this initial work it has been determined that physisorption isotherms and their hysteresis behaviour can be classified in six different groups as outlined below show in Figure 3-3-15 and Figure 3-16.

1- Type I isotherm is concave to the quantity of adsorbed gas (n^a) and p/p^o, and reaches a limiting value as $p/p^o \rightarrow 1$. This kind of curve is given by microporous solids which have small surface area such as activated carbons, molecular sieve zeolites and certain porous oxides. The limitation in uptake depends on micro pore volume instead of internal surface area.

2- Type II isotherm arising from non-porous or macroporous adsorbent refers to unrestricted monolayer and the multilayer growth of adsorbates, the linear line in the

middle after Point B is when multilayer coverage is observed. At point B there is complete monolayer coverage but multilayer coverage has just started.

3- The third type of isotherm III forms an increasing adsorption over its total range, so point B does not exist; it is not a common type but it appears with some materials such as nitrogen on polyethylene, in which isotherm consist on indistinct Point B and gradual curvature. Multilayer coverage occurs early in the adsorption isotherm.
4- Type IV isotherms contain a hysteresis loop related to capillary condensation in mesopores, but show limited uptake at high p/po. The main cause of this isotherm is monolayer-multilayer adsorption, as shown by mesoporous industrial adsorbents. The strength of interaction between the adsorbant and the absorbate is similar to that of adsorbates with each other.
5- V type isotherm is not common, and the interaction between adsorbant and adsorbate is considered weak, it appears in very porous adsorbants.
6- Type VI isotherms occur for multilayer adsorption on a non-porous surface. This involves layer by layer growth of adsorbates and relatively strong van der walls forces between the adsorbate and the surface compared to the adsorbate-adsorbate interactions.

Despite this, there are considerable numbers of isotherms that do not match any of the classifications listed above (Pendleton et al., 1997).

Not only do isotherms have different types, but the hysteresis also has variety. According to (Sing, 1985), there are four kinds which are H1, H2, H3 and H4. In mesoporous materials hysteresis is generated in multilayer physisorption and it is always related with capillary condensation. H1 and H4 are most common while H2 and H3 are represented intermediates as shown in Figure 3-16

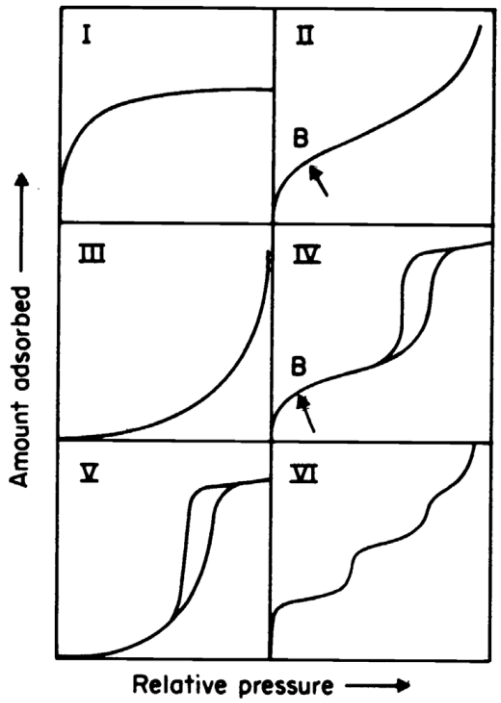

Figure 3-3-15. Types of physisorption isotherms. Adapted from (Sing, 1985).

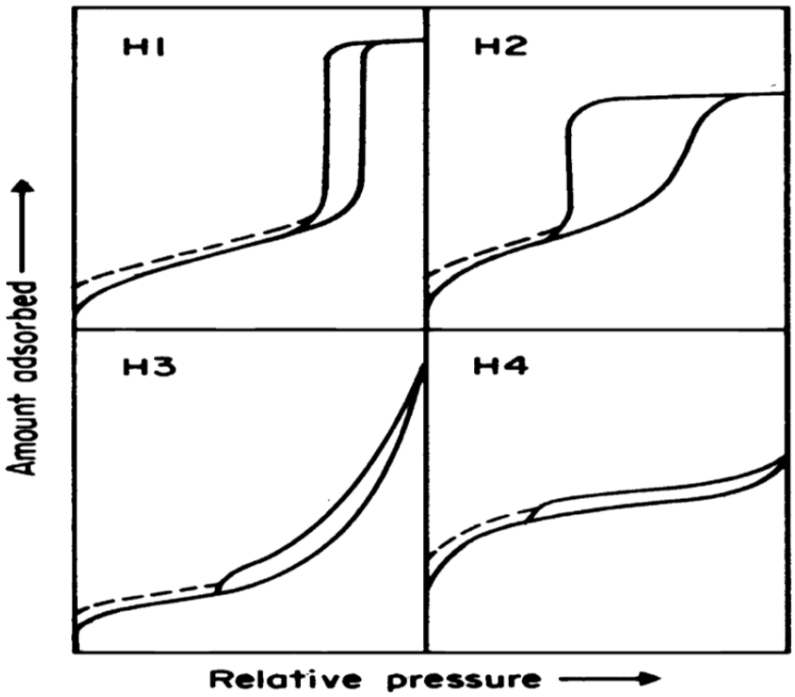

Figure 3-16. Hysteresis cycle for the adsorption desorption isotherm (Sing, 1985)

3.3.6. Inductively Coupled Plasma Mass Spectrometry

The concentration of nickel in solution was measured by using a PerkinElmer Optima™ 7300 DV ICP-OES instrument (PerkinElmer, Inc. Shelton, CT, USA) equipped with WinLab32™ for ICP Version 4.0 software for simultaneous measurement of all analytic wavelengths of interest as shown in Figure 3-17. The Optima 7300 DV was modified to accelerate analysis, by joining an SCD detector and an echelle optical system. The Optima 7300 DV has the ability to measure all elements simultaneously. The wavelength can be changed according to the element to detect. Different solutions (10, 20, 40, 80 and 100 mg/l) were used for the calibration curve. The instrument can be used to measure the concentration of metals in a solution down to parts per trillion, the metal analysis procedure has many steps such as ion generation, skimmer orifices, extraction, and transfer of the ions by ion optics to the detector. A low flow GemCone™ nebulizer and cyclonic spray chamber are used as a sample introduction unit in which the productivity is improved by providing high transfer for the sample to the plasma then good transfer to the ion optics and detector, the results are collected from the computer software (Agatemor and Beauchemin, 2011, Sarojam, 2010).

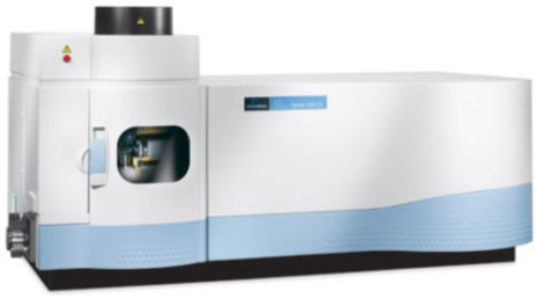

Figure 3-17. PerkinElmer Optima 7300 DV ICP-OES

3.3.7. XRF Spectrometry

The concentration of metals adsorbed onto the surface of PolyHIPEs were measured by x-ray fluorescence (XRF) spectroscopy since this is sensitive to concentrations which are less than 1 wt%. XRF spectrometers are robust elemental composition analysis instruments that are used in industry and research as positive materials identification, and concentration measurement tools. An XRF spectrometer provides simultaneous analysis of a wide range of elements, and can be used as either a qualitative screening tool or a fully quantitative elemental analysis instrument, as shown in Figure 3-18. The diagram in Figure 3-19 shows the electromagnetic radiation spectrum and the regions where excitation of a material by a radiation to produce a measurable signal may occur (Pete, 2010). When a sample is put under any type of radiation such as (X-rays, γ-rays, electrons, protons), its electrons adsorb some of the incident energy. As a result the excited electron can jump between energetic levels. When the radiation is removed the atom tries to lose this energy by another transition to its original orbital with emission of a photon of energy equal to the differences between the two states. The energy difference in most materials between such states will generate x-rays. XRF is a method which utilizes the properties of a photon detector, by detecting the radiation emitted from the sample for different wavelengths (Jenkins, 2000). The precise x-ray energy detached depends on the element which emitted the photon.

Spectro X-Lab 2000 with X-ray fluorescence analysis and a new x-ray tube was used to measure the concentration of the elements on the PolyHIPE surface after filtration with different standard solution of nickel and copper. This equipment has an X-Ray tube in which an electron beam is used to generate x-rays which impinge on the sample surface. After the interaction between the x-ray beam and the sample a spectral background forms, and it is collected by a detection system which is well off the axis of the original x-ray beam. This system has a semiconductor detector synthesised from Si (Li) and it has good sensitivity for low and high x-ray energies. This system linked with integrated software to analyse the results – standard samples with known concentration have been used to calibrate the x-ray intensities produced for all major elements.

Figure 3-18. Spectro X-lab 2000 *equipment*

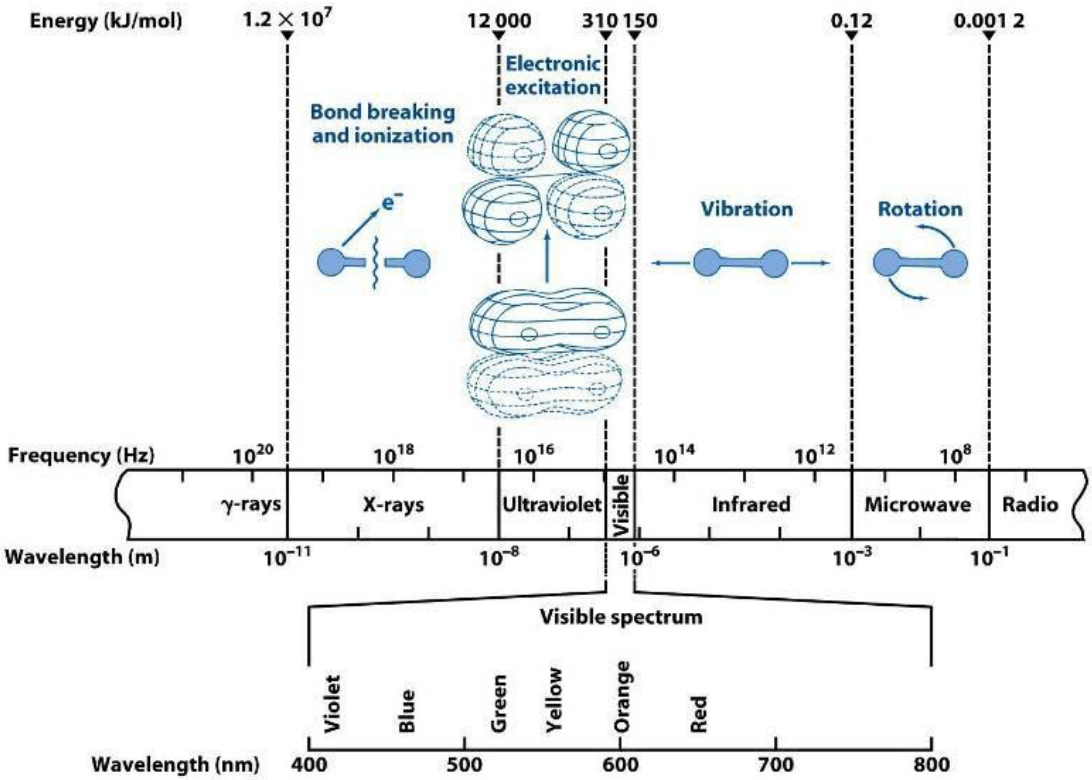

Figure 3-19. Light wavelength range

3.3.8. Ion Chromatography (IC)

Ion chromatography (IC) was used to measure the concentration of anionic species in the standard solutions in this study. The IC instrument used in this work was a Dionne ICS-1000 with an AS40 auto sampler. The column is an Ionpac AS14A, 4x250mm analytical column. The flow rate was 1ml/min and the eluent is an 8.0mM Na_2CO_3/1.0mM $NaHCO_3$ solution. Injection loop is 25µl. The ICS-1000 integrated system performs isocratic ion chromatography (IC) separations and was used to measure the concentration of anions in the solution after filtration and regeneration processes. This machine is linked with an Eluent Regeneration (RFIC-ER™system); a single eluent preparation was used to allow a continuous operation. Additionally, it has a dual-piston pump, thermally controlled conductivity cell, and auto suppression service (SRS 300 electrolytic suppressor). Automation gives full control and the data is collected and analysed by a control PC, as shown in Figure 3-20 below. The sample solution enters the machine by a valve injector, then the pumping system transfers the eluent and sample to a column, it passes through the column and then it is transferred to a detection system after a conversion process of the sample to corresponding acid or base The machine was calibrated by using Fluoride as a reference as shown in Figure 3-21 below.

In the solvent degasser the air and gases are removed from the solvent, then the solution is transferred to the pump to give uniform flow for the solution. The Injector is used to put the sample into the high pressure flow line in a narrow band. After that a filter is used to remove any particulate or chemical components which may be damage the machine. Due to influence of solution temperature on the resulting peaks, a Pre-Column Heat Exchanger is used to control the temperature of the solution, then the solution goes through a the compartment for the ion separation process and a Post-Column Heat Exchanger to cool down the solution before entering the detector as shown in Figure 3-20.

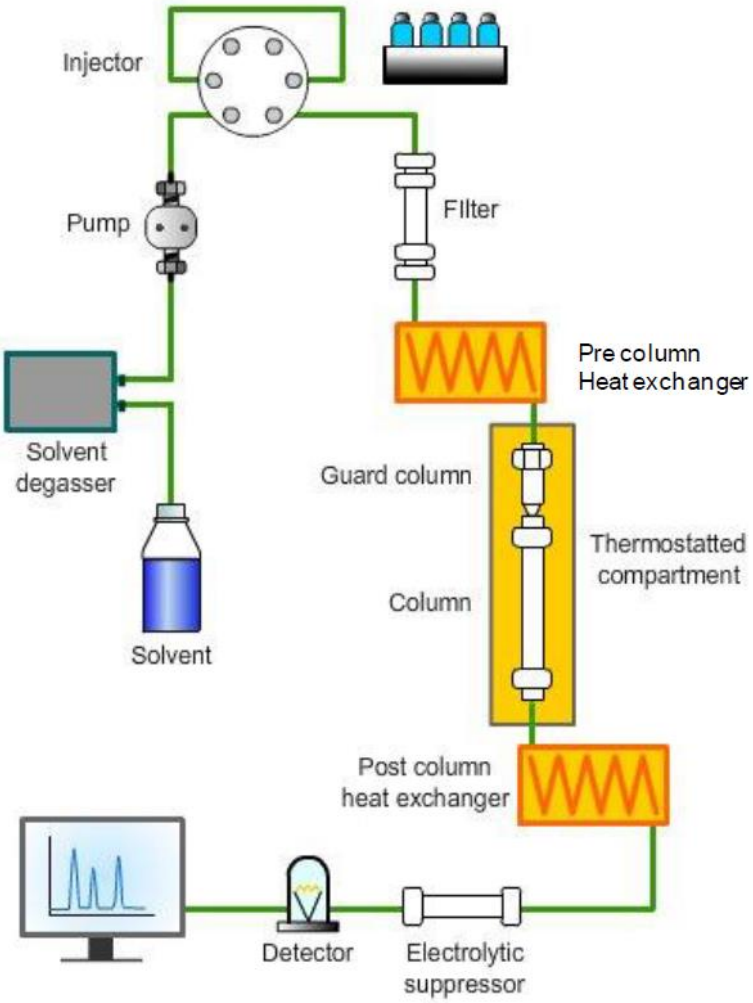

Figure 3-20. Ion Chromatography (IC) System.

Calibration Details	Fluoride					
Calibration Type	Lin			*Offset (C0)*		0.0000
Evaluation Type	Area			*Slope (C1)*		0.1183
Number of Calibration Points	1			*Curve (C2)*		0.0000
Number of disabled Calibration Points	0			*R-Square*		n.a.

ation Results	Fluoride					
Injection Name	Calibration Level	X Value ECD_1 Fluoride	Y Value ECD_1 Fluoride	Y Value ECD_1 Fluoride	Area µS*min ECD_1 Fluoride	Height µS ECD_1 Fluoride
Standard New	1	5.0000	0.5917	0.5917	0.592	1.554

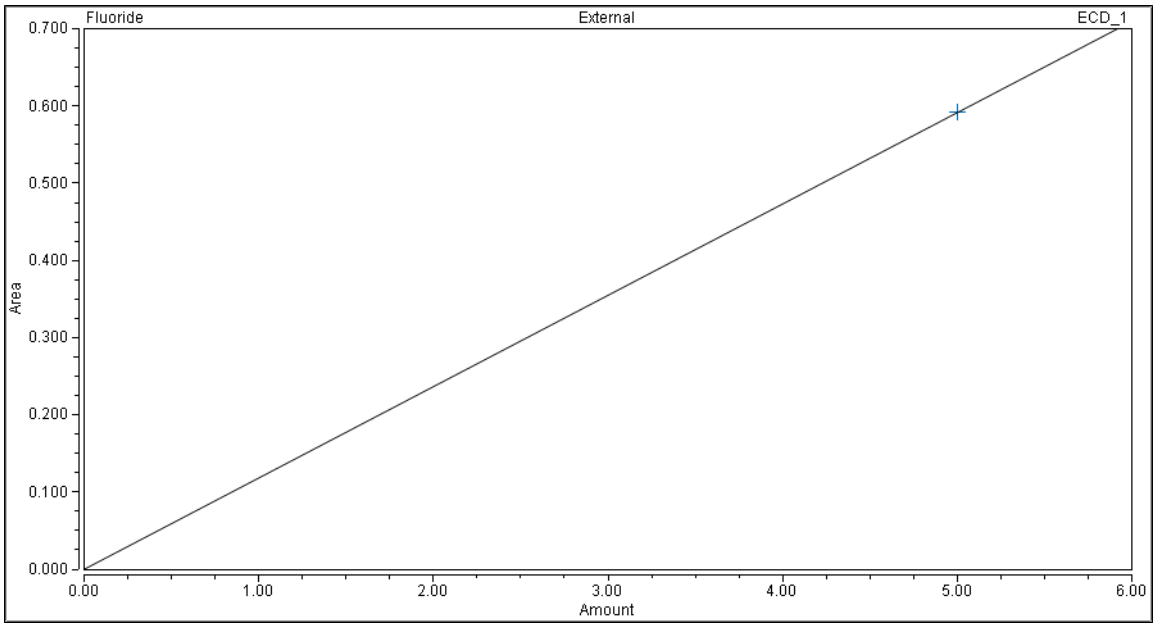

Figure 3-21. The fluoride calibration curve for the equipment.

3.4. Filtration Experiments

The adsorption experiment was done by using a plastic column 7 mm diameter and 70 mm length. PolyHIPE pellets, as shown in Figure 3-6 and Figure 3-8, were placed inside. Then the standard solutions (50 ml) of nickel and copper with different concentrations (20,100,160 ppm) were passed through the beads by using peristatic pump for 8 hours with speed (5 rpm). The outlet from the column was fed into the reservoir for the pump so the liquid was recirculated through the filter many times. Different pH was used during the filtration process (6, 7, 8 and 9). The removal efficiency of nickel and copper was determined by using Eq 3-1 (Adeli et al., 2012).

$$\text{Removal efficiency } (\%) = \frac{Ci - Cf}{Ci} \times 100 \qquad \text{Eq 3-1}$$

Ci: - Initial concentration of metal (mg/l)

Cf: - Final concentration of metal (mg/l).

Table 3-1. The procudure of the filtaration process with different parametres

Type of filtration	Sample	Reducibility	Temperature
Shaking when the samples in vertical direction	Both sample after sulphonation and samples coated with iron oxide	2 times	Room temperature 20℃
Stand filtration	Both sample after sulphonation and samples coated with iron oxide	2 times	Room temperature 20℃
Shaking when the samples in horizontal direction	Both sample after sulphonation and samples coated with iron oxide	2 times	Room temperature 20℃

Two types of filtration were performed cycling static and shaking filtration with different parameters such as temperature and shaking time as shown in figures (*Figure 3-22*). In the shaking filtration the filter bed was filled with the standard solution and the system sealed so no recycling occurred but a smaller volume of solution was required by the test and both shaking and cycling filtration happen in the same time. In addition to that, all standard solutions were filtered through a 0.45m membrane filter (MFS) before using any machine to remove unwanted particulates.

Figure 3-22.The cyclic filtration process

Figure 3-23. The filtration processes with shaking

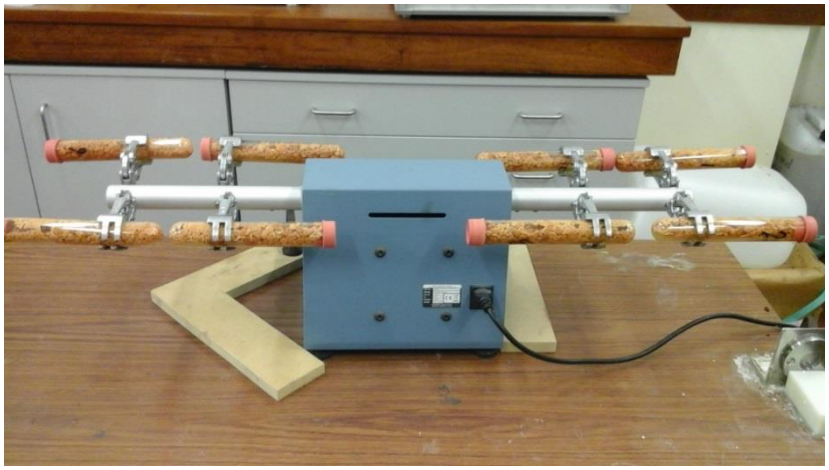

Figure 3-24. The filtration processes with shaking but with different orientation

3.5. Zero point of Charge Measurement

Zero of point charge for iron oxide was measured from solutions with different pH between 5 and 11 made by adding 0.1M NaOH to distilled water, and then adding 0.1 g of the iron oxide (from the coating layer) to each solution with shaking for 2 hours in ultrasonic bath to prepare the suspensions. All these solutions were analysed with a zeta potential equipment to get surface charge data as a function of pH (Boujelben et al., 2009, Bouzid et al., 2008). Zero point of charge (ZPC) is used to determine ions potential to interact with the surface based on surface charge. When a sample dissolves in a solution it gives both positive and negative ions with different concentrations, and at a specific value of pH the surface of the solid become electrically neutral; this pH corresponds to the zero point of charge. At pH higher than this the surface will have negative charge. In contrast, with lower pH value than zero point charge the solution will be acidic (Somasundaran and Agar, 1967)

This system has many parts. A laser illuminates the material particles, as result most of the laser penetrate the sample and some of it is scattered. The scattered beam intensity is measured by a detector. To avoid detector overloading when the light is too much an attenuator is used to decrease the light intensity. A correlator (digital signal processing board) is used to determine the rate at which the intensity is varying, then the computer analyses the data take place and the final results are collected (Instruments, 2004). The zetasizer used here can measure both particle size and surface charge by using different software. Zeta potential is measured by an accessory

well when the samples put between two electrodes ,then when the electric field is applied the sample particles is modified the pattern, this is measured zeta potential at a number of distances from the material particles surface by the detector.

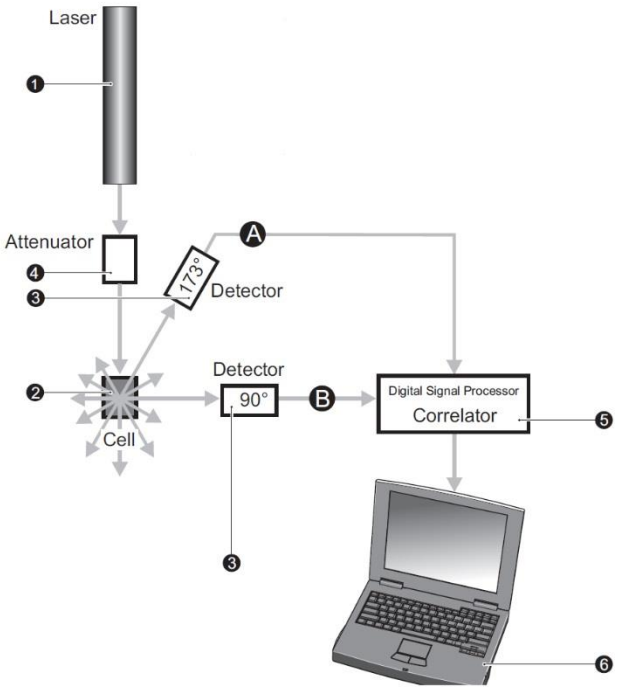

Figure 3-25. Zetasizer Nano S for measuring zeta potential,(Instruments, 2004).

3.6. Regeneration

The regeneration process was done by passing a solution with different pH (3, 5, and 11) through the plastic column which contains the PolyHIPE beads after the filtration process with solutions containing nickel, copper and a binary system between nickel and copper respectively. 0.01M NaOH or HCl were used to prepare these solutions. The plastic column and the peristatic pump were used during the regeneration process to wash the PolyHIPE beads for 8 hours by using cycling filtration. The amount of beads in each column was 3 gm of PolyHIPE beads the same as during the filtration process (Pandey et al., 2007).

4. PolyHIPE Characterization

In order to be a good filter substrate material PolyHIPEs must have certain important characteristics. They must have connected porosity to allow mass transport, they must have a high surface area with a large number of active sites for ion exchange or adsorption, and they must be chemically stable in water and mechanically robust enough to withstand manufacturing and use. This chapter reports the characterisation of PolyHIPE materials under different processing conditions in order to select an optimum material for filtration.

Three types of samples have been developed (see chapter 0)

- In situ sulphonation PolyHIPEs with different structures.
- Post-sulphonation PolyHIPEs with different structures
- Sulphonated and non-sulphonated PolyHIPE coated with iron oxide nanoparticles

4.1. Microstructure

From the SEM images shown in Figure 4-2, the typical PolyHIPE structure is obtained and it can be seen that there are primary pores and secondary pores as well as interconnections between them. There are large walls in some regions, while the image for the sample with 20min mixing time shows few interconnects between the pores. At higher magnification we can see smaller pores inside the structure; pores which are inside the walls which seperate the large pores. Figure 4-2 shows the number of pores inside the wall for a sample with 15 min mixing time is more than in the sample with 30 min mixing time, therefore the surface area for the sample with 15 min mixing time is higher as shown in section 4.2.

4.1.1 Pore size distribution

The average pore size and pore size distribution was calculated by processing the SEM images using Image J software and a manual method of identifying pore diameter; the results are shown in Figure 4-3. It can be concluded that the pore size reduces with increasing mixing time due to decreased water droplet size in the HIPE (see Figure 4-3) (Walsh et al., 1996, Bhumgara, 1995). After reaching a minimum pore size there is an increase with increase mixing time which may be due to droplet coalescense. This would reduce the stability of the emulsion and, ultimately, increase the micro and nano pore size as shown in Figure 4-3 and Figure 4-16 (Jimat, 2011).

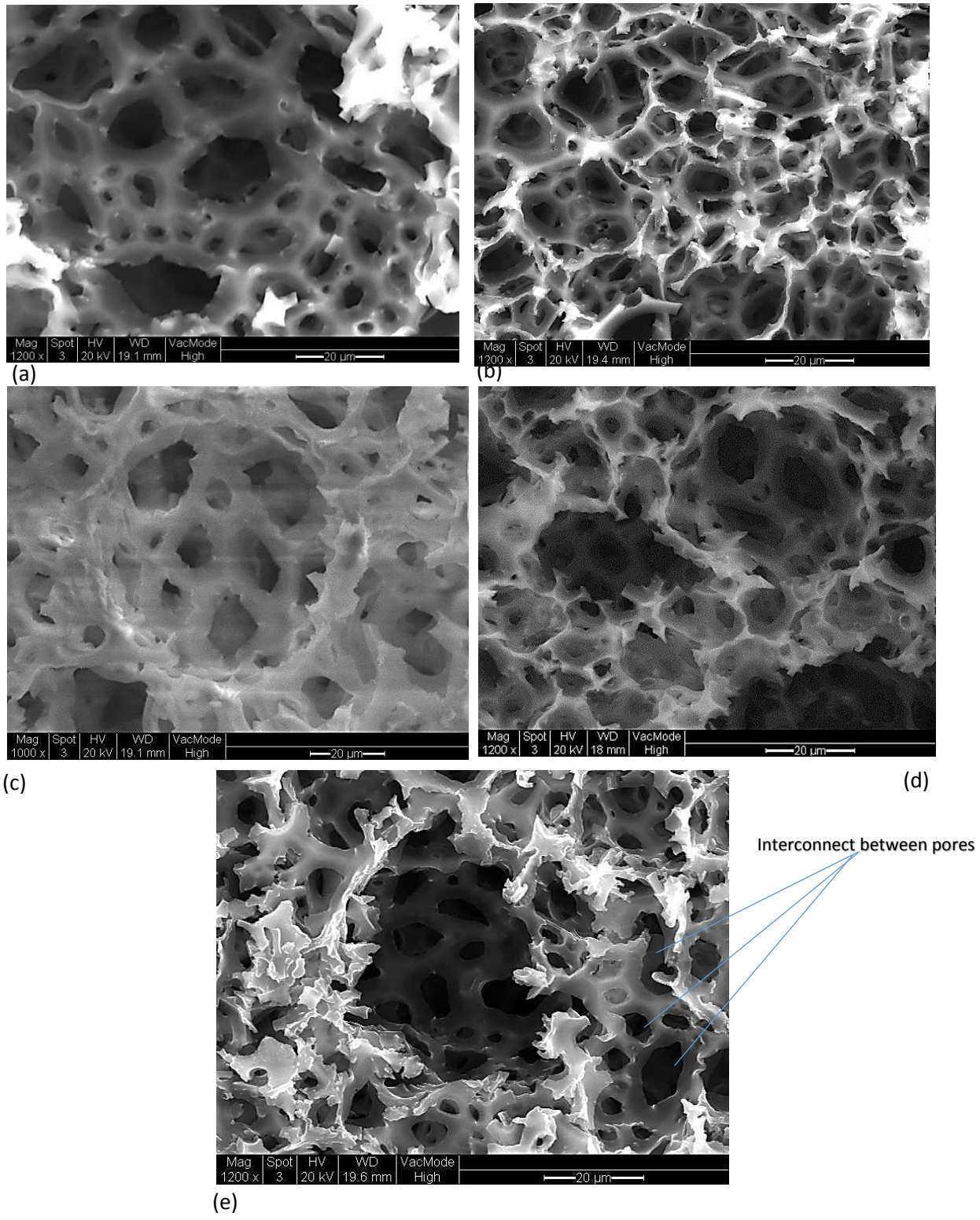

Figure 4-1. Plan view SEM images of the PolyHIPEs structure with different mixing time (a 10, . b15, c20, d25 and d30 min)

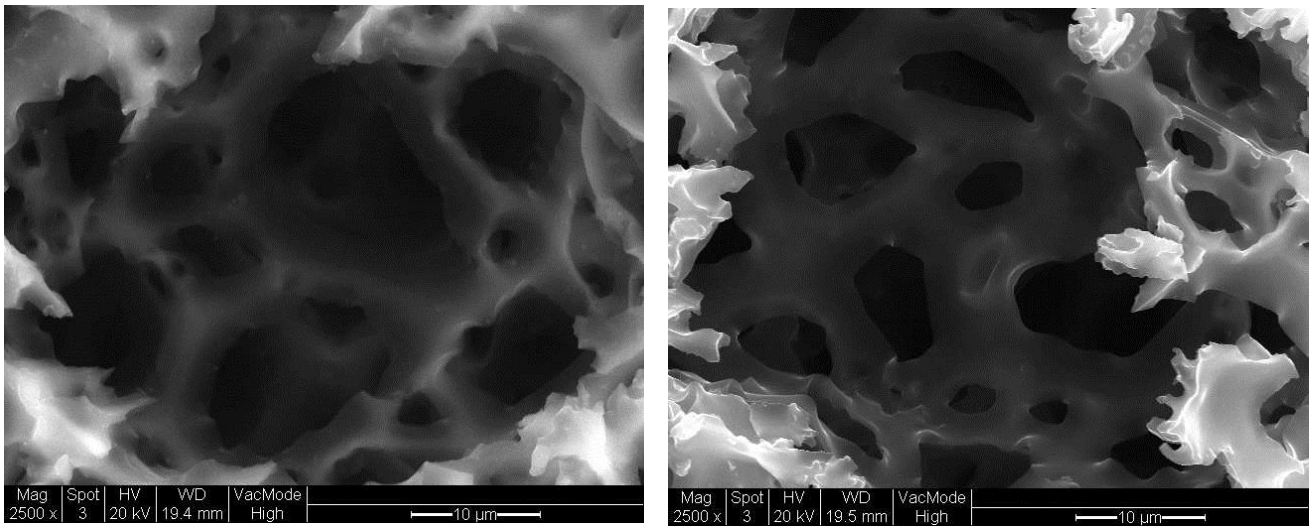

Figure 4-2. The SEM images of the PolyHIPEs structure: (a) 15 minutes, (b) 30 minutes mixing time with higher magnification

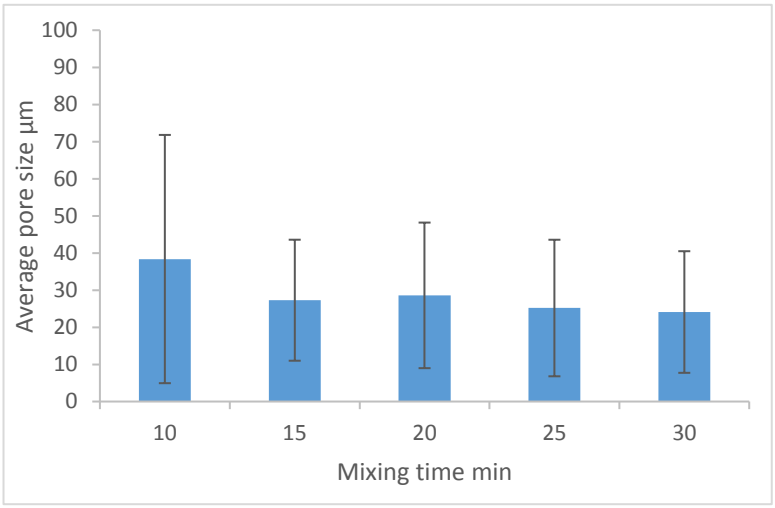

Figure 4-3. Average Pore size for PolyHIPE with different mixing time (10, 15, 20, 25 and 30 min) determined from SEM images using Image J.

The distribution of pore size for PolyHIPE samples with different mixing times (10, 15, 20, 25 and 30 min) was determined by analysing figures Figure 4-2 using Image J software. The diameter of a large number of pores was analysed for each sample (46, 63, 63, 63 and 82 respectively). The Histograms of pore size are plotted in Figure 4-4 to Figure 4-8 and show the micropore size distribution for each PolyHIPE sample. The figures show that the majority of micropores are between 10 and 30 micron diameter, but the samples with 15 and 20 min mixing time have smaller average pore sizes.

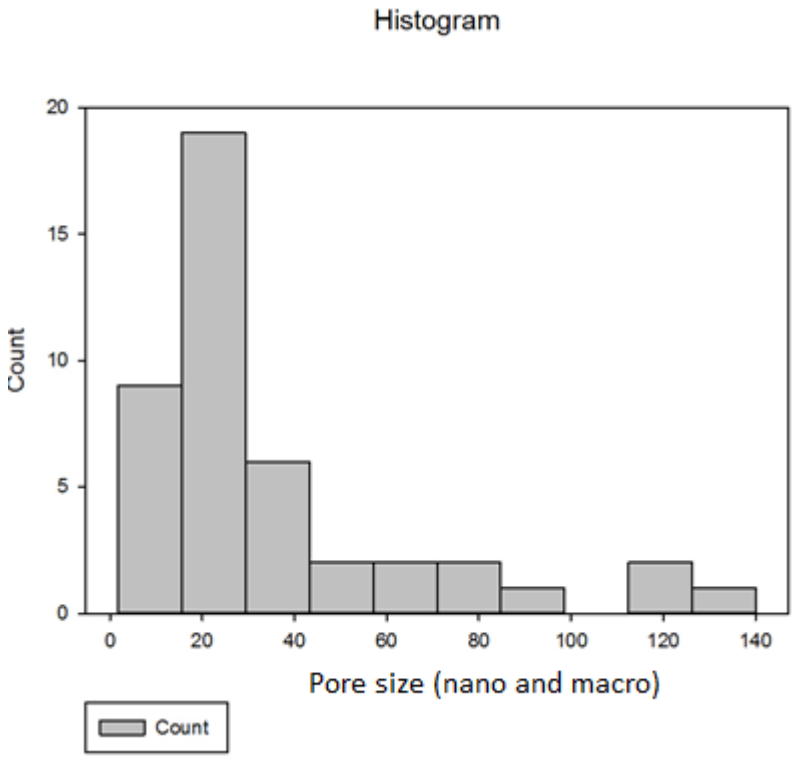

Figure 4-4. Pore size histogram from PolyHIPE sample with 10 min mixing time

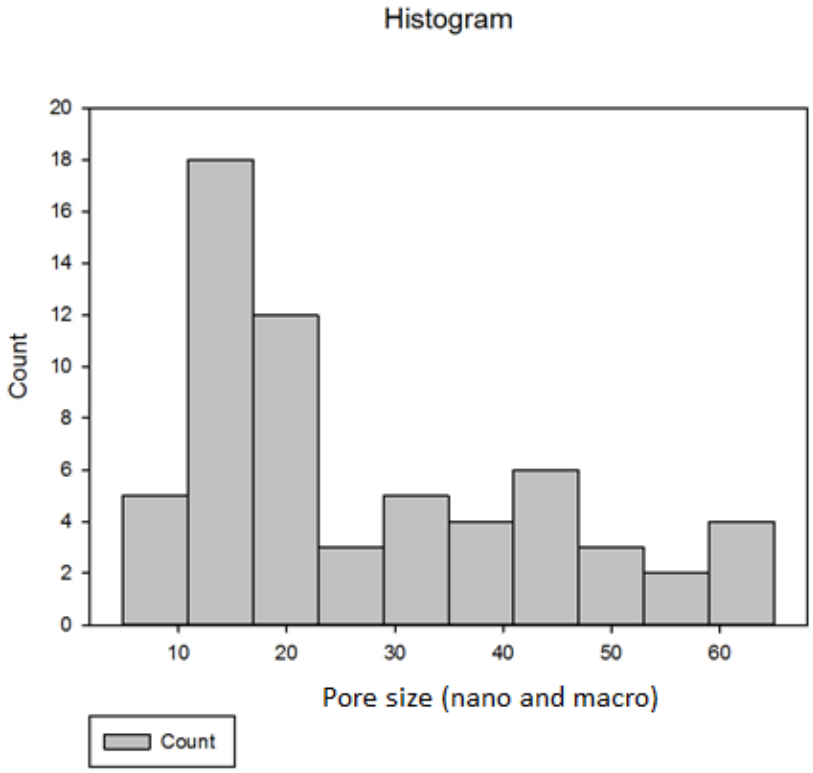

Figure 4-5. Pore size histogram from PolyHIPE sample with 15 min mixing time

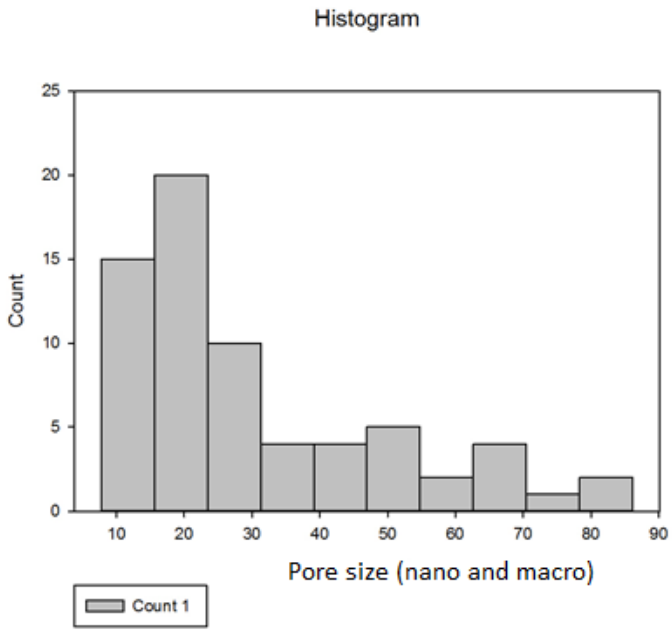

Figure 4-6. Pore size histogram from PolyHIPE sample with 20 min mixing time

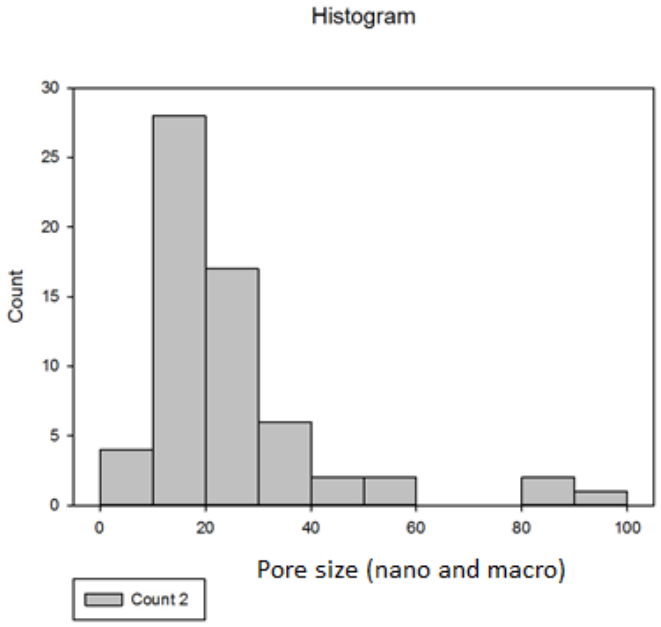

Figure 4-7. Pore size histogram from PolyHIPE sample with 25 min mixing time

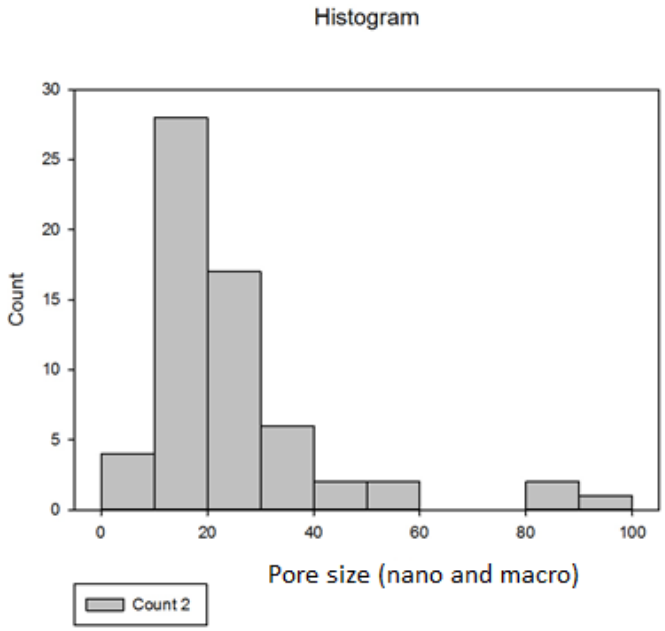

Figure 4-8. Pore size histogram from PolyHIPE sample with 30 min mixing time

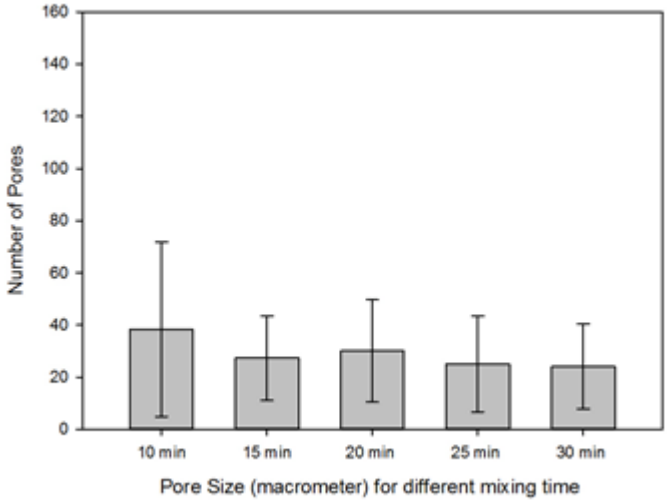

Figure 4-9. Show the Standard error for the pore size masurements from PolyHIPE sample with different mixing time

Figure 4-9 show the standard error for all samples and it show that the sample with 10 min mixing time has the hightest varasion range in the pore size diameter , so it used in the filtaration process.

4.2. BET Analysis

Samples were tested for pore size and surface area using the adsorption-desorption isotherm. Isotherms were analysed by the BET method. The porosity measured by BET in the nanoporosity which are present in the walls of microporous PolyHIPE revelled in SEM analysis**.**

4.2.1. Adsorption desorption isotherm

Figure 4-10 to Figure 4-14 show the volume adsorbed against relative pressure, where relative pressure was calculated by dividing sample pressure (ps) by the saturation pressure (po). They show the adsorption desorption isotherm for PolyHIPE samples obtained with different mixing times (10, 15, 20, 25 and 30 min). From the shape of the adsorption desorption isotherms the adsorption process takes place on a macro porous structure when we compare it with the standard diagram as shown in Figure 3-14 especially for the PolyHIPE samples with 15 and 20 min mixing time (Sing, 1994). From that figure we could conclude that the adsorption desorption isotherm follows the Type II isotherm and it appears from the first part of the isotherm that the adsorption process for nitrogen is initially monolayer and then multilayer. In all samples the isotherm is reversible and no hysteresis was observed as compared with the standard diagram in Figure 3-16 (Sing et al., 1985; Gregg and Sing, 1982).

When adsorption hysteresis occurs for a solid with pores it shows the difference between the mechanisms of adsorption and desorption. All figures show that the adsorption isotherm is rapidly increasing which is related to macropores of large size, and there is no hysteresis in any isotherm due to the macropores being more significant than mesopores which agrees with SEM images as shown in Figure 4-2and Figure 2-1. (Sing et al., 1985).

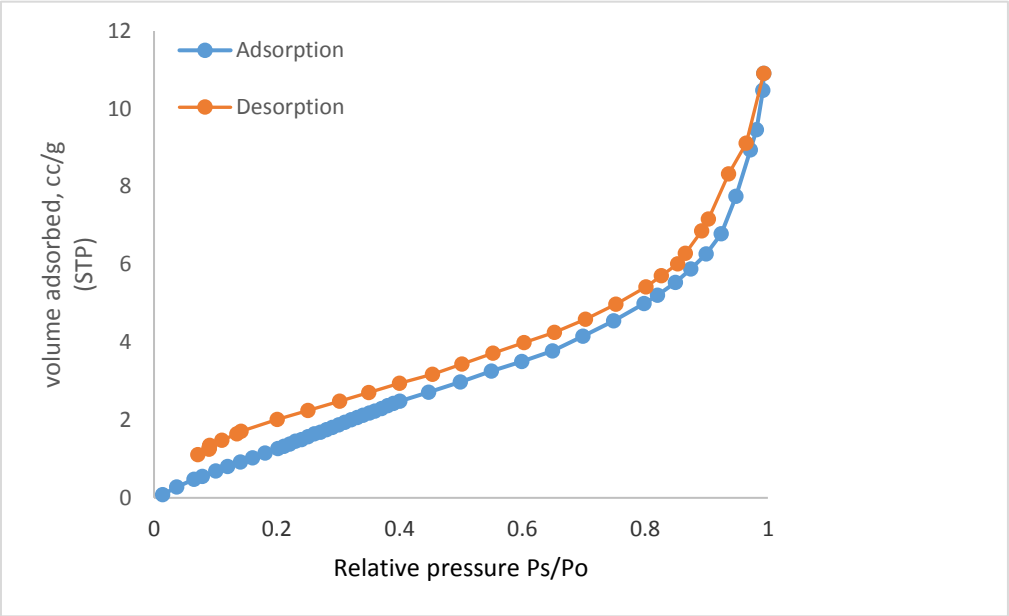

Figure 4-10. Isotherm plot for surface area and pore size analysis for PHP sample produced with 10 (min) mixing time after sulphonation, when Relative pressure is sample pressure (ps) over saturation pressure (po)

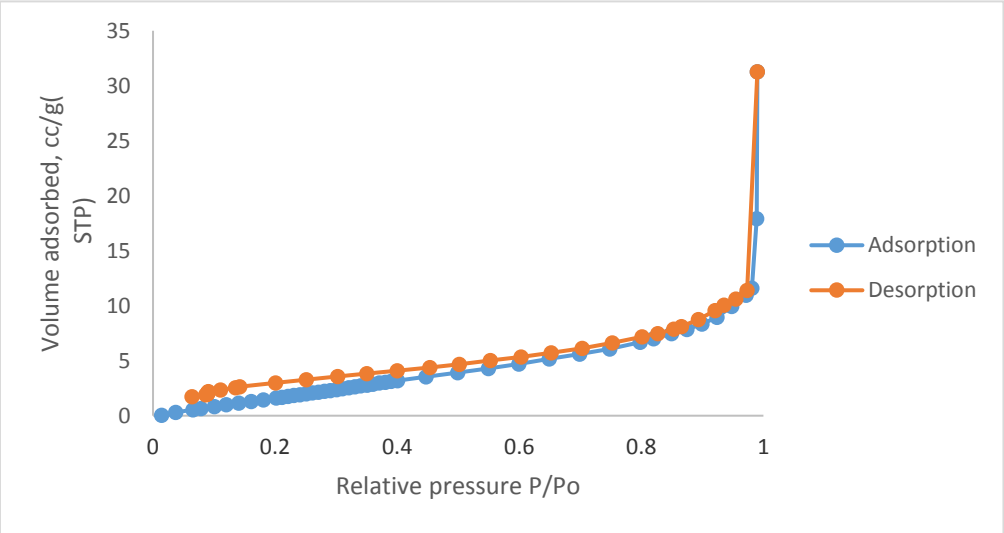

Figure 4-11. Isotherm plot for surface area and pore size analysis for PHP sample produced with 15 mixing time, when Relative pressure is sample pressure (ps) over saturation pressure (po)

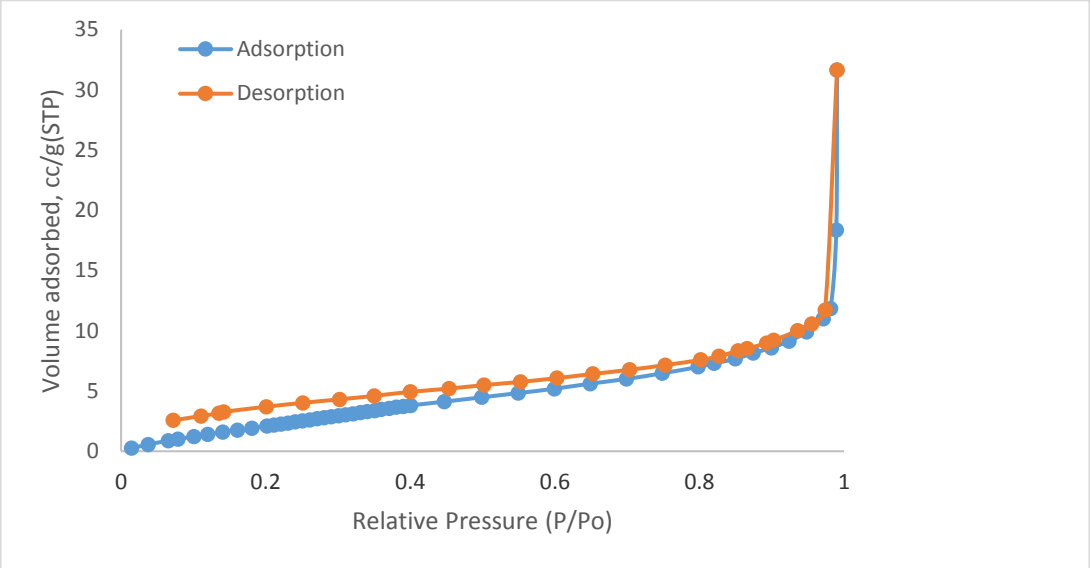

Figure 4-12. Isotherm plot for surface area and pore size analysis for PHP sample produced with 20 mixing time, when Relative pressure is sample pressure (ps) over saturation pressure (po)

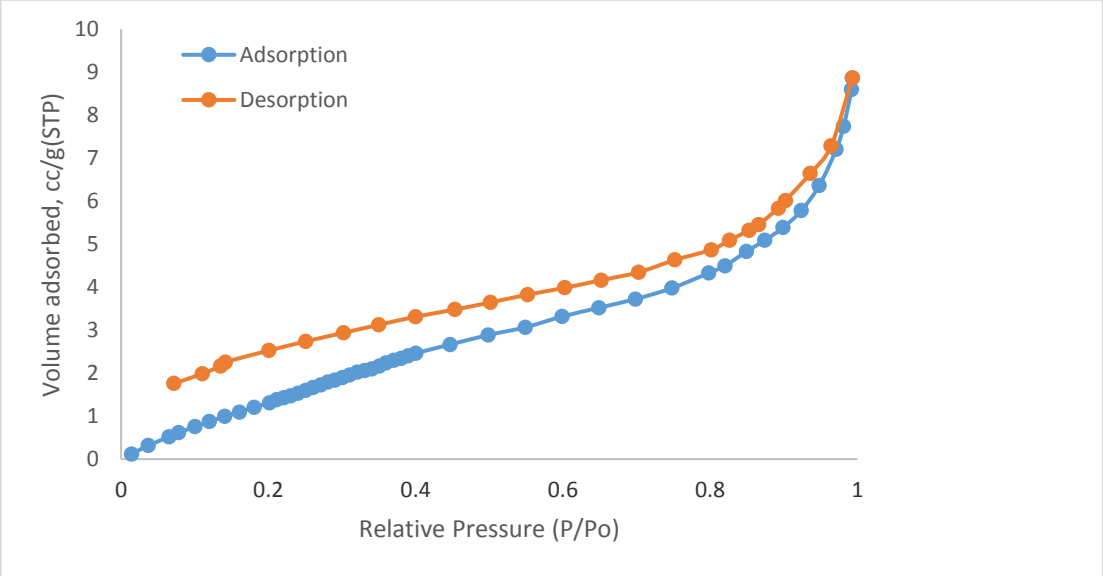

Figure 4-13. Isotherm plot for surface area and pore size analysis for PHP sample produced with 25 mixing time, when Relative pressure is sample pressure (ps) over saturation pressure (po)

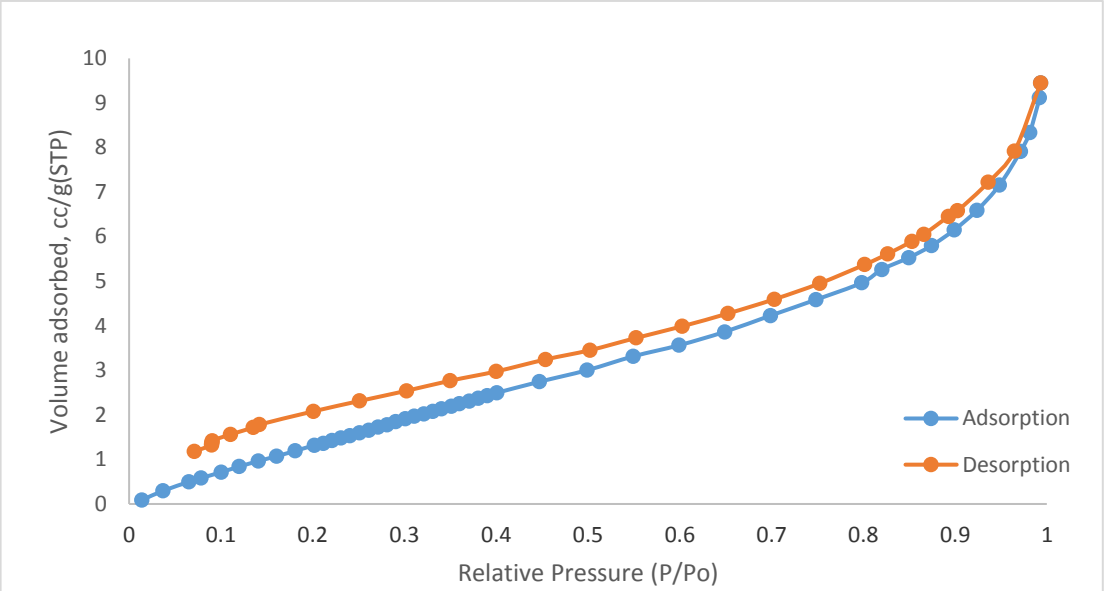

Figure 4-14. Isotherm plot for surface area and pore size analysis of PHP sample produced with 30 mixing time, when Relative pressure is sample pressure (ps) over saturation pressure (po)

4.2.2. BET Analysis

The adsorption isotherm were used to determine the surface area and porosity of the sample using the BET method (Sing, 1985). The varation of pore volume, pore size and surface area for the samples as a fuction of stirring time is shown in Figure 4-15 to Figure 4-17. The pore volume, pore size and surface area are approximentally constant except for the case of the sample which was stirred for 15 minutes which has a higher surface area and larger pore volume. An area of 10 m^2/g is reasonable for the required filtaration behaviour so any of the materials would be sutable. The surface area for the sample with 15 min mixing time is highest due it having lower pore size as shown in Figure 4-16.

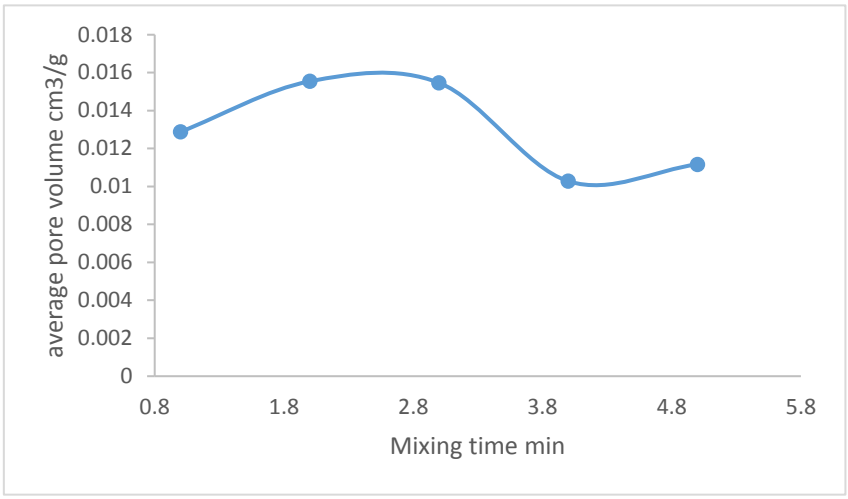

Figure 4-15. Average pore volume of PolyHIPE structure determined from BET analysis, the figure plotted from single data

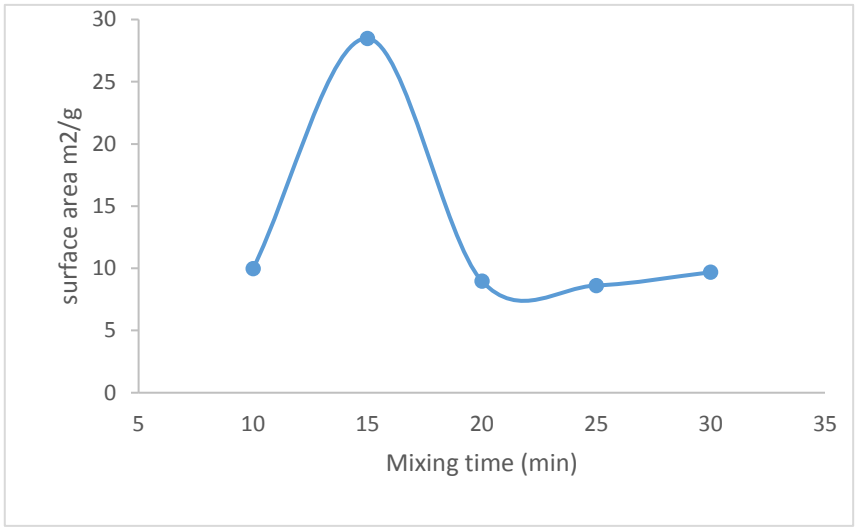

Figure 4-16. Surface area determined from BET analysis. The figure plotted from single data

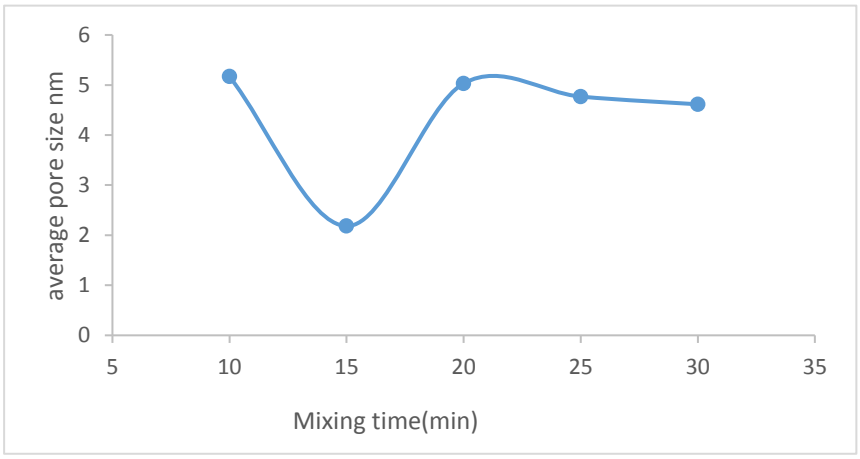

Figure 4-17. Average pore size determined from BET analysis. The figure plotted from single data

4.3. FTIR Analysis

It is essential to determine the composition and stability of the materials so that suitable materials can be selected for filtration studies. Accordingly, FTIR analysis was undertaken to see it stirring affects the structure of the material which was sulphonated in situ. Figure 4-18 to Figure 4-22 show the FTIR spectra for the samples prepared with different mixing time (10, 15, 20, 25 and 30 min). While Table 4-1 lists the major peaks identified in each spectrum and their chemical origin. From these figures it can be seen that the structure is the same with changing the mixing time, since the bonds which represent the vinyl ring and the benzenesulphonicacid group appear in all figures. These come from styrene and sulphuric acid which was added to the aqueous phase during in situ sulphonation.

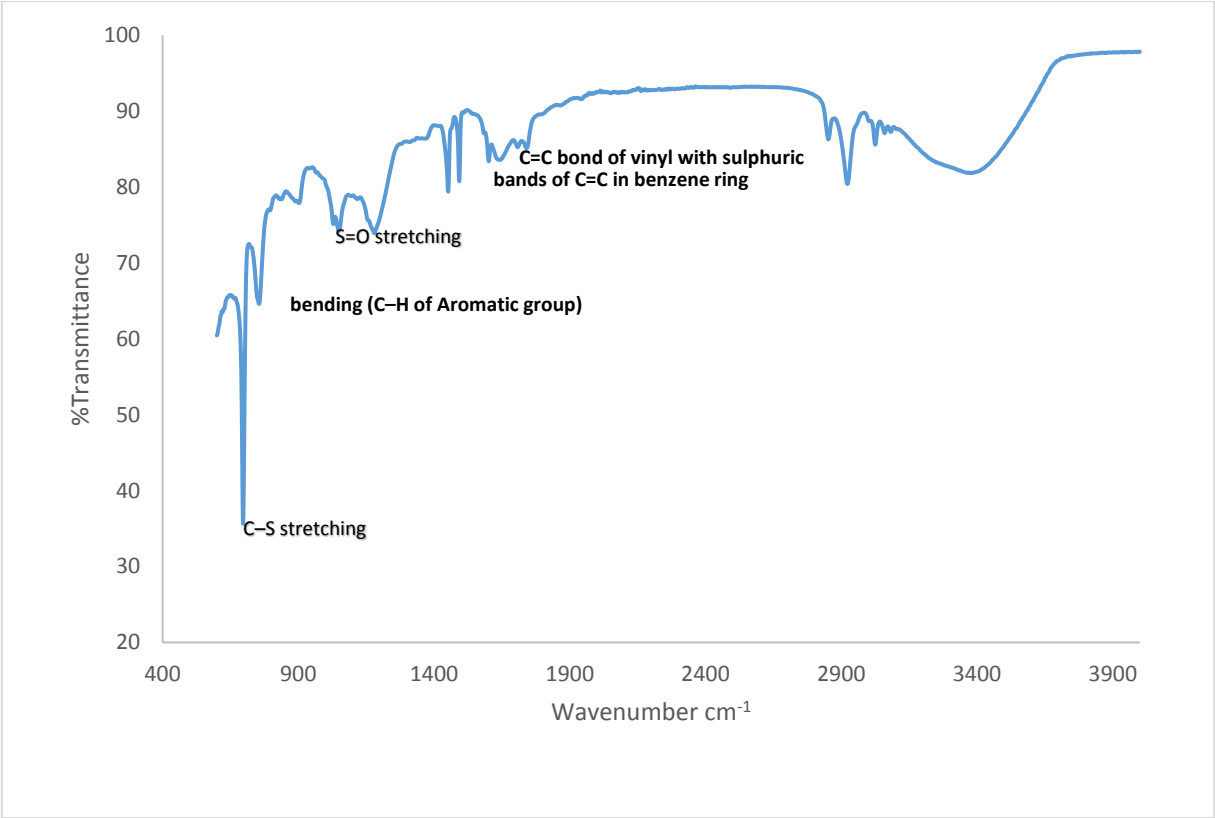

Figure 4-18. FTIR spectrum for the PolyHIPE with 10 minutes mixing time.

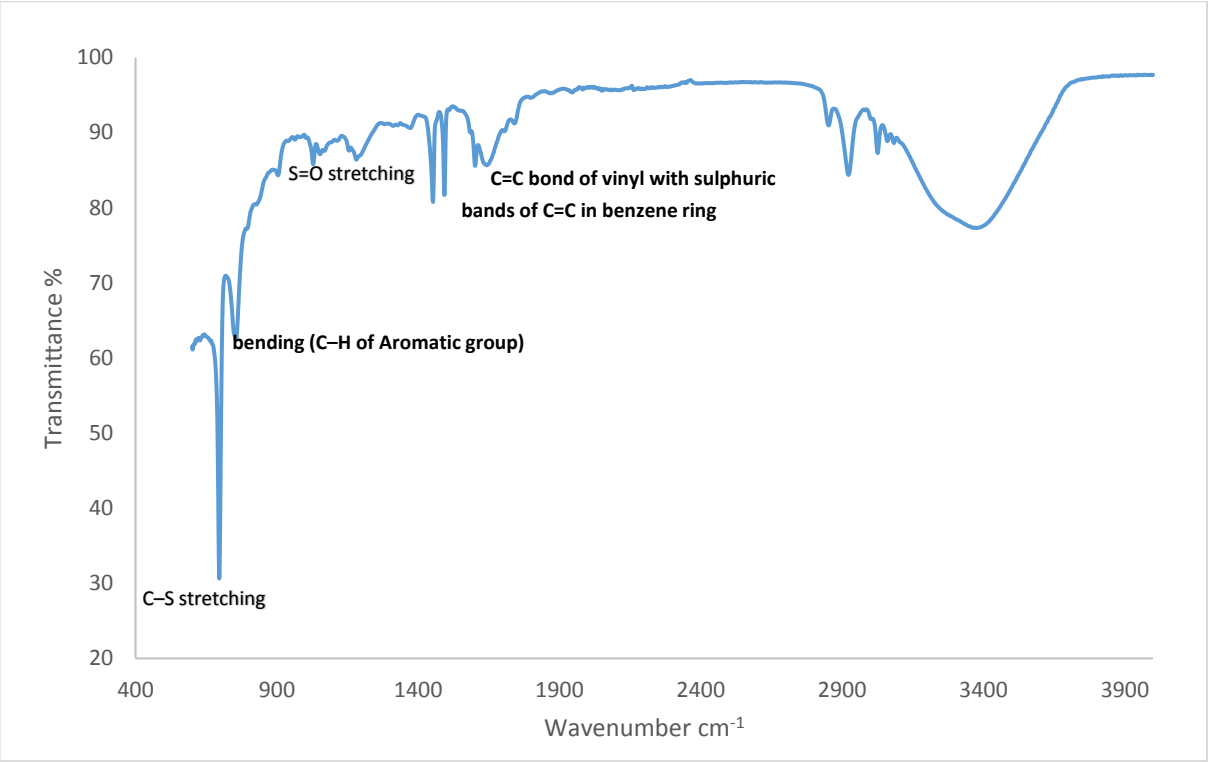

Figure 4-19. FTIR spectrum for the PolyHIPE with 15 minutes mixing time.

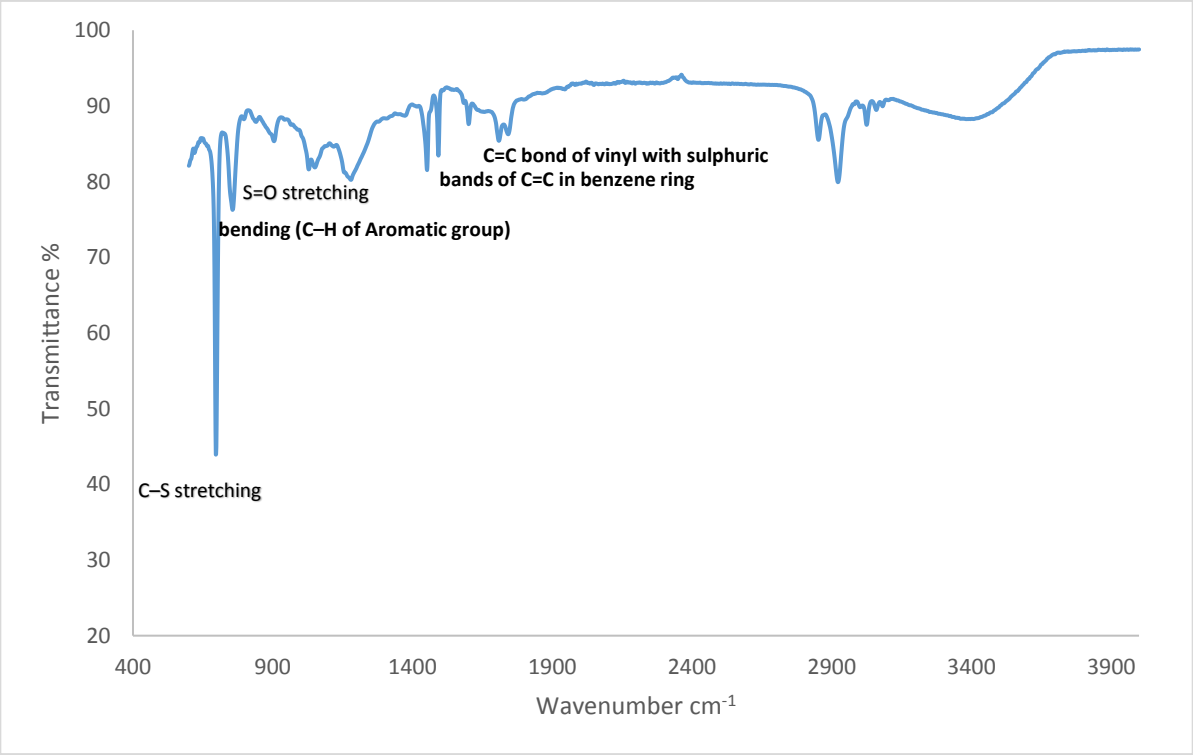

Figure 4-20. FTIR spectrum for the PolyHIPE with 20 minutes mixing time.

The intensity of the peaks at 3300cm^{-1} varies between samples; this is associated with water and OH bonds in the structure and suggests a different amount of drying of the samples has occurred during processing.

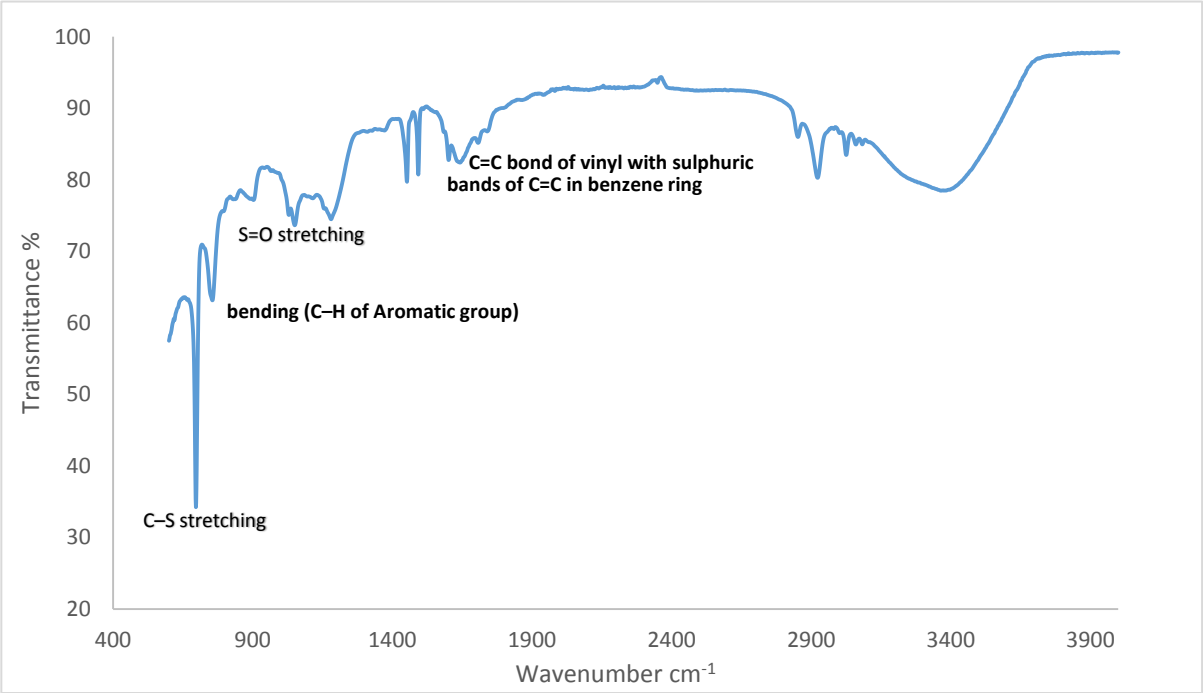

Figure 4-21. FTIR spectrum for the PolyHIPE with 25 minutes mixing time.

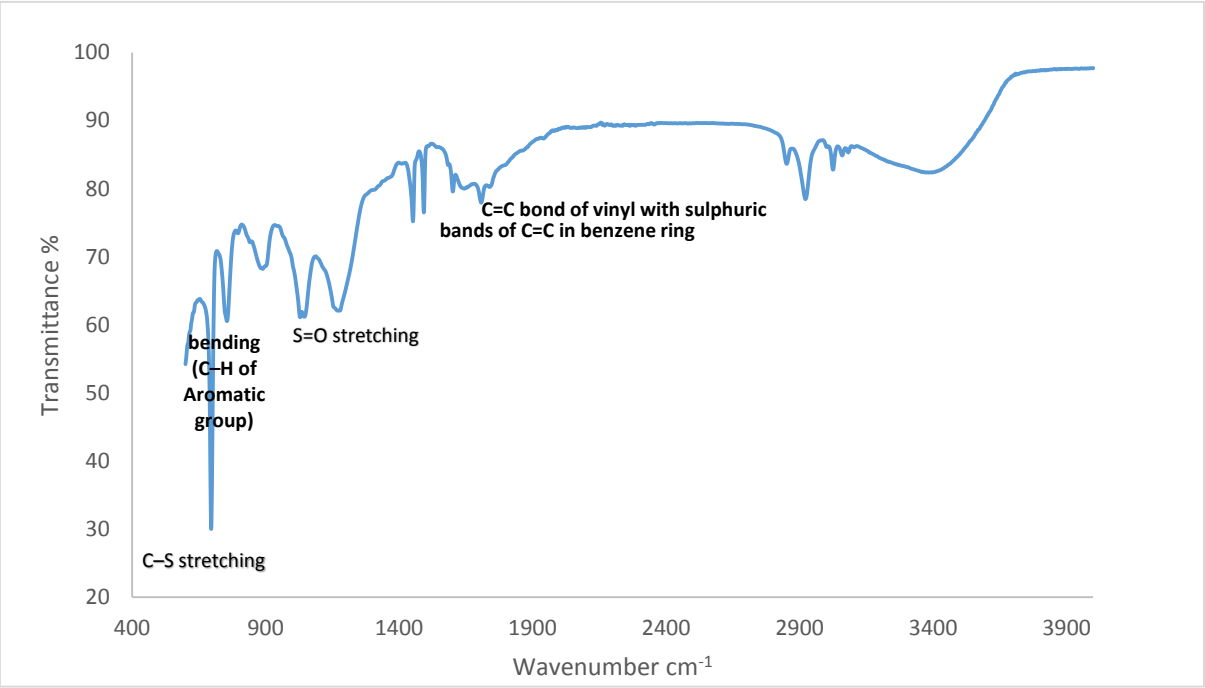

Figure 4-22. FTIR spectrum for the PolyHIPE with 30 minutes mixing time.

As shown in Table 4-1 there are small differences in the minor peaks from FTIR spectroscopy for the samples with different mixing time but with predominantly the same structure. Direct comparison of the spectra (Figure 4-22) shows that the same peaks are present for all samples but their intensity varies. This due to the variability is sample processing and drying and the sampling of different volumes of material for FTIR analysis. The high intensity peak in each sample (C-H bending of the aromatic ring) is characteristic of the styrene monomer.

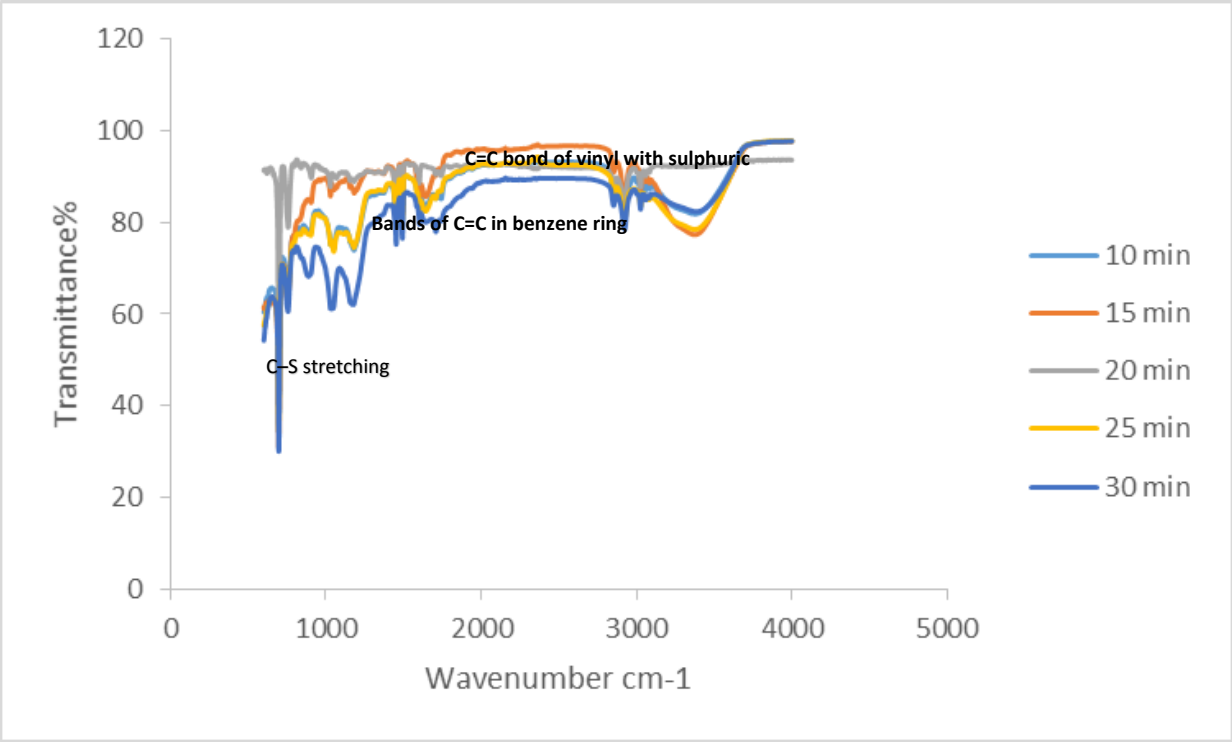

Figure 4-23. FTIR spectra for all PolyHIPE samples.

Table 4-1. The functional groups from FTIR.

Number	Sample peak cm^{-1} with 10 min	Sample peak cm-1 with 15 min	Sample peak cm-1 with 20 min	Sample peak cm-1 with 25 min	Sample peak cm-1 with 30 min	Peak name	References
1	696.5	696.3	696.9	696.5	696.4	C–S stretching	(Stuart, 2005)
2	755.3	755	756.5	755.4	755.6	out of plane bending (C–H of Aromatic group)	(Stuart, 2005)
3	838.7	-	839.8	836.5	841.4	C=C phenyl ring,	(Pretsch et al., 2009)
4	902.7	904.1	905.5	902.6	-	C=C phenyl ring,	(Pretsch et al., 2009)
8	1029.2	1028.6	1028.4	1029.2	1029.5	S=O stretching	(Stuart, 2005)
9	1049.5	1052.9	-	1050.3	1045.4	S=O stretching	(Stuart, 2005)
11		1155.1	-	-	-	Symmetric SO2 stretching	
12	1180.2	1181.6	1180.6	1180.4	1172.4	sulfonic acid group, –S=O	(Stuart, 2005)
13	-	-	1372.4	1372		Methyl symmetrical C–H bending	(Stuart, 2005)
14	1452	1452.1	1451.8	1452	1451.9	Carbonyl group	(Stuart, 2005)
15	1492.8	1492.9	1492.7	1492.8	1492.8	bands of C=C in benzene ring	(Burrows et al., 2013)
16	1601.6	1601.7	1601	1601.6	1601.5	bands of C=C in benzene ring	(Burrows et al., 2013)
22	1740.7	1740.7	1741.6	1739.4	1739.5	Attributed to C=C bond of vinyl ring subsisted with sulphuric group	(Pretsch et al., 2009)
25	2852.9	2852.3	2851.2	2852.6	2851.9	Methylene symmetric C–H stretching	(Stuart, 2005)
26	2923	2922.8	2922.1	2922.9	2922.4	Methylene asymmetric C–H stretching	(Stuart, 2005)
27	3025.6	3025.8	3025.2	3025.5	3025.5	benzyl CH group	(Stuart, 2005)
29	3060.1	3060.4	3059.3	3060.1	3060.1	C-H stretching	(Burrows et al., 2013)

4.4. Compression Test

Mechanical properties of the PolyHIPE are important for the filter material is to be healable or to withstand the fluid pressures achieved in filtration if used as a bead or monolith. PolyHIPEs with different stirring time were compressed between the platens of a mechanical test machine. A typical stress-strain curve for each sample type is shown in Figure 4-25 to Figure 4-29 and the tangent to the curve at zero strain was used to measure the Young's Modulus of the material assuming the time-dependent deformation was minimal.

The compression test was performed for three samples from each mixing time and the average and the standard error were computed as shown in Figure 4-24. The Young's modulus depends on the pore size of the PolyHIPE. Its seems to be that, Young's modulus decreases with increasing the pore size (Alikhani and Moghbeli, 2014). There is a small decrease in the Young's Modulus at the 20, 25, 30 minutes mixing times which is due to the formation of larger pores (in Na no scale) as shown from the BET measurement as shown in Figure 4-17.

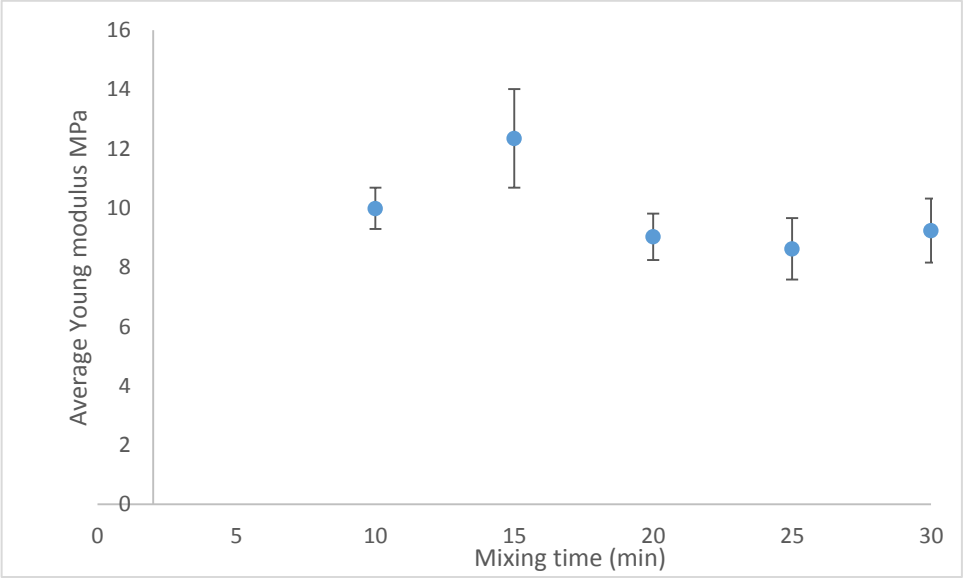

Figure 4-24. Young's Modulus for PolyHIPE with different mixing times (10, 15, 20, 25, 30 min)

There was a small of time-dependent elastic recovery at the end of the test once the load was removed but viscoelastic behaviour was not significant as test speed did not affect the measured results. There was no evidence of fracture in the compression test samples.

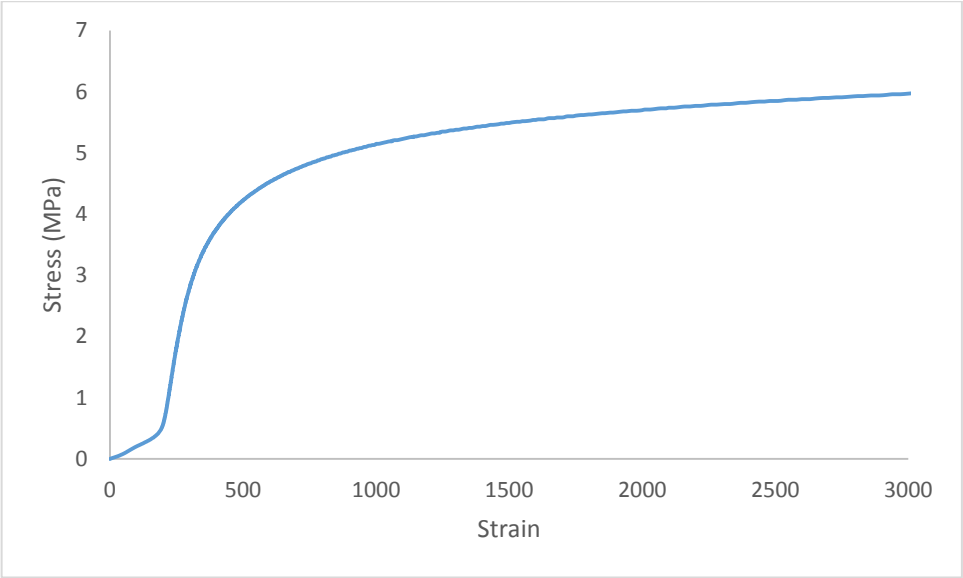

Figure 4-25. Stress strain curve for PolyHIPE sample with 10 min mixing time

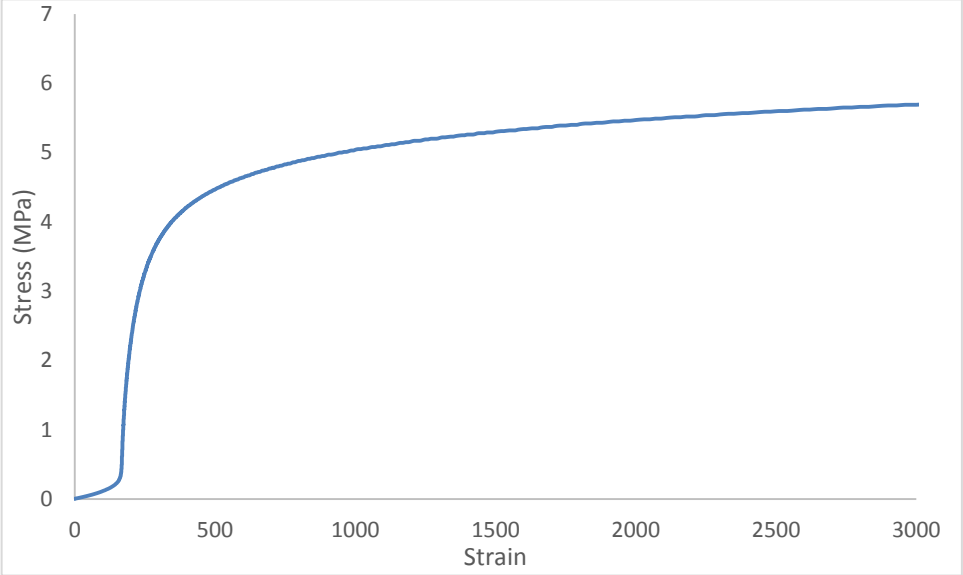

Figure 4-26. Stress strain curve for PolyHIPE sample with 15 min mixing time

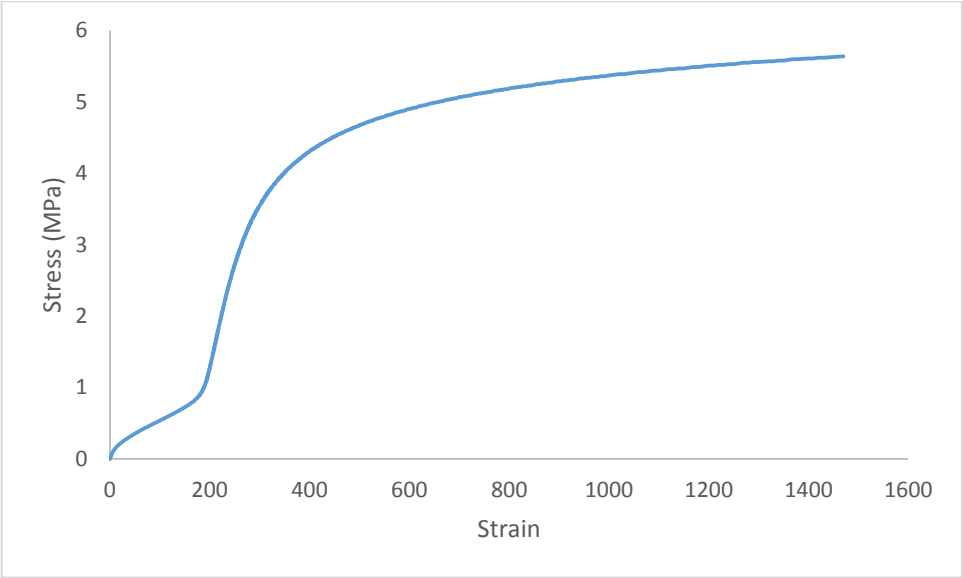

Figure 4-27. Stress strain curve for PolyHIPE sample with 20 min mixing time

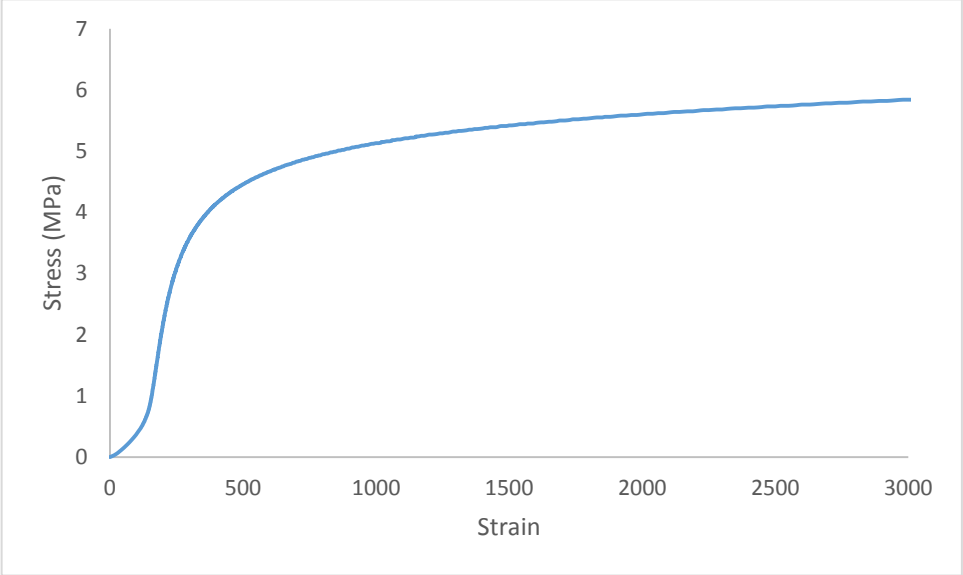

Figure 4-28. Stress strain curve for PolyHIPE sample with 25 min mixing time

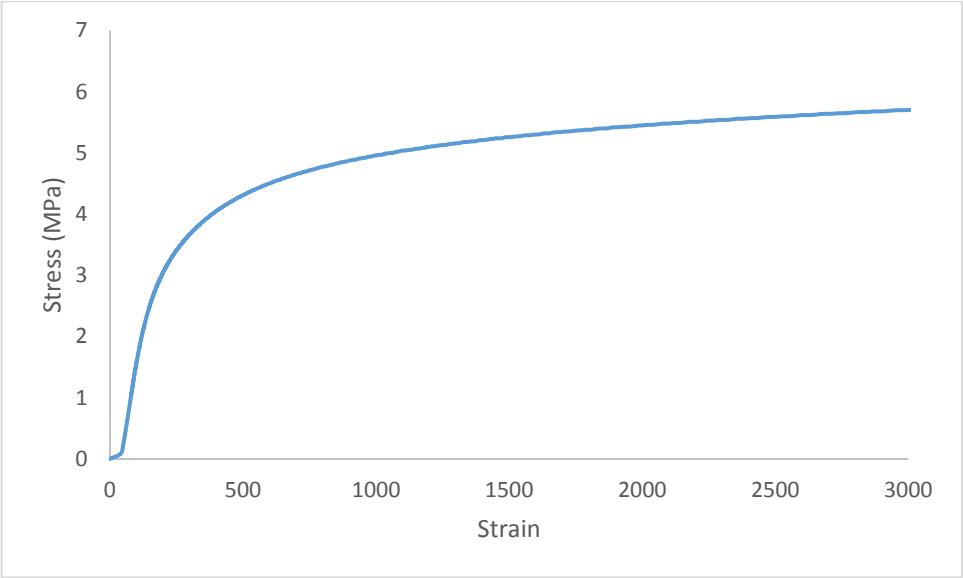

Figure 4-29. Stress strain curve for PolyHIPE sample with 30 min mixing time

4.5. Summary

In summary the PolyHIPE produced in this work has a hierarchical structure with many nano and micro pores in its structure and good surface area which will help in the filtration and iron oxide coating process where it will allow the nanoparticles to enter into the internal structure leading to an increase in total iron oxide surface area. Additionally, it might be has many functional groups like SO_3H which help to use the polyHIPE as an ion exchange material. All the results in this chapter show that a PolyHIPE with a well-defined structure has been produced but it still has a hydrophobic surface, so its water uptake is low and might be not enough to use it as a filter for water treatment. Thus post sulphonation is required as this will convert its surface structure to hydrophilic as demonstrated in the next chapter.

5. PolyHIPE after Post Sulphonation

Two types of sulphonation were investigated in this study. In situ sulphonation where 5% sulphuric acid was added to the aqueous phase during PolyHIPE manufacture and post sulphonation where the PolyHIPE was soaked in concentrated sulphuric acid and microwaved to functionalise the surface after polymerisation. This chapter describes material produced by the second method.

5.1. Microstructure

Figure 5-1 shows the effect of the sulphuric acid on the morphology of the PolyHIPEs structure after post sulphonation. The PolyHIPEs have smooth and granular areas due to the deposition of the sulphate on the surface (Fleming, 2012). The images show interconnected pores and also the increase in the wall thickness (Shakorfow, 2012) which is due to the sulphonation process. In addition there are more pores in the walls compared with the samples before the sulphonation (see Figure 4-2and Figure 4-2) which may be due to creation new pores during the sulphonation process. It is clearly seen that the surface is much smoother after post sulphonation as well. FTIR analysis shows that there is more sulphur in the structure after post sulphonation (Figure 5-2 to Figure 5-6)

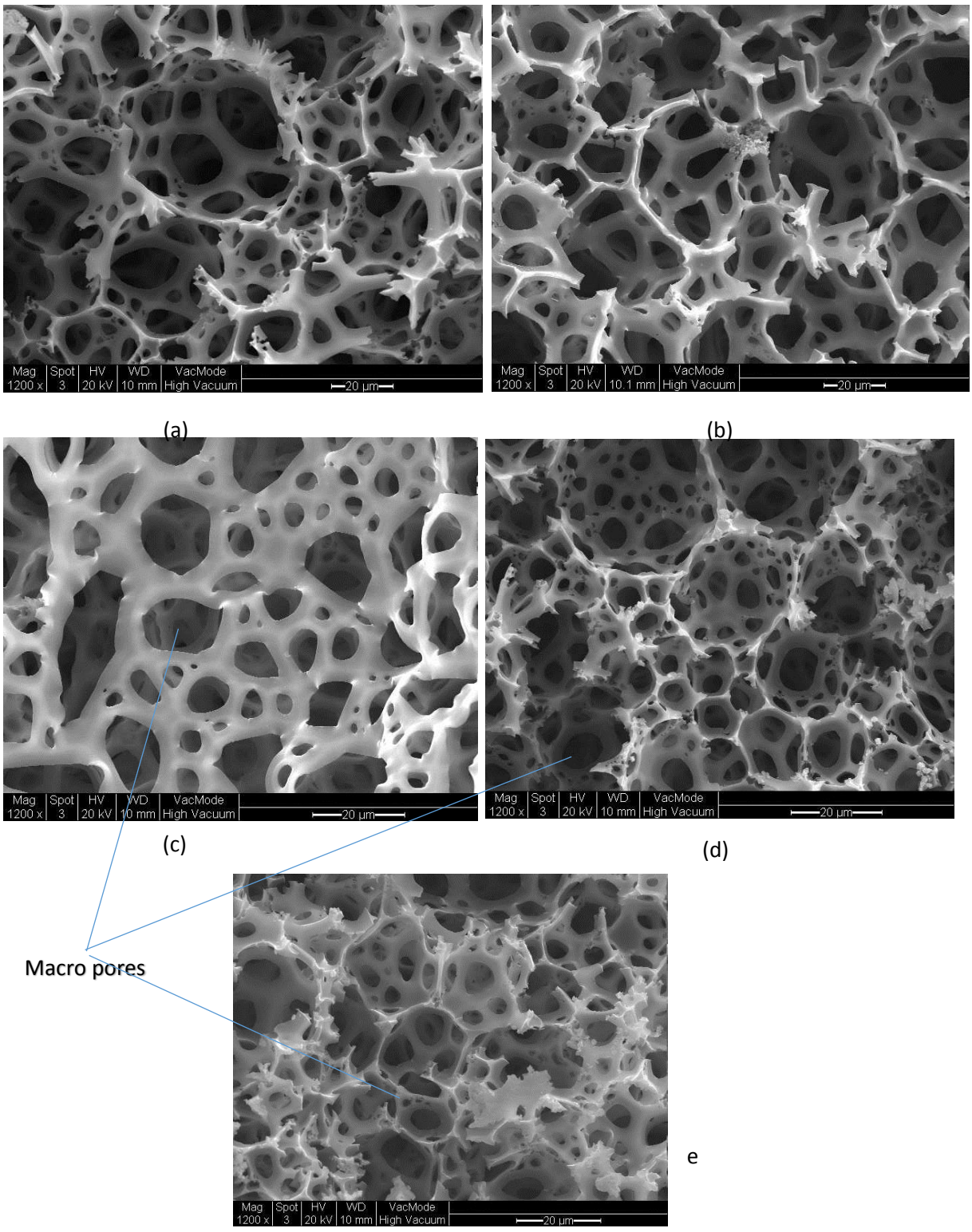

Figure 5-1. SEM images of PolyHIPEs after sulphonation: (a) 10 minutes mixing time, (b) 15 minutes mixing time, (c) 20 minutes mixing time, (d) 25 minutes mixing time, (e) 30 minutes mixing time, x100Mag.

5.2. FTIR Spectroscopy after Sulphonation

Figure 5-2 to Figure 5-6 show the FTIR spectra for the PolyHIPE samples with different stirring time after the post sulphonation process. There are differences in the intensity of some peaks and also fewer peaks appear in some samples. For instance, the difference in intensity for the peak at 696 cm-1 (C–S stretching) for the samples with (10, 20, 25 min) is larger than for the other samples which may be due to a better degree of sulphonation. The groups that appear around 1150cm-1 are due (S=O) stretching. The (S=O) stretching peaks for post sulphonated PolyHIPE are much higher intensity than the samples with in situ sulphonation (see Figure 4-18 to Figure 4-23) due to the increased concentration of sulphuric acid in contact with the polymer during post rather than in situ sulphonation. Because of the sulphuric acid in the aqueous phase (5% concentration) the peaks which come from the sulphonate group appear before and after the post sulphonation process. Thus there are very strong peaks for sulphur containing groups in post sulphonated material as well as a variable intensity peaks at 3320 cm $^{-1}$ due to water and OH groups in each sample.

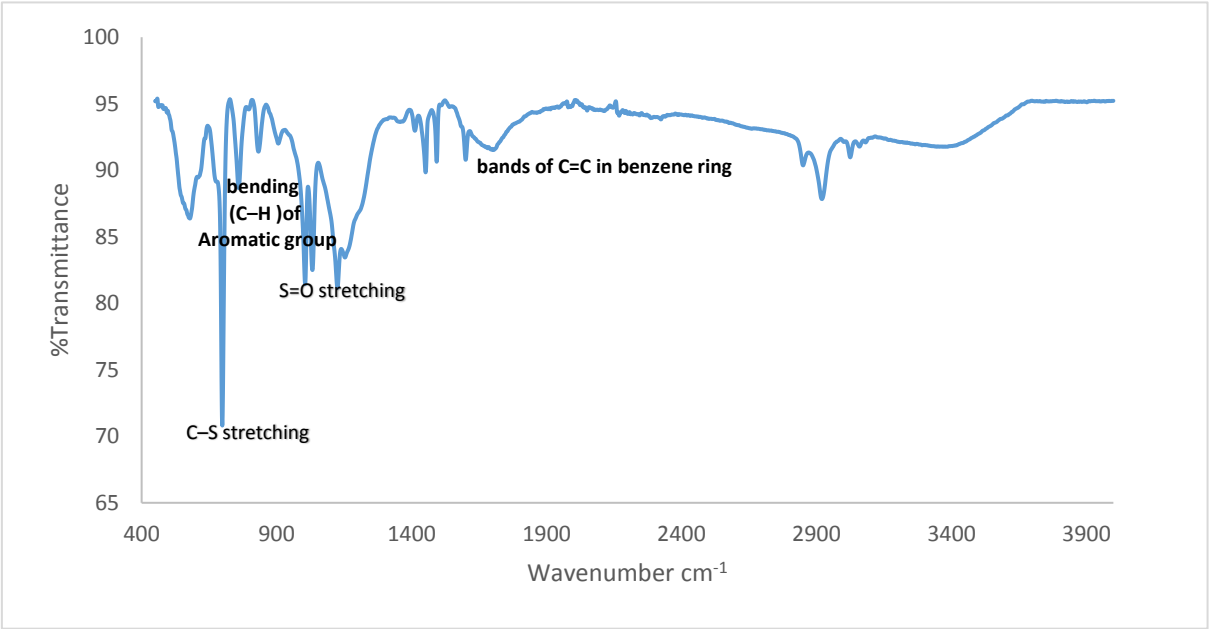

Figure 5-2. FTIR spectrum for PolyHIPE with mixing time 10 min

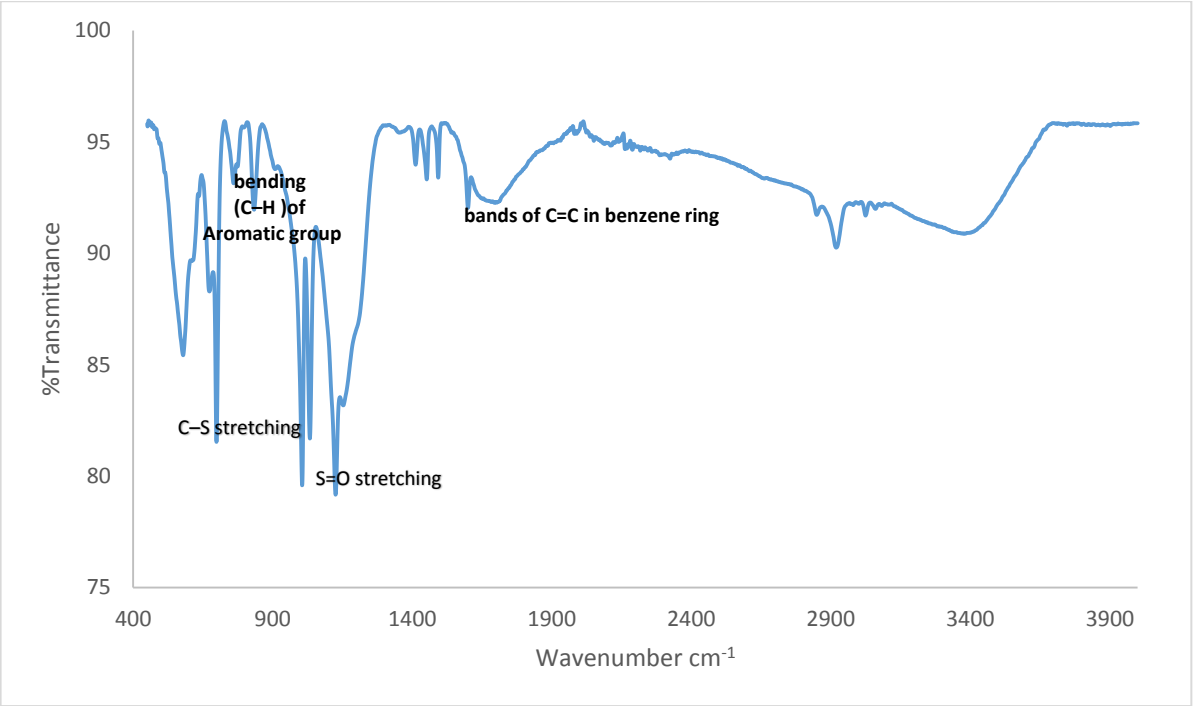

Figure 5-3. FTIR spectrum for PolyHIPE with mixing time 15 min

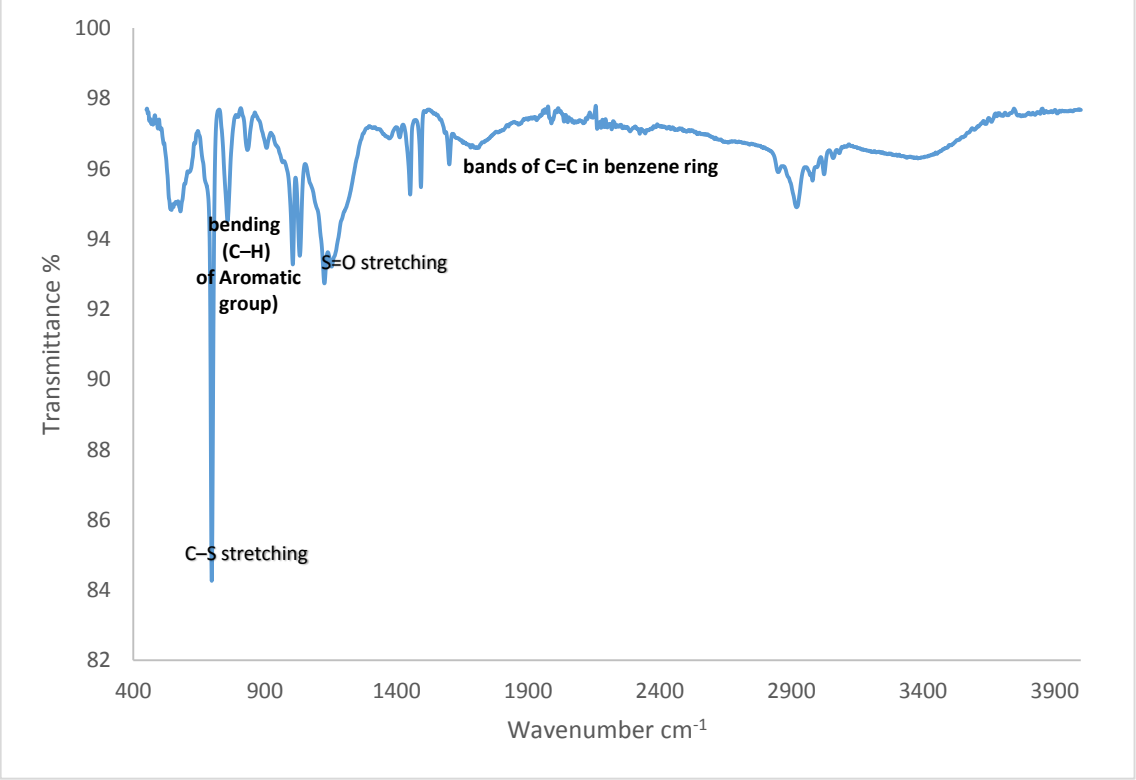

Figure 5-4. FTIR spectrum for PolyHIPE with mixing time 20 min

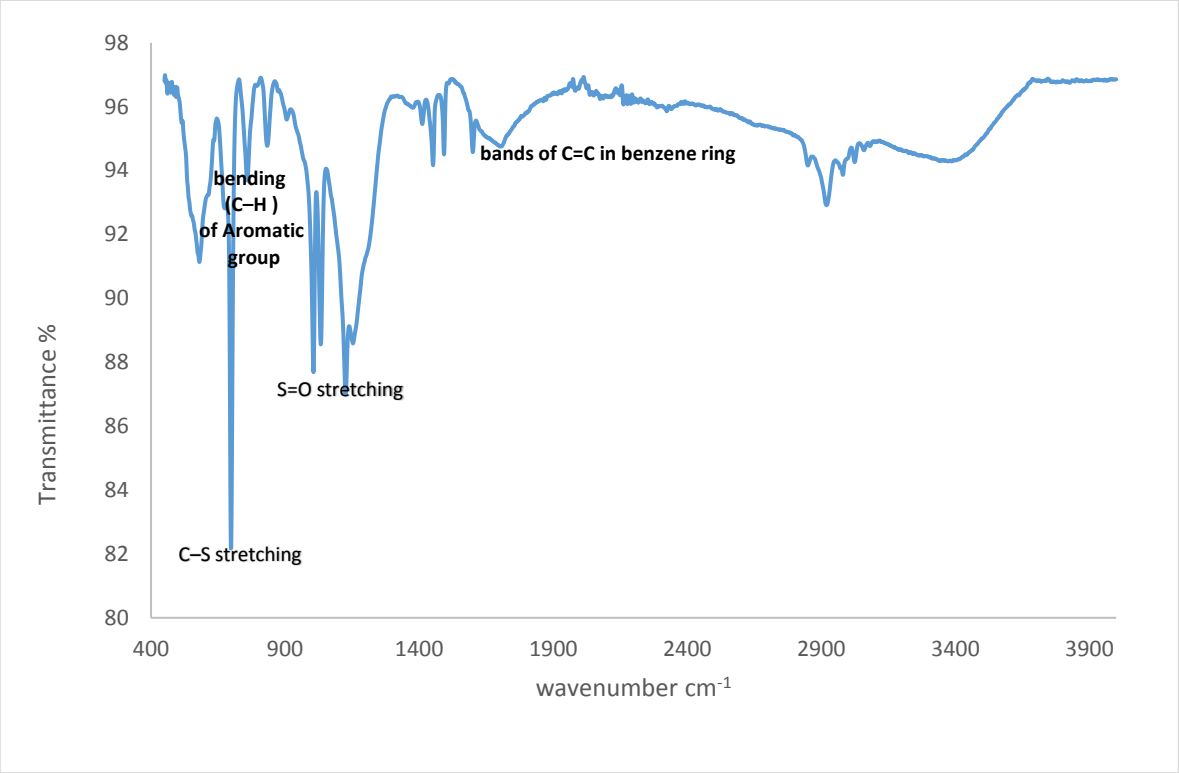

Figure 5-5. FTIR spectrum for PolyHIPE with mixing time 25 min

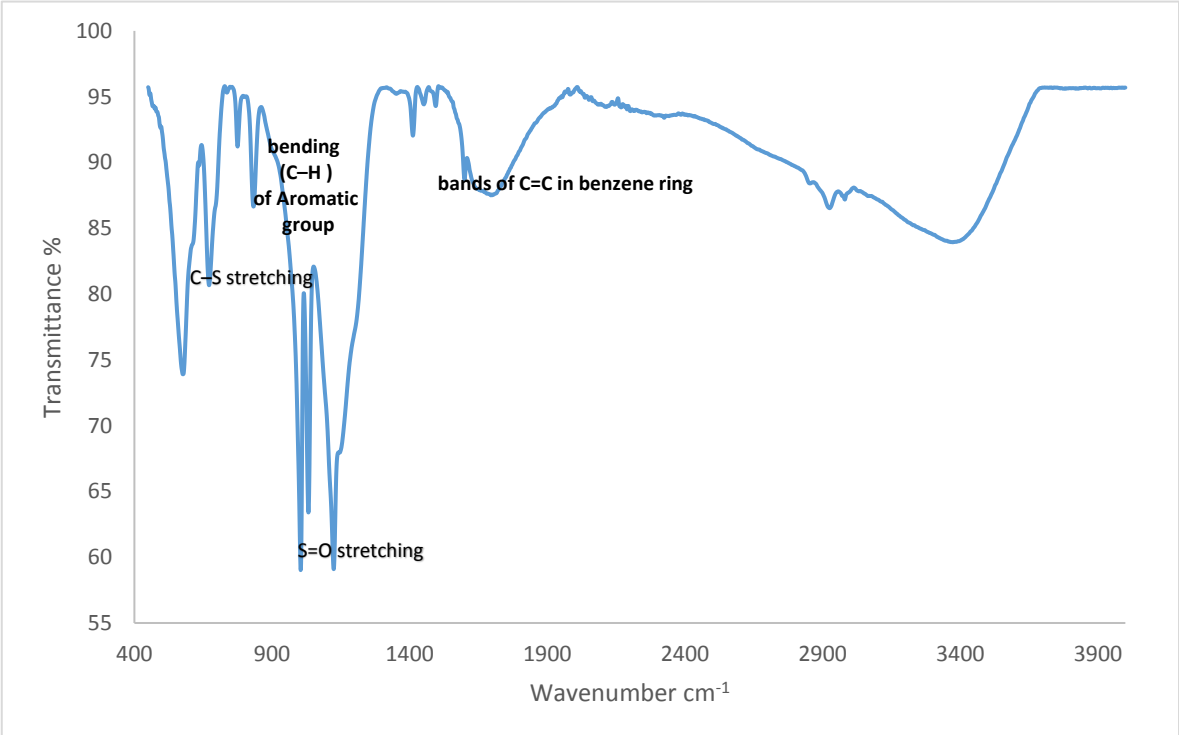

Figure 5-6. FTIR spectroscopy for PolyHIPE with mixing time 30 min

It is clear that post sulphonation increases dramatically the amount of sulphur functionality at the PolyHIPE surface which is expected to make the surface more hydrophilic. This has been assessed in water uptake tools in the next section.

5.3. Water Uptake

Water uptake was measured for the PolyHIPE samples before and after post sulphonation, by immersing the samples in water and measuring the weight before and after immersion. The samples were kept in water for 48 hours until the saturation state was achieved. The water uptake was calculated using Eq 5-1.

$$water\ uptake = (wf - wi)/wi * 100 \qquad Eq\ 5\text{-}1$$

w_f = final weight of PHPs

w_i = initial weight of PHPs

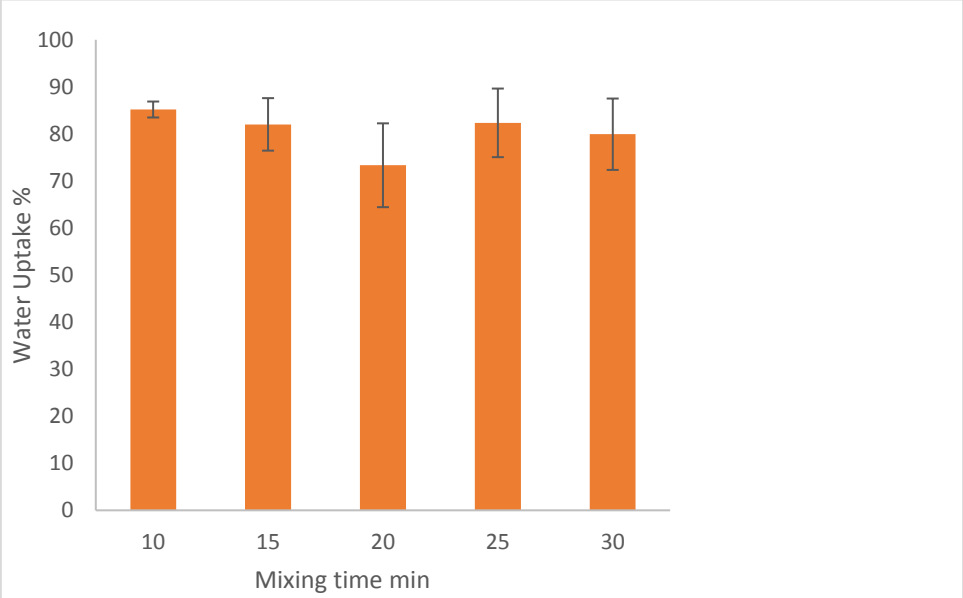

Figure 5-7. Water uptake function of the mixing time before the sulphonation.

For the in situ sulphonation samples the water uptake decrease with mixing time and then rises Figure 5-7. Water uptake thus increases with an increase in the pore size (Feuerabendt et al.) and the size and amount of interconnects between them. But, after post sulphonation the water uptake increases as shown in *Figure 5-8* due to the surface conversion from hydrophobic to hydrophilic (Yee et al., 2013). These results agree with the FTIR results (see Figure 5-2 to Figure 5-6) which demonstrate the increasing in the sulphur content after post sulphonation

which leads to an increase in the hydrophilicity of samples, and thus the water uptake increases. The increase in sulphur content between in situ and post sulphonation has been confirmed by energy dispersive x-ray microanalysis (EDX) in the scanning electron microscope.

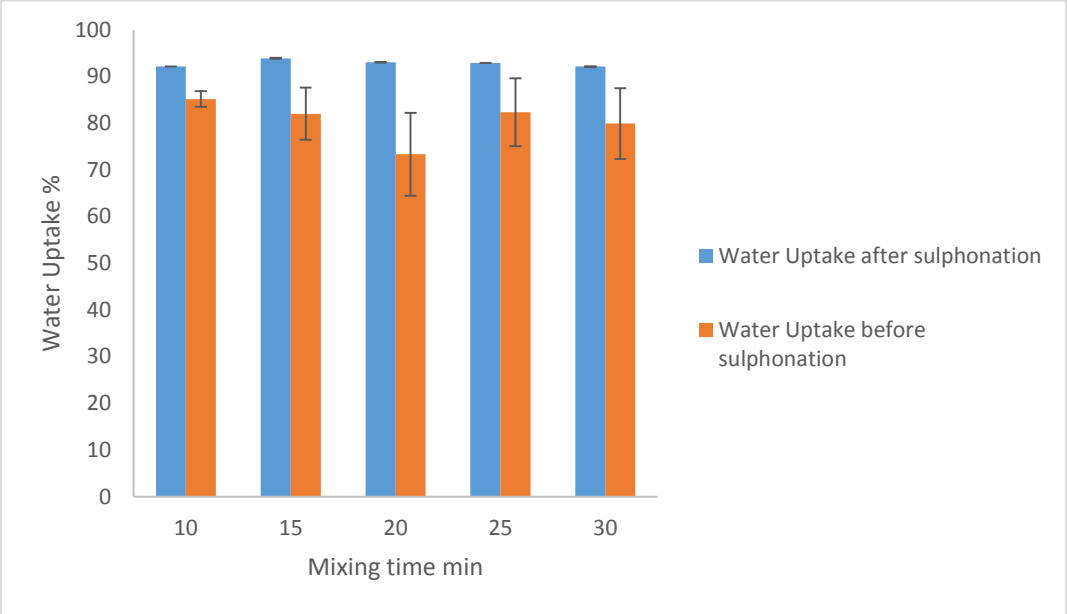

Figure 5-8. Water uptake before and after sulphonation.

Water uptake appears to be dependent on the macropore structure and surface chemistry of the sulphonated PolyHIPE but nano porosity may also have an effect. Thus adsorption isotherms and BET analysis have been carried out on the post sulphonated material (see next).

5.4. Can we measure sulphur content and heavy metal removal from contaminated solutions?

Filtration trials were undertaken to determine what analysis techniques would be required to assess the effectiveness of polyHIPE as an adsorbant filter material. Figure 5-9 shows the EDX spectrum for the PolyHIPE samples with 10 min mixing time after the filtration process (see Chapter 6) when the concentration of nickel in the standard solution was increased to a very high level (160 mg/l). It shows the peaks of elements such as S which originates from the sulphonation process, Na comes from the ion exchange between sodium ions from sodium hydroxide which was used to fix the pH of the solution and H^+ ions from the benzensulphonic acid group according to Eq 5-2, but EDX couldn't detect the nickel ions which mean the concentration of nickel less than 1%.

$$NR - SO_3H + Mn^+ \rightarrow (R - SO3)n\ Mn + \ + nH^+ \qquad \text{Eq 5-2}$$

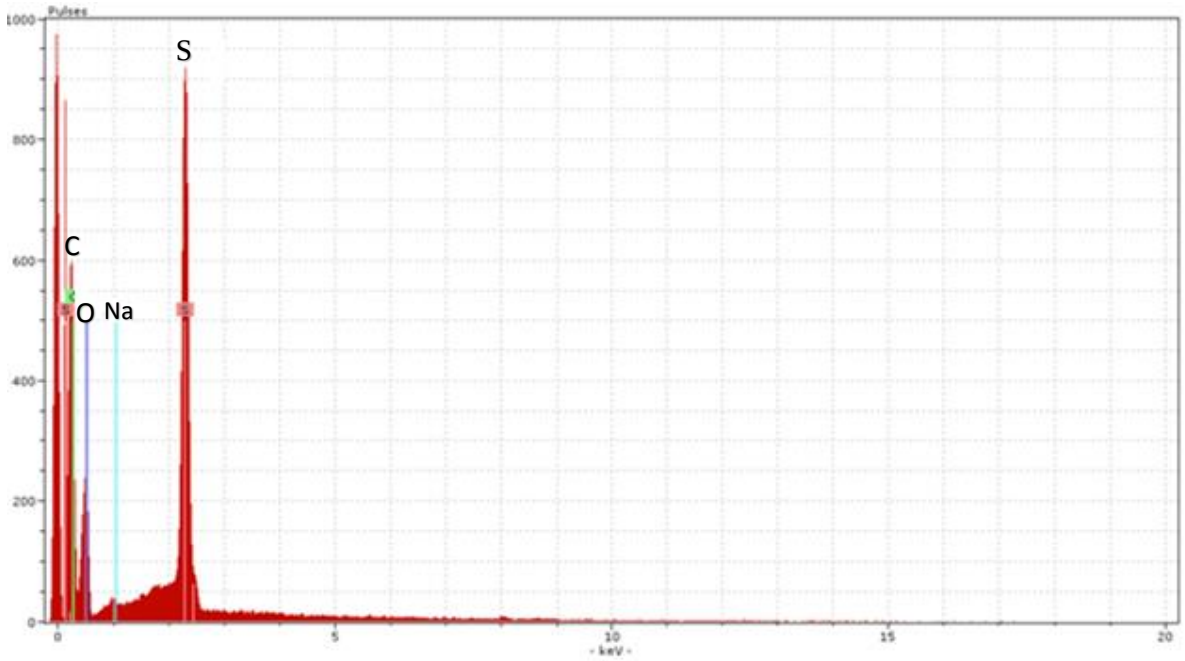

Figure 5-9: Figure: - EDX images for the sample after sulphonation and filtration

Thus nickel needs a more sensitive analysis method and tests have been done to determine if XRF analysis is suitable as discussed in the next section.

5.5. XRF Analysis

X-ray fluorescence measurement has been done to determine the concentration of nickel in the solid beads from the trial experiment when 0.6136 g from the whole sample (which is 3g) was taken for analysis. The results are shown in Table 5-1 and the concentration is presented in terms of arbitrary units. Standard samples with known concentration can be used to convert this to real concentrations and this has been done for nickel and copper here – the reliability of these standards is a significant source of error which may be as high as 25%. The data in Table 5.1 indicate there is 0.26 g of nickel in the PolyHIPE sample demonstrating that the material has acted as an adsorber. Signals from many elements were present in the analysis data – the erroring the analysis is ±20 units so anything with a lower concentration is likely to be experimental error. Concentrations in the range 20-200 units come from environmental contamination. Clearly the most significant element in the analysis is sulphur showing that the

sulphonation process has been successful. There are also significant amounts of phosphorus in the material as well as nickel, calcium, potassium and iron. The potassium comes from the polymerisation initiator (potassium persulphate). The nickel comes from the filtration but the phosphorus and iron are likely contaminants that arise from the fact that the stirred tank used in polyHIPE manufacture has been used to make polyHIPE containing phosphoric acid previously.

Table 5-1. X-ray fluorescence test to measure the concentration of metal in polyHIPE beads

N	Symbol.	Name	C.ppm
0	L.O.I.	Loss of Ignition	906216.6
1	Si	Silicon	86.3
2	P	Phosphorus	743.1
3	S	Sulfur	90502.1
4	Cl	Chlorine	52.2
5	K	Potassium	282.7
6	Ca	Calcium	166.9
7	Ti	Titanium	4.5
8	Fe	Iron	278.6
9	Ni	Nickel	434
10	Zn	Zinc	402.5

XRF appears to be a suitable method for metal analysis in the polyHIPE samples to be tested in the next chapter.

5.6. Adsorption Desorption Isotherm and BET analysis

Figure 5-10 to Figure 5-13 show the adsorption desorption isotherms for PolyHIPE samples with different mixing time after the post sulphonation process. The form of the curve is same as for the sample before the sulphonation process as show in Figure 4-10 to Figure 4-14. Type II isotherms are observed with initial monolayer adsorption followed by multilayer adsorption at higher pressures of nitrogen. All samples show a reversible isotherm and no hysteresis in any of them, except with sample with 15 min mixing time which has hysteresis due to capillary condensation at mesopores, which corresponds to a type IV isotherm in the IUPAC classification (Sing et al., 1985; Gregg and Sing, 1982). Capillary condensation processes

happen on the PolyHIPE surface at a lower pressure than that which is required to reach the saturation state for the surface by vapor. As a result, capillary walls are covered with a liquid layer. Normally adsorption hysteresis occurs on solids with pores which give different mechanisms of adsorption and desorption.

The isotherm shows that the structure has mesopores where physisorption happens and it is in condition capillary condensation and monolayer-multilayer adsorption. All samples show that the adsorption isotherm was rapidly increasing which is due to macropores of large size which agrees with the SEM images as shows in Figure 5-1. All the samples, except the sample with 15 min mixing time (see Figure 5-11), show that there is no hysteresis in the isotherm due to the macropores dominating mesopores which agrees with the SEM images as show in Figure 5-1(Sing et al., 1985).

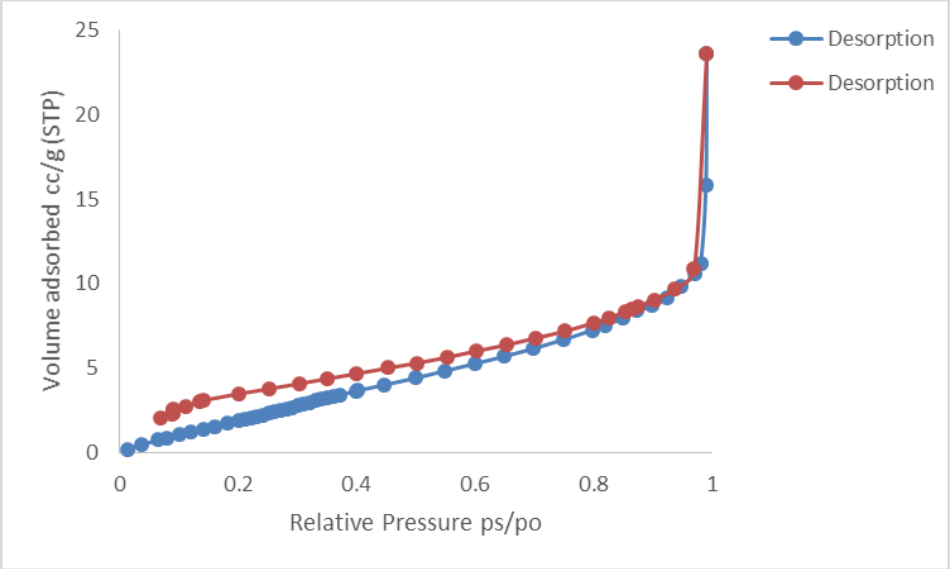

Figure 5-10. Isotherm plot for surface area and pore size analysis of PHP with 10 mixing time after sulphonation, when Relative pressure is sample pressure (ps) over saturation pressure (po)

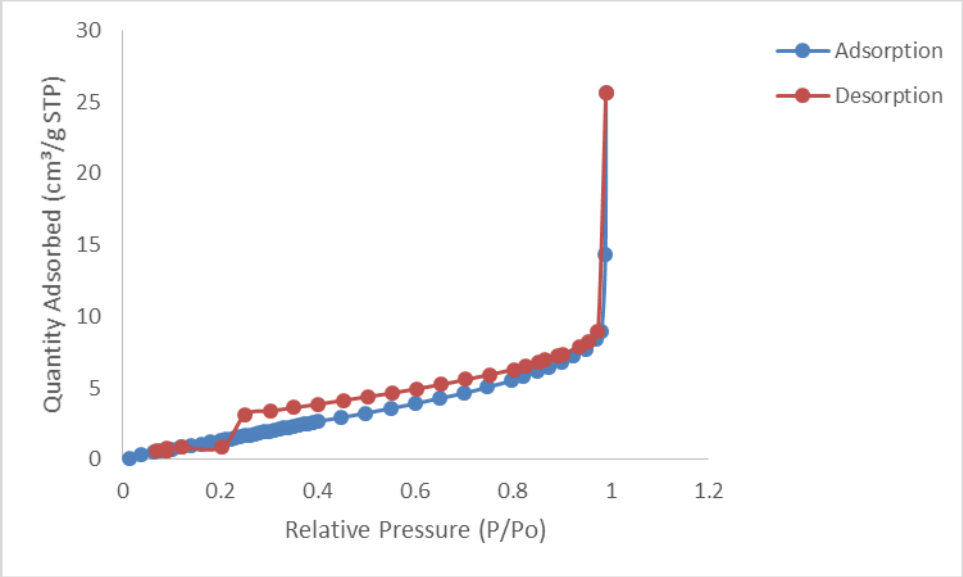

Figure 5-11. Isotherm plot for surface area and pore size analysis of PHP with 20 mixing time after sulphonation, when Relative pressure is sample pressure (ps) over saturation pressure (po)

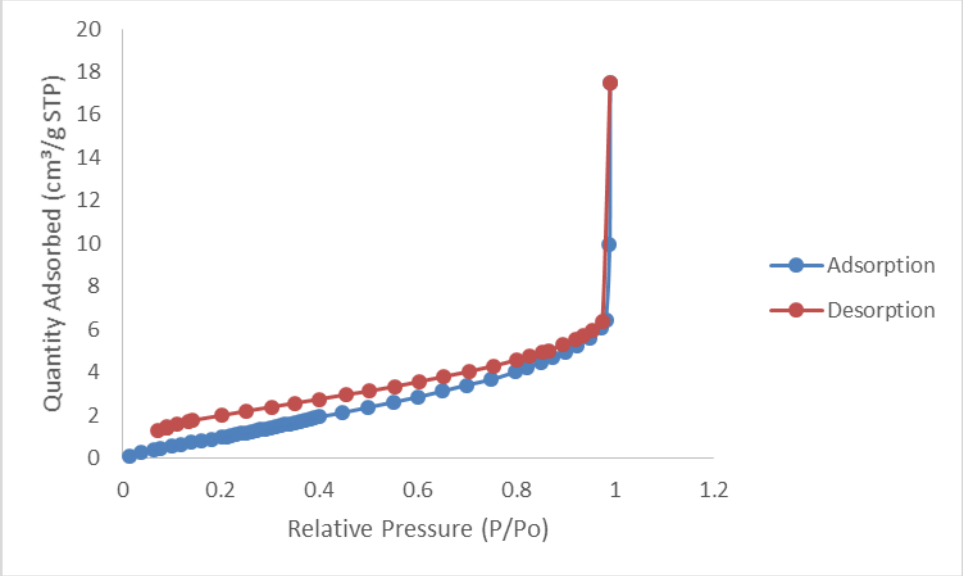

Figure 5-12. Isotherm plot for surface area and pore size analysis of PHP with 25 mixing time after sulphonation, when Relative pressure is sample pressure (ps) over saturation pressure (po)

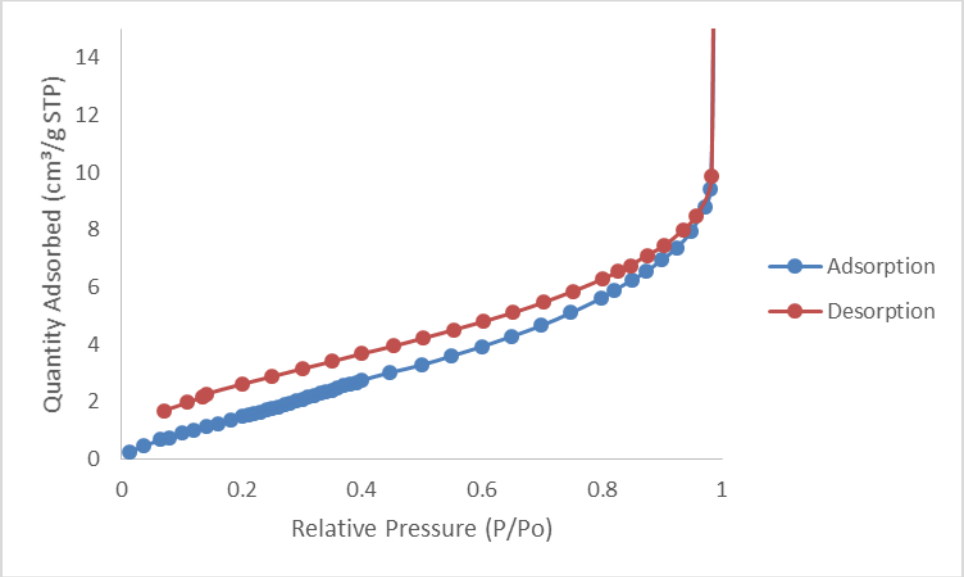

Figure 5-13. Isotherm plot for surface area and pore size analysis of PHP with 30 mixing time after sulphonation, when Relative pressure is sample pressure (ps) over saturation pressure (po)

Figure 5-14, Figure 5-15 and Figure 5-16 show the average pore size, the average pore volume and the average surface area measured by BET from the adsorption isotherm for polyHIPE after post sulphonation. Before sulphonation the surface area was 10 m^2/g and the pore volume was 0.0129 cm^3/g but after sulphonation the surface area increased up to 11.9 m^2/g and the pore volume to 0.0156 cm^3/g

It clearly shown that the adsorption process take place in the macroporous structure of PolyHIPE and the adsorbate-absorbant and adsorbate–adsorbate interaction was strong and weak respectively when we compare it with standard curves Figure 3-14 as explained in chapter three (Sing, 1994). Figure 5-14, Figure 5-15 and Figure 5-16 show that the sample with 15 min mixing time has higher surface area and smaller pore size and pore volume than the others which means the behavior after the post sulphonation process is approximately the same as before; these results show no large differences before and after sulphonation which agrees with research done previously (Hasan, 2013). In addition to that these figures clearly show that the sample with 10 min mixing time after sulphonation has larger pore volume and surface area and pore size, which explains the water adsorption value as shown in Figure 5-8 so it was used for the filtration process assessment in the next chapter.

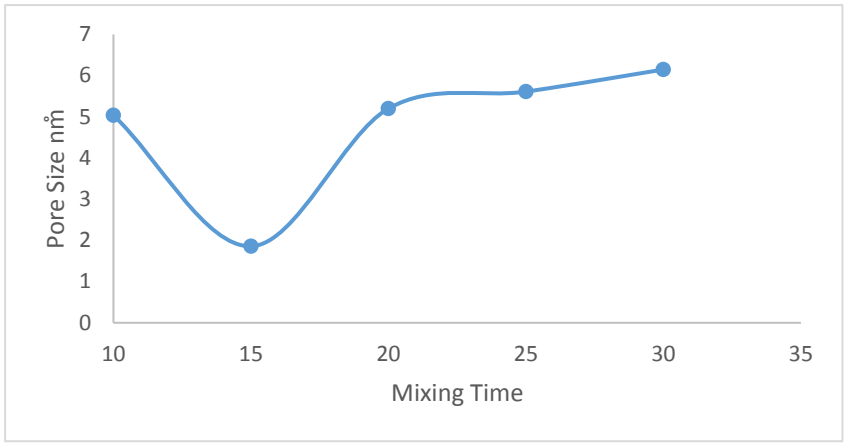

Figure 5-14. Average pore size for PolyHIPE structure determined from BET. The figure plotted from single data

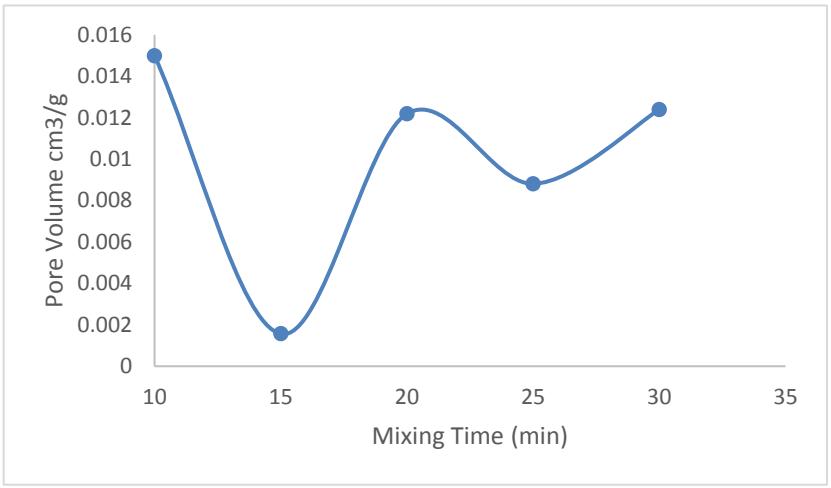

Figure 5-15. Average pore size for PolyHIPE structure determined from BET. The figure plotted from single data

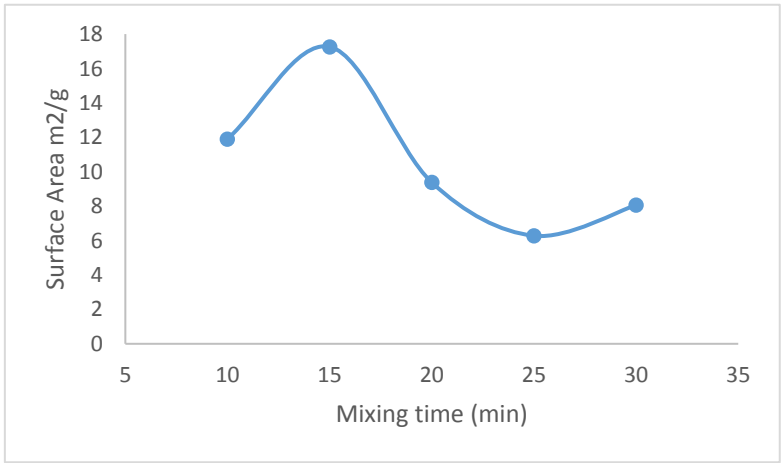

Figure 5-16. Average pore size for PolyHIPE structure determined from BET analysis. The figure plotted from single data

5.7. Summary

Post sulphonation has increased the water uptake by converting the PolyHIPE structure from low hydrophilic to high hydrophilic. This is clear from FTIR results by the increase in the sulphonate peaks intensity compared with the PolyHIPE samples with in situ sulphonation. Additionally, more (SO_3H) groups are added to the structure, which are considered as strong cation exchangers and thus can be used to remove heavy metals such as nickel and copper from water as shown in next chapter.

6. Filtration studies

The previous chapter has shown that the surface area of PolyHIPE is not changed very much by processing but the macropore structure and water transport into the material is controlled by mixing time and the sulphonation method. Water penetrates the PolyHIPE and there is large surface area for ion exchange or adsorption. Thus filtration studies were undertaken with 3 g of the PolyHIPE beads after the sulphonation process placed in plastic tube, then the solution was passed through the samples by a pump for 8 hours.

6.1. Removal Efficiency

The removal efficiency was calculated after filtration by using PolyHIPE beads after sulphonation with three solutions containing (Ni^{+2} (20mg/l), Cu^{+2} (20 mg/l) and (Ni^{+2} (10mg/l) + Cu^{+2} (10 mg/l)) respectively. Each system will be discussed in individual sections where the removal efficiency was calculated according to Eq 6- below.

$$\text{Removal efficiency (\%)} = \frac{Ci - Cf}{Ci} \times 100 \qquad \text{Eq 6-1}$$

Ci: - Initial concentration of metal (mg/l)

Cf: - Final concentration of metal (mg/l).

6.2. Nickel Removal Efficiency

Benzenesulfonic acid groups as shown in Figure 6-1, might be present in the PolyHIPE structure after sulphonation and are a strong cation exchanger, so are widely used in removing cations from waste water. They have strongly acidic behavior. The SO_3H can lose H^+ ion and thus act as an exchanger for metal cations (Kearney and Rearick, 2003).

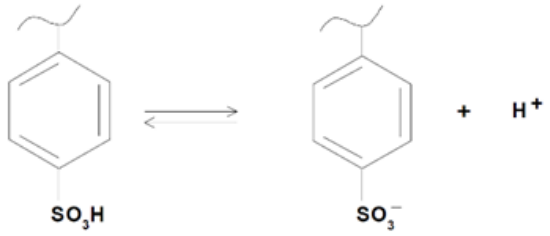

Figure 6-1. Structure of Strong Acid Cation Exchange Resin (Kearney and Rearick, 2003)

Post sulphonated PolyHIPE samples with 10 (min) mixing time were washed twice by using the soxhlet as shown in chapter three (3.2) and were then used for the removal efficiency analysis. From Figure 6-2, it can be seen that the removal efficiency is constant with increasing the pH from 6 to 8. It might be expected that increasing removal of nickel with increasing pH would occur due to the reduced concentration of hydrogen ions with the increasing the pH value. As a result of that, the competition between H^+ and nickel ions towards the active sites (SO_3H) groups available in the PolyHIPE structure reduces (Ismail et al., 2012). However, it seems from the results here that the dominant factor is the number of available sites and there are plenty to exchanging with the metal.

Furthermore, changing the pH of the solution may lead to new compound formation such as nickel hydroxide at pH 8.2, which precipitate at the bottom of the container (Gupta et al., 2003). Therefore the removal efficiency decreases after pH 8 as is observed to a small extent in Figure 6-2. The interaction mechanism between Benzenesulfonic acid groups and nickel could follow Eq 6-2 and Eq 6-3 (Cheremisinoff, 2001). The best removal efficiency was at pH 8 (0.83) but this was still above the acceptable limit specified by the world Health Organization which is about 0.07 mg/l (Edition, 2011).

$$2(R-SO_3H)+NiSO_4 \rightarrow (R-SO_3)2Ni+H_2SO_4 \quad \text{Eq 6-2}$$

$$NR-SO_3H+M^{n+} \rightarrow (R-SO_3)n\,M^{n+}+nH^{+} \quad \text{Eq 6-3}$$

Where R is the monomer , N is number of unit , n
atomic number

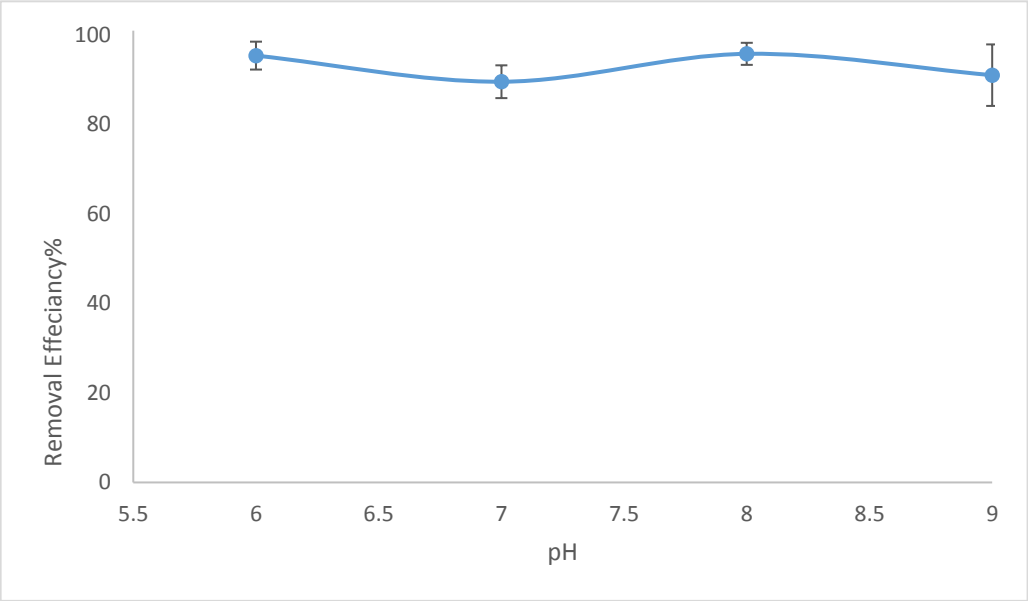

Figure 6-2. Removing efficiency versus pH for PolyHIPE sample after sulphonation and filtration with 20 ppm nickel solution.

Figure 6-2 and Table 6-1 shows the remaining concentration of nickel ions in solution (as determined by ICP) as a function of pH. The lowest concentration is achieved at pH 8. This may be attributed to the high concentration of H^+ ions at pH6. The interaction between heavy metals and functional groups is due to the tendency of these heavy metals to be attracted towards functional groups with high electron density (Benzenesulfonic acid) to make chemical bonds. Additionally, bonding between the strong positive charge and the multiple functional group may be arising in the same time (Rivas et al., 2003). The concentration of nickel before and after filtration Table 6-2. The ICS-1000 (Ion Chromatography System) was used to measure the concentrations of other anions after the filtration process with (20mg/l) of nickel solution, and the results (see Table 6-1, Figure 6-4 and Figure 6-5) show that, the concentrations of all of these ions is below the acceptable limits determined by the World Health Organization,(Edition, 2011).

Table 6-1. Concentration of anions in water after filtration

PH	Fluoride	Chloride	Nitrite	Bromide	Sulphate	Nitrate	Phospate
6	0.346	18.81	2.81	3.55	426.54	161.28	6.51
7	0.174	3.70	1.20	1.76	168.06	67.63	1.20
8	0.176	4.52	1.28	1.58	256.87	98.78	2.62
9	0.172	3.32	0.95	1.12	179.53	53.75	2.13
c. in deionised water	n.a.	n.a.	n.a.	n.a.	n.a.	n.a.	n.a.
Acceptable Limit(mg/l)	Not concern	70 mg/L	3	Not concern	Not concern	50	Not concern

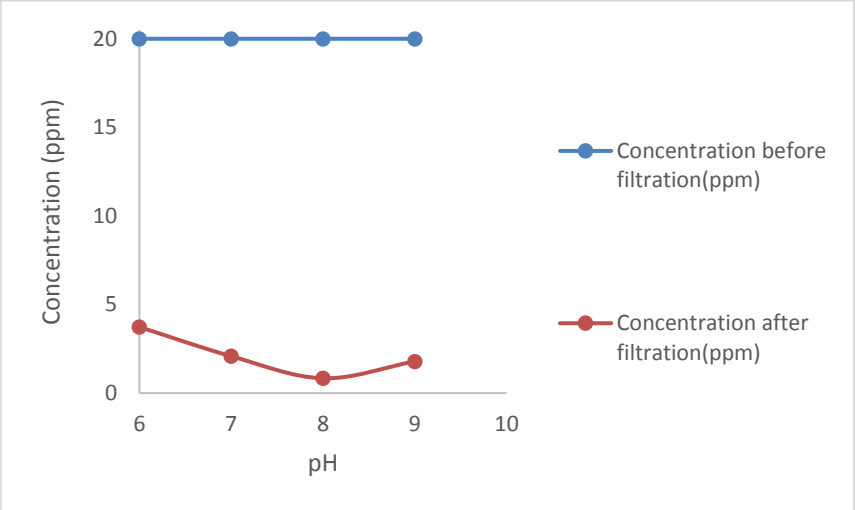

Figure 6-3. Show the change in the concentration of Nickel ions before and after filtration

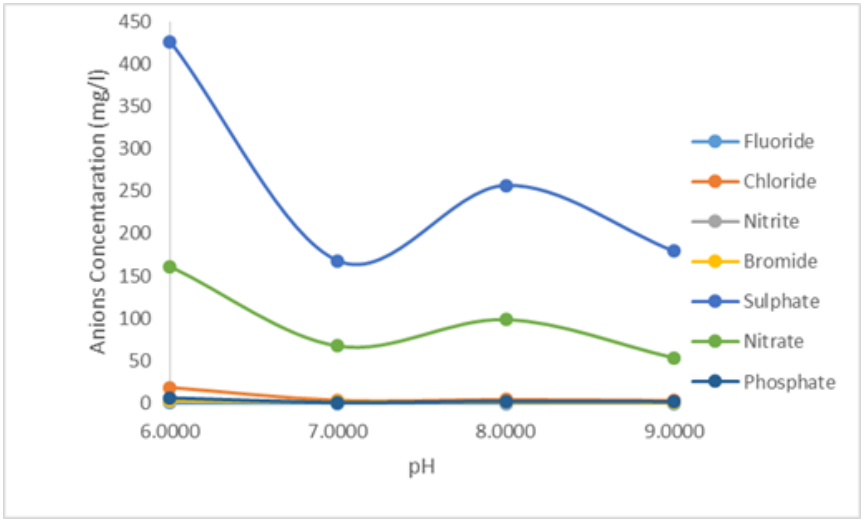

Figure 6-4 show the change in the concentration of anions before and after filtration

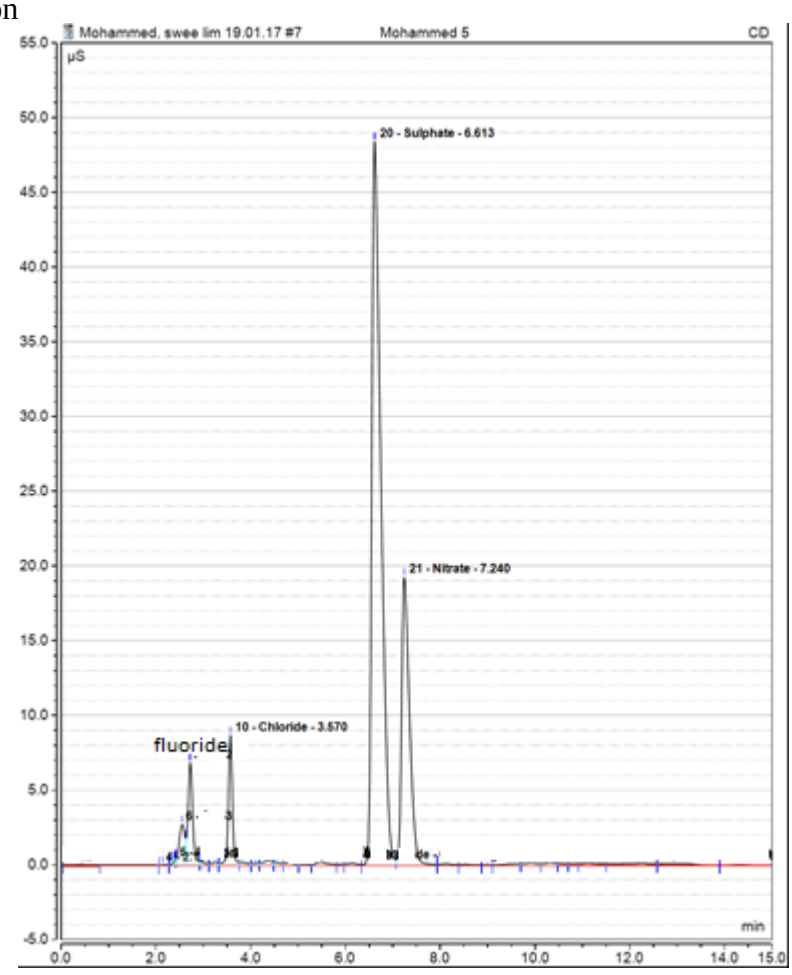

Figure 6-5. IC for anions is a Dionex ICS-1000 with an AS40 auto sampler for the samples after filtration with PolyHIPE beads after sulphonation.

Figure 6-5 shows the results from Ion chromatography on the filtered solution that shows that the sulphate peak was highest when compared with other anions which may be due to unreacted sulphuric acid within PolyHIPE structure and the release of sulphate groups from the material during filtration.

6.3. Removal Efficiency after Total Washing

The washing process for PolyHIPE beads was repeated many times to reduce the concentration of sulphate in the solution after filtration. The process was repeated until the pH of the deionised water which was used for washing was the same pH value before and after washing. The removal efficiency was increased as shown in Figure 6-6 compared with the last results (see Figure 6-2), which may be attributed the effect of unreacted sulphuric acid, when it reacted with the Ni^{2+} shown in..Eq 6-4 below (Fierro et al., 2008) but the compound is removed after filtration. However, the removal efficiency for nickel ions by PolyHIPE after sulphonation still has maximum value at pH 8 as in last results which were obtained after twice washing as shown in Figure 6-2. Then it plateaus it due to the formation of nickel hydroxide at pH 8.2 because of the decrease in the concentration of free nickel ions in the solution (Gupta et al., 2003).

$$Ni + H_2SO_4 \rightarrow NiSO_4 + H_2 \quad \text{..Eq 6-4}$$

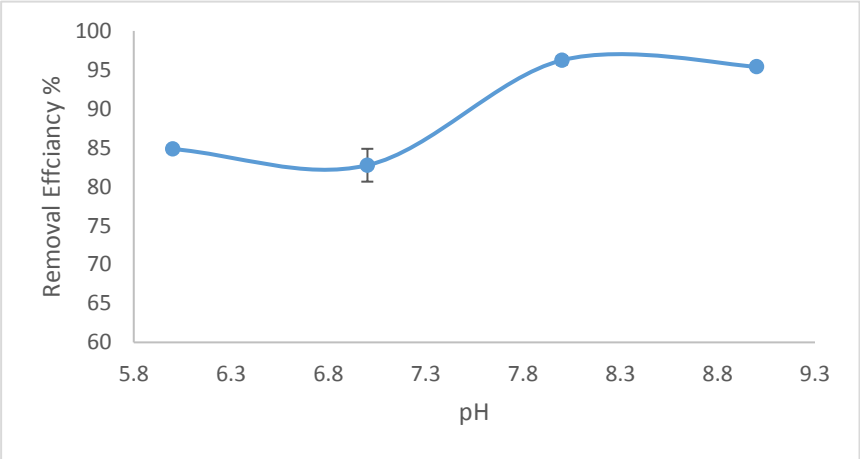

Figure 6-6.Removal efficiency for Nickel with the pH after total washing of the sample

Figure 6-3 and figures Figure 6-7 to Figure 6- show the concentration of anions in the solution after the washing and filtration process with a nickel standard solution of 20mg/l. The concentration is reduced to an average value of approximately 157 mg/l, which is below the acceptable limit determined by The World Health Organization (see Table 6-1). This filtration was done after total washing for PolyHIPE beads after sulphonation process, until the pH for distilled water was the same before and after the washing process, while the concentration of

sulphate after only twice washing was approximately 2248 mg/l Table 6-2. This means that the PolyHIPE beads need complete washing until the pH is the same for the solution before and after washing it they are to be used. The concentration of other anions is considered low in both cases which means it came with the distilled water and equipment that was used to prepare the nickel standard solution and not from PolyHIPE structure itself.

No. ECD_1	Peak Name ECD_1	Amount ppm pH6	Amount ppm PH7	Amount ppm PH8	Amount ppm pH9	c.anions in deionised water
1	Fluoride	0.76	0.09	0.39	0.15	n.a.
2	Chloride	3.62	1.24	11.14	2.06	n.a.
3	Nitrite	n.a.	0.58	n.a.	n.a.	n.a.
4	Bromide	n.a.	n.a.	n.a.	n.a.	n.a.
5	Nitrate	58.68	109.27	57.10	74.99	n.a.
6	Phosphate	n.a.	n.a.	n.a.	n.a.	n.a.
7	Sulphate	133.29	141.41	191.08	165.33	n.a.

Table 6-2. Ion chromatography measurement for the solution after total washing and filtration with 20mg/l nickel solution with different pH

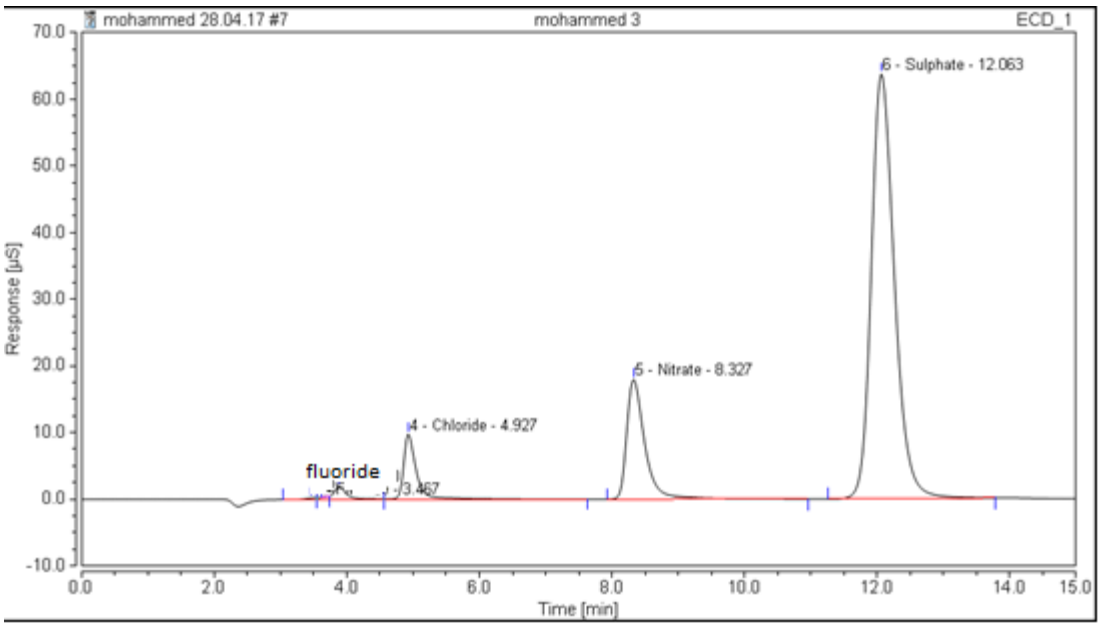

Figure 6-7. Ion chromatography measurement for the solution after total washing and filtration with 20mg/l nickel solution at pH6

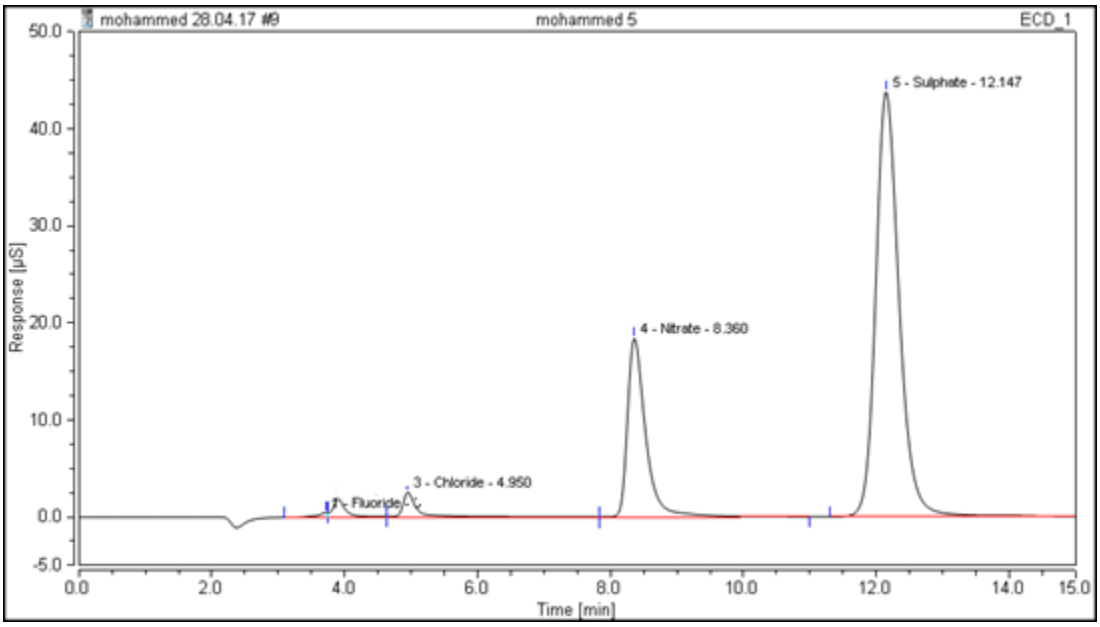

Figure 6-8. Ion chromatography measurement for the solution after total washing and filtration with 20mg/l nickel solution at pH7

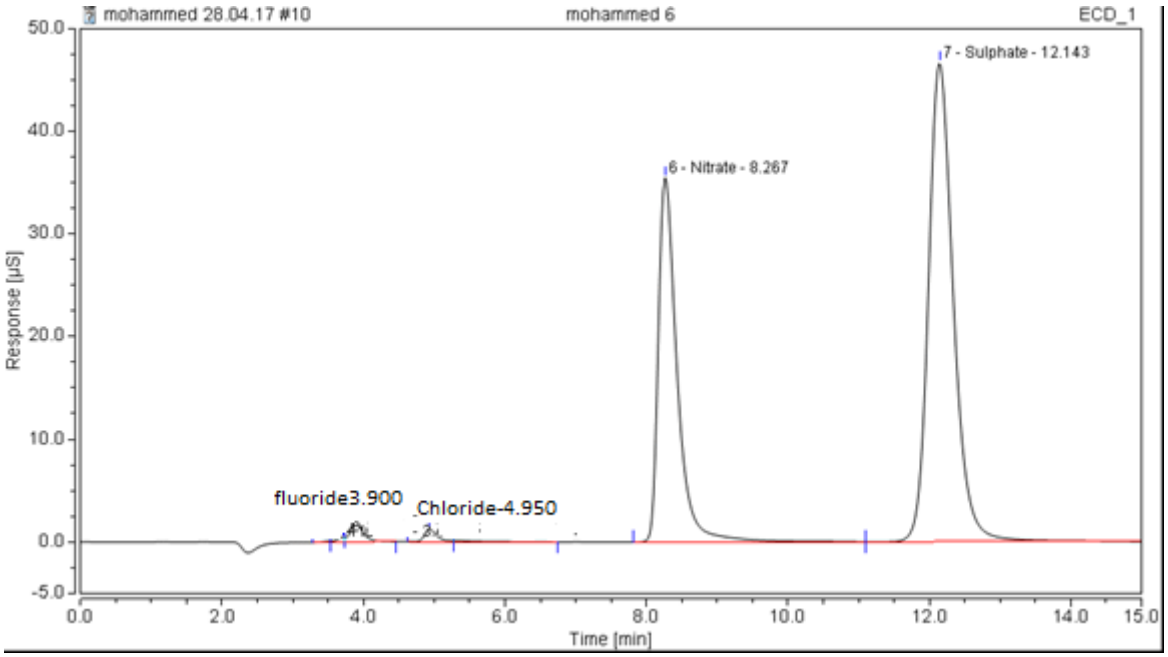

Figure 6-9. Ion chromatography measurement for the solution after total washing and filtration with 20mg/l nickel solution at pH8

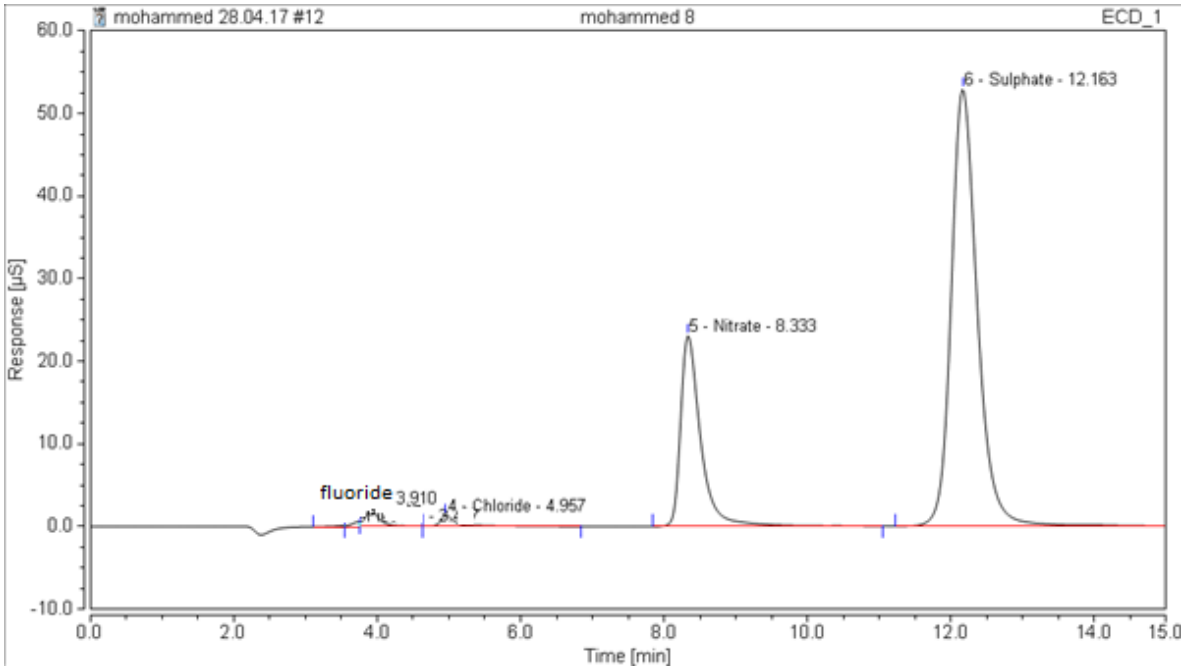

Figure 6-10. Ion chromatography measurement for the solution after total washing and filtration with 20mg/l nickel solution at pH9

Figure 6-7 to Figure 6- show the peaks for many anions like nitrate, chloride and sulphate etc. These peaks represent the anion concentrations in the water after the filtration process with nickel standard solution by PolyHIPE after post sulphonation. The results show that nitrate and sulphate have the highest concentration due to using nickel nitrate in the preparation step for the nickel standard solution, while the sulphate comes from unreacted sulphuric acid within the PolyHIPE beads. Other anions are shown in Table 7-3 which come from the deionized water since the PolyHIPE after sulphonation is considered as a strong cation exchanger, so these anions do not have the ability to react with it, and therefore are still in the water after the filtration process.

6.4. X-ray fluorescence

In the filtration process 50ml of nickel solution with 20mg/l concentration was used, and in the previous section the ICP test shows that the majority of the nickel bonds with the PolyHIPE beads after the sulphonation process. Therefore, XRF has been used to measure the concentration of nickel in the solid beads when 1.216 mg from the whole sample (which is 3g) was analysed. The results shown in there is Table 6-3 1.22 mg of nickel in the PolyHIPE sample, this confirms the ICP results which show that most of the nickel bond with the beads. A simple calculation would indicate for 100% nickel removal there should be 1mg of nickel in the 3g sample so these results suggest that that complete removal has taken place. The fact that XRF indicates more nickel that was in the standard solution implies that there are other sources of nickel which contribute to the results (e.g. from corrosion of the stainless steel mixing chamber during PolyHIPE preparation with acid in the aqueous phase) or may be due to experimental scatter in the XRF measurements. The nickel concentration in the beads used in this test may not be uniform. Excess nickel may also come from the tools which were used to set up the experiment. However the amount of nickel in this sample higher than the sample with single washing as mentioned in section 6.1.This results agree with increasing the removal efficiency for the sample after total washing. In addition to that there are many metals in the solution which come from deionized water such as calcium and there may be some nickel in this as well.

Table 6-3. X-ray fluorescence test to measure the concentration of metal in polyHIPE beads after total washing with distilled water.

N	Symbol.	Name	C.ppm
1	S	Sulfur	62164.1
2	Cl	Chlorine	29.4
3	K	Potassium	271.7
4	Ca	Calcium	176.1
5	Ti	Titanium	4
5	Cr	Chromium	6.5
6	Mn	Manganese	10.2
8	Ni	Nickel	552.1

6.5. Copper Removal Efficiency

The removal of copper after post sulphonation follows the mechanism shown in equation Eq 6-3, in that Benzenesulfonic acid replaces two hydrogen ions (H^+) with copper ions. However, from Figure 6-8 it can be seen that, the removal efficiency increases with increasing the pH and the maximum value was at pH 9 and it reaches values specified by the World Health Organization acceptable concentration Guideline value which is (2mg/l) (Edition, 2011). At the pH range 6.2 to 6.8 copper hydroxide ($Cu(OH)_2$) starts to form (Vengris et al., 2001). Therefore, the removal efficiency decreases above pH 7. The high removal efficiency at pH 9 might be due an insufficient amount of copper in solution for precipitation processes (Arai, 2008, Eick and Fendorf, 1998, Rajapaksha et al., 2012). However, there are enough free ions in the solution to participate in the ion exchange process.

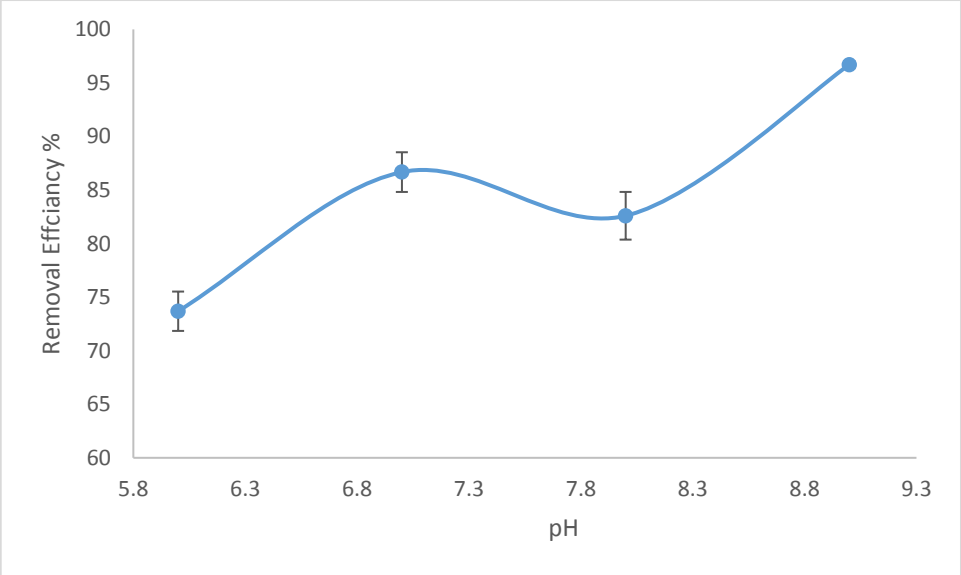

Figure 6-8. Removal efficiency of copper with pH

Table 6-4 and figures Figure 6-7 to Figure 6- show the concentration of anions in the solution after the filtration process with copper standard solution of 20mg/l concentration. The calculation of sulphate anions is higher than the nickel ions and represents material not completely washed from the PolyHIPE. This filtration was done after total washing of the PolyHIPE beads after the post sulphonation process, when the pH for the distilled water wash was the same before and after the washing process. The concentration of other anions is considered low in both cases which means it came with the distilled water that was used to prepare the nickel standard solution and not from the PolyHIPE structure itself.

Table 6-4. Ion chromatography measurement for the solution after total washing and filtration with 20mg/l copper solution with different pH

No.	Peak Name	Amount ppm pH6	Amount ppm pH7	Amount ppm pH8	Amount ppm pH9	c.anions in deionised water
1	Fluoride	0.6888	0.0805	0.5979	0.5588	n.a.
2	Chloride	137.5765	53.9419	181.2654	156.0115	n.a.
3	Nitrite	15.1404	20.7777	22.0251	17.8086	n.a.
4	Bromide	n.a.	n.a.	n.a.	n.a.	n.a.
5	Nitrate	22.7443	9.0026	4.1526	6.3466	n.a.
6	Phosphate	n.a.	n.a.	n.a.	n.a.	n.a.
7	Sulphate	140.2268	374.6893	226.2583	66.9112	n.a.

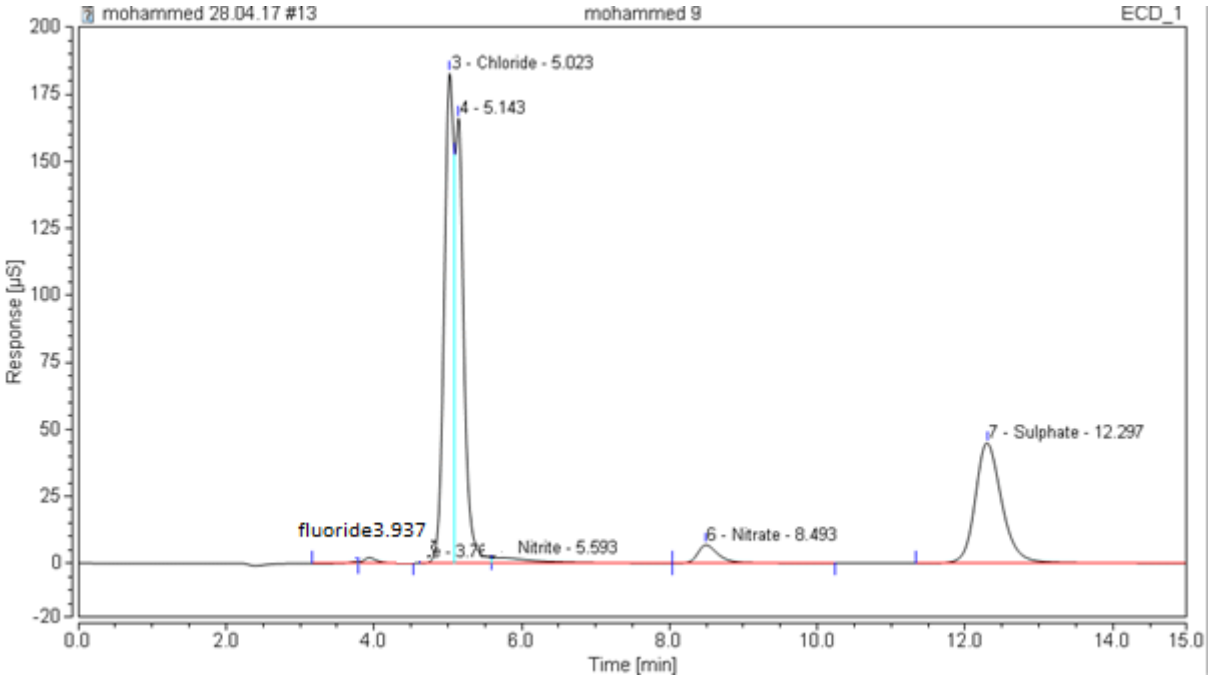

Figure 6-9. Ion chromatography measurement for the solution after total washing and filtration with 20mg/l copper solution at pH9

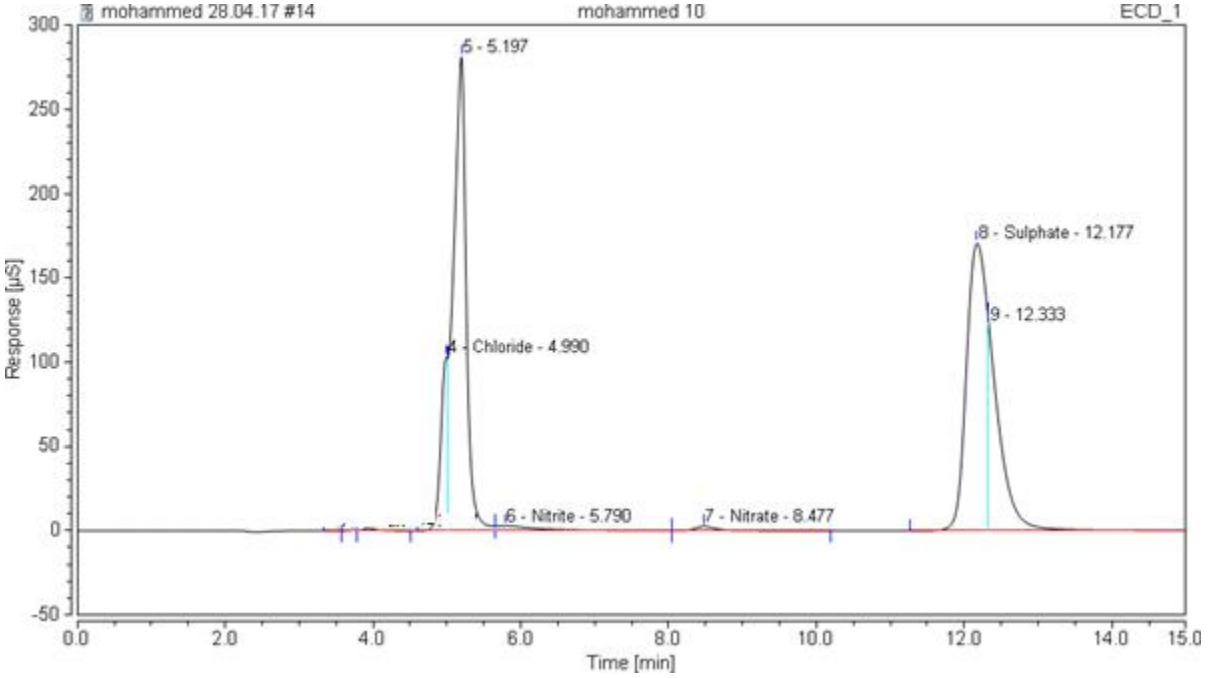

Figure 6-12. Ion chromatography measurement for the solution after total washing and filtration with 20mg/l copper solution at pH9

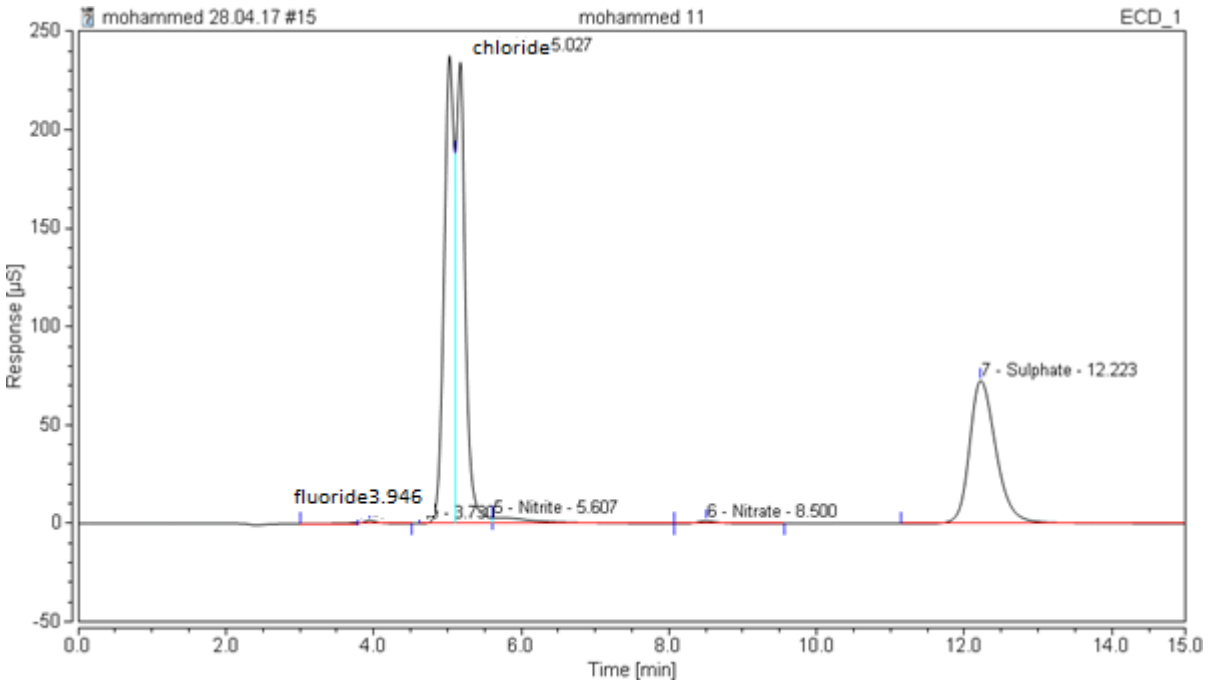

Figure 6-13. Ion chromatography measurement for the solution after total washing and filtration with 20mg/l copper solution at pH9

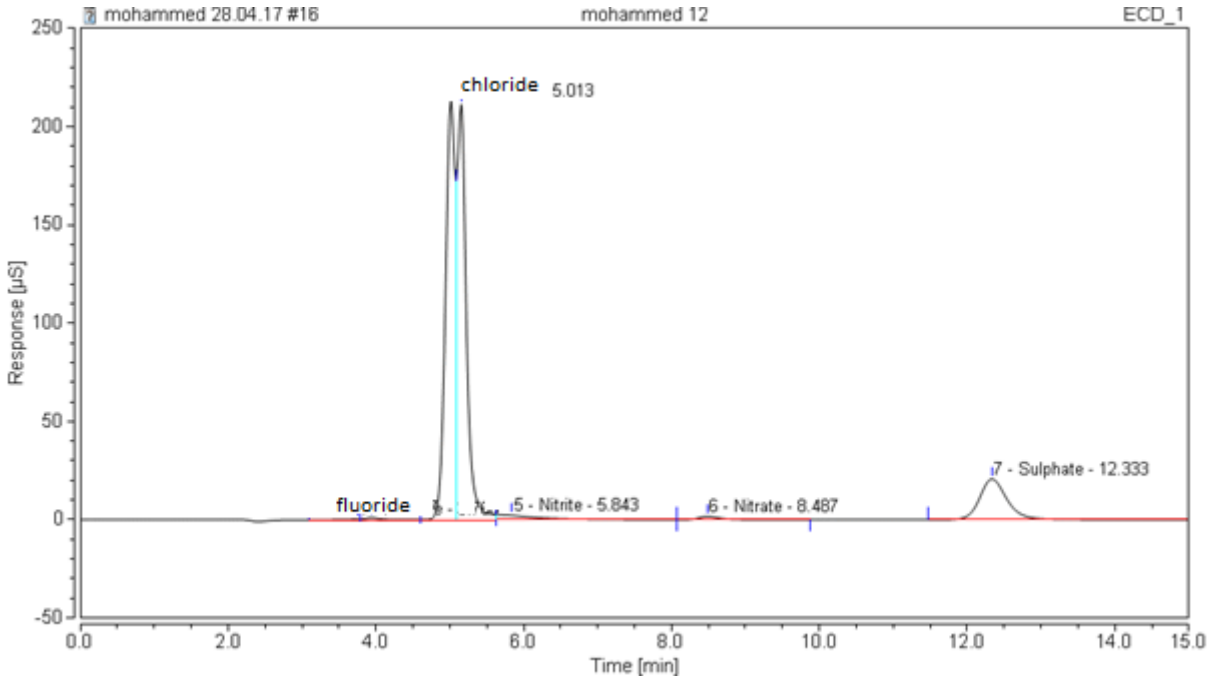

Figure 6-14. Ion chromatography measurement for the solution after total washing and filtration with 20mg/l copper solution at pH9

Figure 6-7 to Figure 6-14 show the peaks for many anions like nitrate, chloride and sulphate etc. This peaks represent the anions concentrations in the water after the filtration process with nickel standard solution by PolyHIPE after sulphonation. The results show that chloride, nitrate and sulphate have the highest concentration due using nickel nitrate in the preparation step for

the nickel standard solution, while the sulphate comes from unreacted sulphuric acid within the PolyHIPE beads. Other anions such as chloride as show in Table 7-3 come from the deionized water. Due PolyHIPE after sulphonation being considered as a strong cation exchanger, so these anions do not have the ability to react with it, therefore are still in the water after the filtration process.

6.6. X-ray fluorescence

In the filtration process 50ml of copper solution with 20mg/l was used. The ICP test shows that the majority of copper is bound with the PolyHIPE beads after the sulphonation process. Therefore X-ray fluorescence analysis has been done to measure the concentration of copper in the solid beads when 0.25 g from the whole sample (which is 3g) was taken for the test. The results shown in Table 5-1 indicate there is 1.44 g of copper in the total PolyHIPE sample, this supports the ICP results which show that most of the copper is bound with the beads. As in the case for nickel the amount of copper in the sample is greater than the total amount in the solution (1g) probably due to a combination of experimental error and other sources of copper contamination.

Table 6-6. X-ray fluorescence test to measure the concentration of metal in polyHIPE beads after total washing with distilled water.

N	Symbol.	Name	C.ppm
0	L.O.I.	Loss of Ignition	980463.8
1	S	Sulfur	12825.6
2	Cl	Chlorine	37.6
3	K	Potassium	44.6
4	Ca	Calcium	80.4
5	Ti	Titanium	1.8
6	Cr	Chromium	7.6
7	Mn	Manganese	4.1
8	Fe	Iron	184.4
9	Ni	Nickel	45.1
10	Cu	Copper	3183.8

6.7. Binary System (Nickel and Copper) Removal Efficiency

In this experiment both nickel and copper ions were in the solution before filtration and the ratio was 50/50 for each one (10mg/l Ni^{++} and 10 mg/l Cu^{++}). The removal efficiency behaviour of the two metals is shown in Figure 6-10 and follows approximately the behaviours as the same single metal ion system when the concentrations of these metals was 20 mg/l as shown in Figure 6-6 and Figure 6-8, except at pH 8 when the removal efficiency for nickel is at minimum value instead of constant in the single system which may be attributed to the formation of cooper hydroxide at pH between 6.2 and 6.8, which is less than the pH required to form nickel hydroxide (pH=8.2) (Vengris et al., 2001, Gupta et al., 2003). This copper hydroxide may act as barrier between nickel and the active sites. At pH higher than 8 and close to 9.5 the amount of nickel and copper in solution may not be enough for the precipitation processes, because the precipitation process required a certain minimum concentration of metal in the water to occur (Arai, 2008, Eick and Fendorf, 1998, Rajapaksha et al., 2012, Gupta et al., 2003, Ismail et al., 2012). Thus there were more free ions in the solution which participate in the ion exchange process leading to an increase of the removal efficiency.

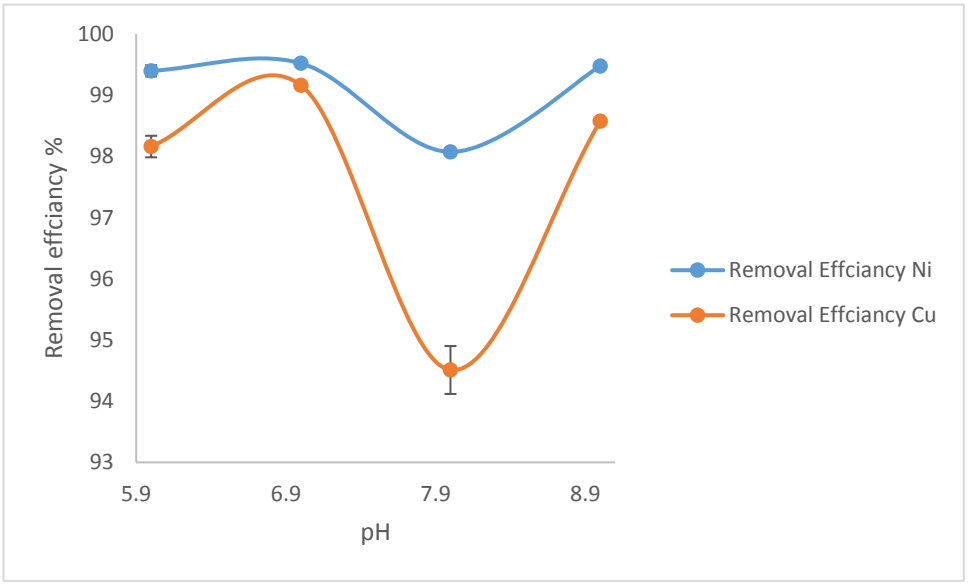

Figure 6-10. Removal efficiency of copper and nickel in a binary system with pH

Table 6-5 and figures Figure 6-7 to Figure 6- show the concentration of anions in the solution after the filtration process with the mixed solution. This filtration was done after total washing for PolyHIPE beads after the post sulphonation process, when the pH for distilled water was the same before and after washing process. The sulphate concentration is lower than for either of the single metal ion cases. The concentration of other anions is considered low in both cases which means it came with the distilled water that was used to prepare the nickel and copper standard solutions and not from the PolyHIPE structure itself.

Table 6-5. Ion chromatography measurement for the solution after total washing and filtration with 20mg/l nickel-copper solution with different pH

No.	Peak Name	Amount ppm PH6	Amount ppm PH7	Amount ppm Ph8	Amount ppm pH9	Deionised water
1	Fluoride	0.2843	0.2772	n.a.	0.3641	n.a.
2	Chloride	76.2304	77.0584	5424	82.5840	n.a.
4	Nitrite	10.2637	7.3523	n.a.	8.4178	n.a.
5	Bromide	n.a.	n.a.	n.a.	n.a.	n.a.
6	Nitrate	20.6539	22.6833	5036	25.1010	n.a.
7	Phosphate	n.a.	n.a.	n.a.	n.a.	n.a.
8	Sulphate	116.4835	82.3613	58.93	91.7272	n.a.

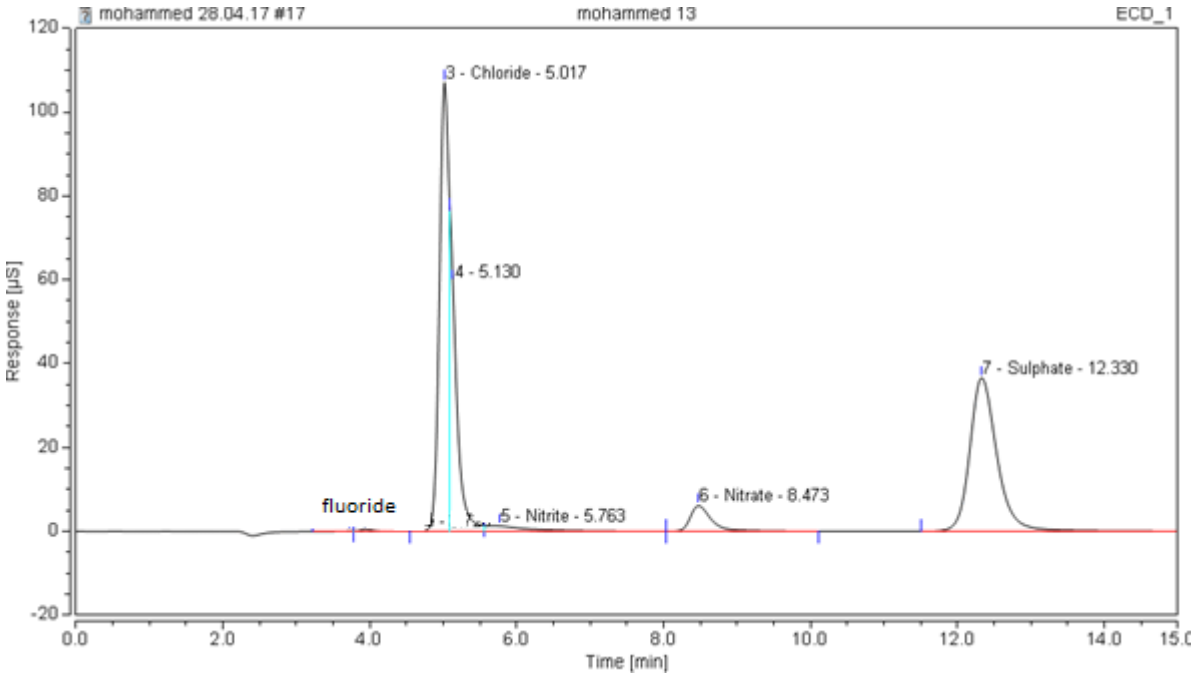

Figure 6-11. Ion chromatography measurement for the solution after total washing and filtration with 20mg/l nickel-copper solution at pH6

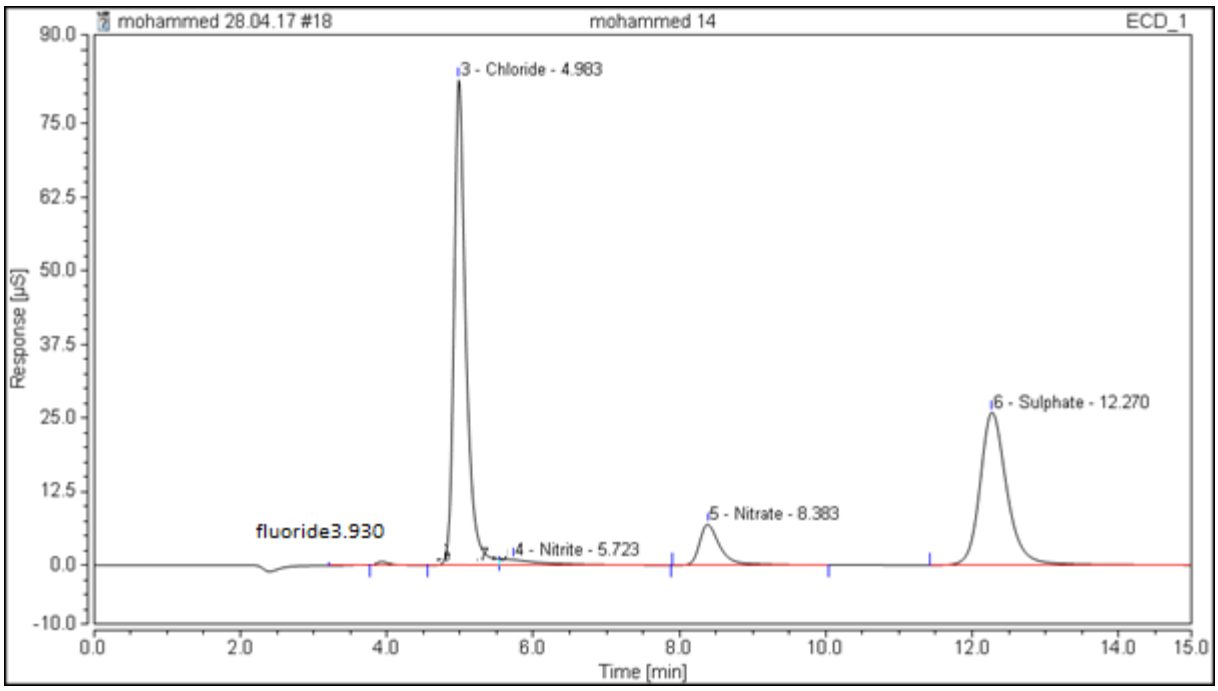

Figure 6-12. Ion chromatography measurement for the solution after total washing and filtration with 20mg/l nickel-copper solution at pH7

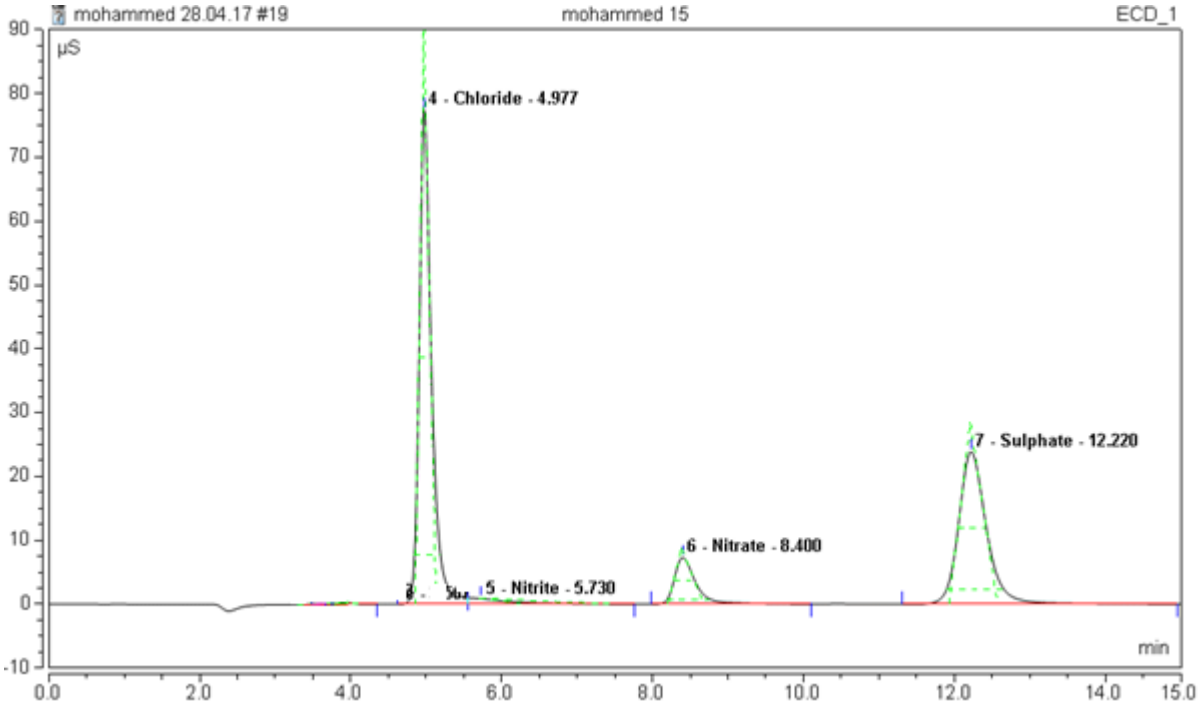

Figure 6-13. Ion chromatography measurement for the solution after total washing and filtration with 20mg/l nickel-copper solution at pH8

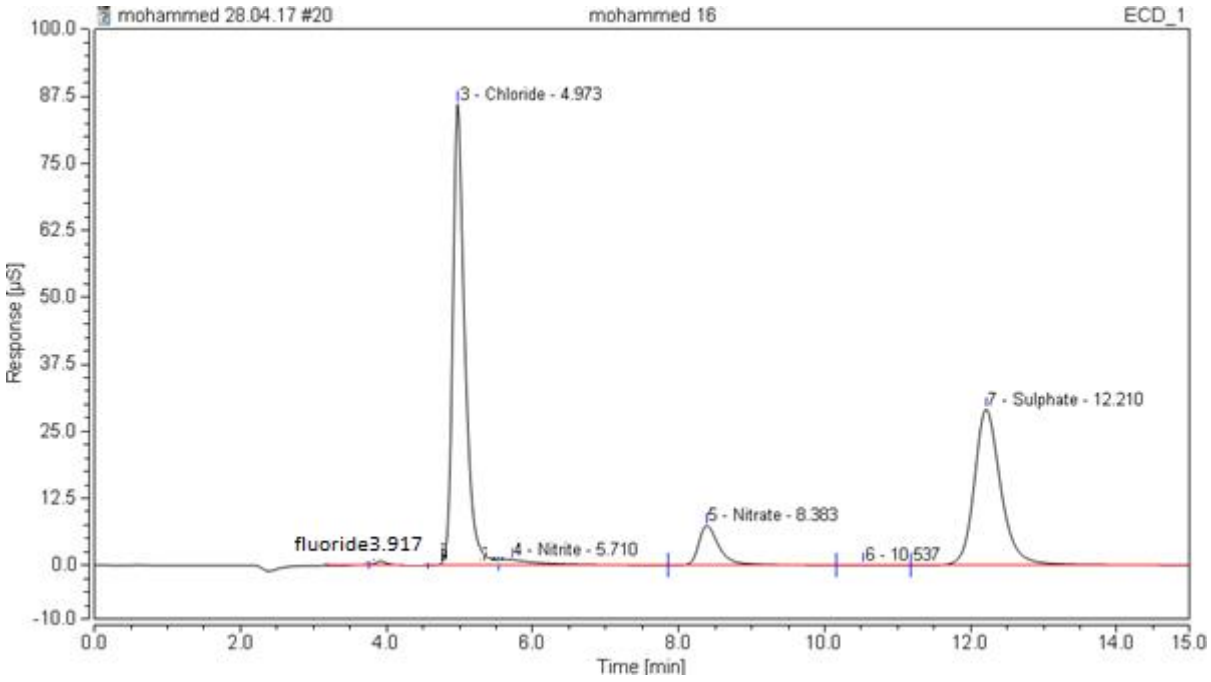

Figure 6-14. Ion chromatography measurement for the solution after total washing and filtration with 20mg/l nickel- copper solution at pH9

Figure 6-7 to Figure 6-18 show the peaks for many anions like nitrate, chloride and sulphate etc. These peaks represent the anions concentrations in the water after the filtration process with the mixed standard solution by PolyHIPE after post sulphonation. The results show that chloride, nitrate and sulphate have the highest concentration due using nickel nitrate in the preparation step for the nickel standard solution, while sulphate comes from unreacted sulphuric acid within the PolyHIPE beads. Other anions such as chloride as show in Table 7-3 which come from the deionized water. PolyHIPE after sulphonation is considered a strong cation exchanger, so these anions do not have the ability to react with it, therefore are still in the water after the filtration process.

6.8. X-ray fluorescence

X-ray fluorescence data is shown in Table 6-6 in test have done for the PolyHIPE beads after filtration with the solution containing the binary system nickel-copper (10mg/l each). The results show after simple calculation 0.054gm from the sample contains equal amounts of nickel and copper (1.44gm of nickel and 1.40 of copper respectively) which may be due to the removal efficiency being approximately the same and no selectivity occurring during the filtration process as mentioned in the last section. Again the total mass of metal in solution is 1g so these results indicate complete adsorbing of metal ion including those from other sources of contamination. In addition to that there is many elements in the solid which come from the deionized water such as chlorine and calcium or the other metals which come from the tools which were used in the experiment such as titanium and iron etc.

Table 6-6. X- Ray fluorescence test to measure the concentration of metal in polyHIPE beads after total washing with distilled water

N	Symbol.	Name	C.ppm
0	L.O.I.	Loss of Ignition	7141966
1	Si	Silicon	0
2	S	Sulfur	265481.3
3	Cl	Chlorine	389.412
4	K	Potassium	38498.08
5	Ca	Calcium	860.884
6	Ti	Titanium	55.204
7	Cr	Chromium	151.438
8	Mn	Manganese	85.044
9	Fe	Iron	6061.25
10	Ni	Nickel	481.916
11	Cu	Copper	727.35

6.9. SEM Analyses after Sulphonation and Filtration

After the sulphonation process the PolyHIPE becomes acidic due to SO_3H in its structure. The SO_3H group joins the benzene ring and the degree of sulphonation depends on how many sulphuric groups will attach to the ring (Bhumgara, 1995), therefore the morphology changed as well. The Sample obtained after 10 min mixing time was used for the filtration experiments

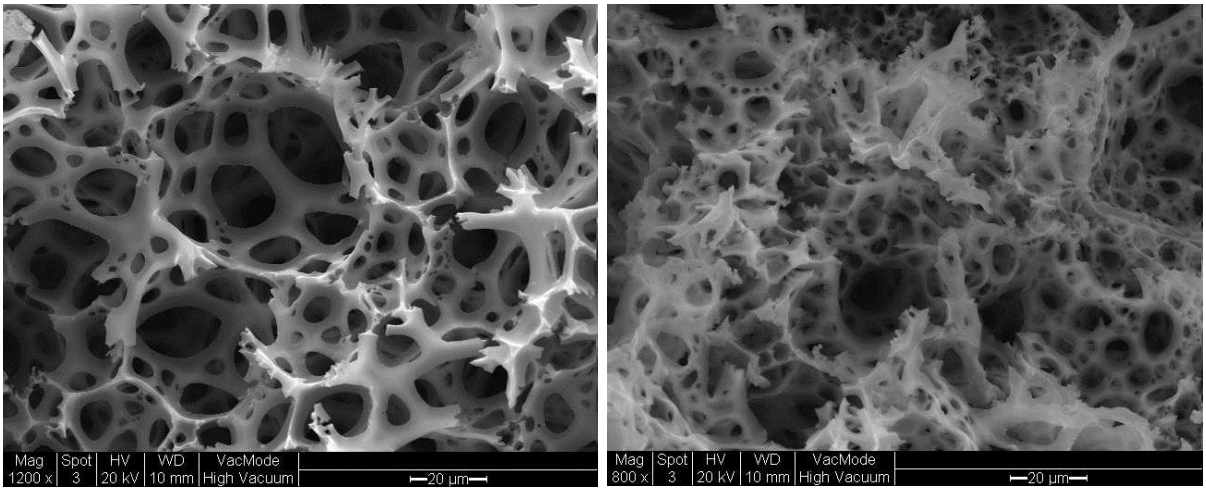

(a) (b)

Figure 6-15. SEM images for PolyHIPE (a) after sulphonation (b) after sulphonation and filtration with 10 min mixing time

The stability and structure of the materials before and after filtration was assessed using SEM images. There are many small pores in the wall between the large pores due to the treatment process with the sulphuric acid, but there are no differences between the samples after sulphonation and after filtration with the nickel standard solution. This is due to the low amount of nickel which was less than 1%, so it was not detected by the SEM and EDX analysis as shown in Figure 5-9 (Yabe and de Oliveira, 2003).

6.10. Summary

From the previous results, we can conclude that the PolyHIPE after the post sulphonation process could be used as ion exchanger to remove heavy metals from waste water. The functional group (SO_3H) can be added to the PolyHIPE structure by bin situ or post sulphonation processes which can be used as a strong cation exchanger to remove the heavy metals. XRF and EDX results show the high concentration of the sulphur in the PolyHIPE structure due to a good degree of sulphonation and show sulphur concentration after the post sulphonation process. BET measurements show there is no huge difference in the surface area and pore size for the sample before and after the post sulphonation process. However, it was good enough to get excellent removal efficiency for all systems but the amount of nickel and copper remaining in solution is still above the acceptable limit which is determined by World Health Organization Guidelines, so we are looking for another method to improve this. Using PolyHIPE coated with iron oxide nanoparticles to reach this limit is discussed in the next chapter.

7. PolyHIPE coated with Iron Oxide nanoparticles for filtration

Iron oxide nanoparticles have been found to be an excellent absorber for heavy metal ions (Boujelben et al., 2009). In this chapter PolyHIPE has been coated with iron oxide nanoparticles and its filtration performance tested to remove the nickel from waster with a concentration of 100 mg/l. The coated material has been characterised by SEM, BET and EDX to determine the morphology of the PolyHIPE after the coating process and its surface area, pore size and pore volume. In addition the presence of iron over the surface was confirmed by these tests. In this chapter high level of nickel concentration is used in the filtration process to give the coated PolyHIPE a high driving force for the interaction with the metal. In addition the zero of point charge is measured to determine the pH value which is required to make the surface charge for the iron oxide has zero value. This sets the conditions where metal ion removal by adsorption is most effective.

7.1. Scanning Electron Microscopy

Figure 7-1, shows SEM images of the coated PolyHIPE structure obtained after 10 min mixing time for the sulphonated and non sulphonated samples. All samples were in situ sulphonated to make the surface hydrophilic so the iron oxide containing solution could penetrate but the water uptake was increased by subsequent post sulphonation. The concentartion of iron oxide which was used during the coating process was 200g/l .

From Figure 7-1, we can conclude from the surface of the PolyHIPE after sulphonation and coating that, due to the hydrophilic behaviour of the sulphonated sample the iron oxide coating solution goes into the internal structure of the polyHIPE and it does not accumulate on the surface as in samples without sulphonation, therefore there are many open pores still on the surface. Figure 7-1 (c) shows that iron oxide agglomerates on the surface due to its high surface energy. This tends to close up small surface pores and reduce the amount of iron oxides available for adsorption. The agglomeration is also the result of Van der Waals attraction between oxide particles (Pradeep, 2009).

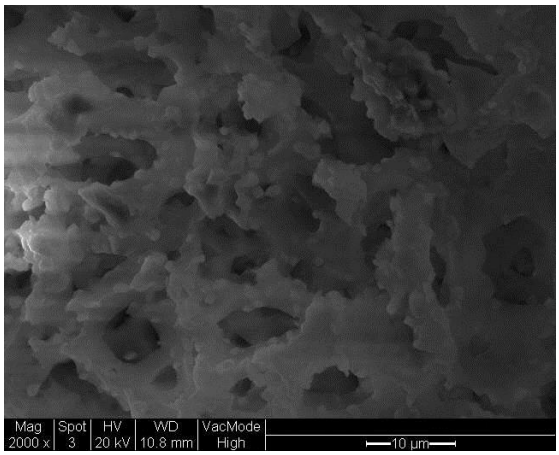

(a)

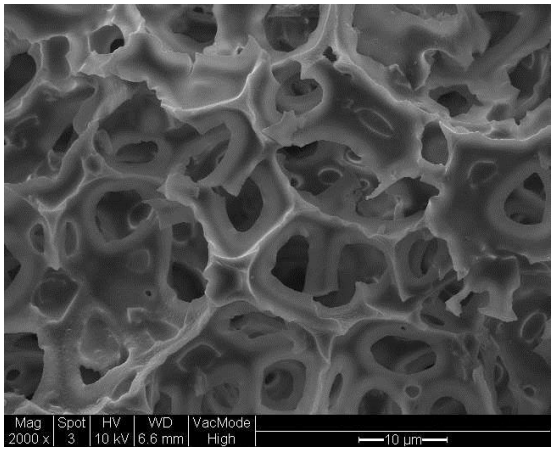

(b)

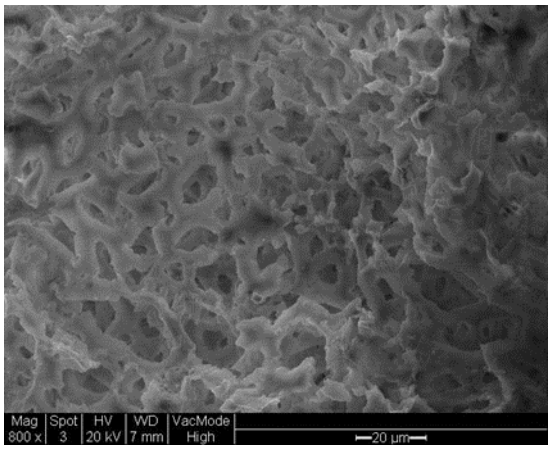

(c)

Figure 7-1. SEM images for the coated polyHIPE. (a), Post sulphonation, coating and filtration. (b), after sulphonation and coating, (c) after coating and filtration but without sulphonation.

7.2. Adsorption Desorption Isotherm

The adesorption desorption isotherm in Figure 7-2 shows a monolayer-multilayer physisorption process (Hasan, 2013) similar to the other PolyHIPE tested in this project. It clearly shows that the adsorption process takes place in a macroporous structure of PolyHIPE and the adsorbate – adsorbant and the adsorbate-adsorbate interaction was strong and weak respectively (Sing, 1994). However, the Iron oxide structure consists on both micropores and mesopores which means it has higher surface area. The surface area after coating with iron oxide was 50 m^2/g which means that coating with iron oxide increases the surface area of this polyHIPE considerably (see Figure 4-16) (Jusoh et al., 2007, Kang et al., 2004, Hua et al., 2012).

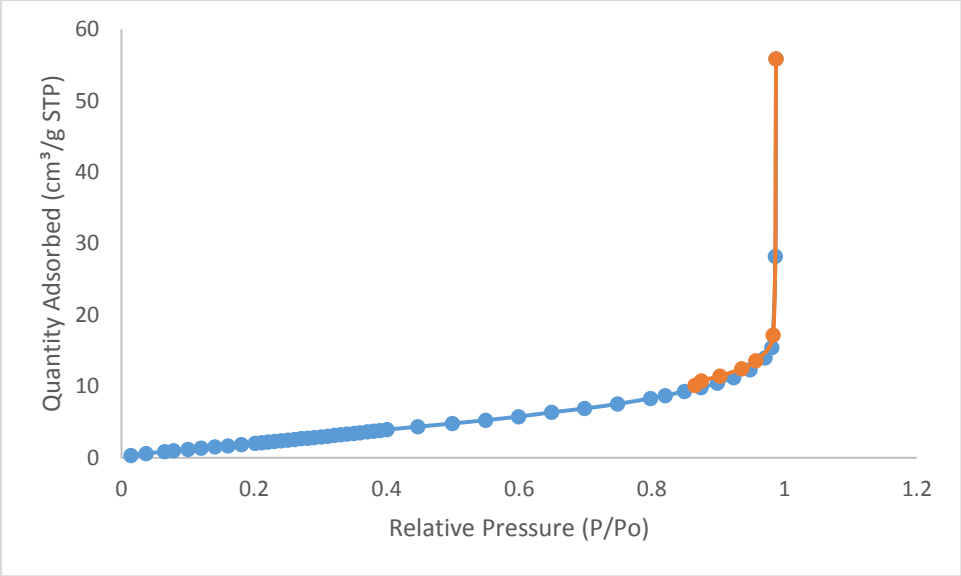

Figure 7-2:- Isotherm plot for surface area and pore size analysis of PHP with 10 (min) mixing time after coating with iron oxide.

7.3. XRF Analysis

As shown in Table 7-1, three samples from each post sulphonated and in situ sulphonated samples after coating with iron oxide and filtration with nickel solution with concentration 160 mg/l were analysed by XRF, to determine the ratio of elements in the PolyHIPE samples surface. From the results we can conclude that, the amount of the nickel absorbed by the in situ sulphonated sample was more than the amount of nickel absorbed by the post sulphonated sample. This may be because the in situ sulphonated samples have a more uniform distribution of internal active sites which can bind to iron oxide nanoparticles. This is supported by the higher iron content of the in situ sulphonated samples (Table 7.1). In addition to that, samples coated with iron oxide have higher surface area than the post sulphonated sample and would attract more nickel if the amount of iron oxide is increased.

Table 7-1. XRF analysis for the PolyHIPE samples after filtration for PolyHIPE sample after coating with iron oxide and after sulphonation and coating

	Values (Wt. %)	
Sample	Fe	Ni
Post Sulphonated 1	93.65	0.34
Post Sulphonated 2	92.21	0.72
Post Sulphonated 3	92.07	0.55
insitu Sulphonated 1	96.07	1.09
insitu Sulphonated 2	93.81	2.37
insitu Sulphonated 3	95.67	1.32

7.4. Removal Efficiency

To assess removal efficiency the filtration process has been done by using nickel standard solution with different concentrations (160, 100, and 20 mg/l). The measurement of the nickel concentration in solution by ICP shows there is low reduction in nickel concentration with removal efficiency 11% at high concentration as shown in

Table 7-2. Medium and low nickel concentrations did not show any difference in nickel concentration before and after the filtration process as shown in Table 7-3; in fact there is some increase in the nickel concentration above the standard in some samples after filtration which may be attributed to measurement error and other sources of nickel contamination. These results suggest a higher driving energy for interaction between the active sites and nickel ions at high concentrations, so iron oxide is suitable as an adsorber to remove high concentrations of heavy metals rather than low concentration used in the previous chapter as has been observed previously (Sahmoune et al., 2011, Taha et al., 2011). It was found by many others that the adsorption capacity increased with increasing in initial concentration for iron oxide adsorption systems (Kumar et al., 2012).

Table 7-2. Parameters (pH, contact time, amount of the iron oxide used in the coating processes) changed to get better absorption for the nickel from the standard solution.

The sample mixing time	Sample type	Amount of the adsorbate g	Amount of the liquid	Ph.	The concentration before the filtration processes	The contact time	The concentration of iron oxide	The concentration after the filtration process mg/l%
10 min	Sulphonated and coated with iron oxide Second filtration	80g	100 ml	5	160 mg/l	25 min cycle	10%	134.6
10 min	Coated with iron oxide	80g	100 ml	5	160 mg/l	25 min cycle	10%	141.8
10 min	Coated with iron oxide second filtration	80g	100 ml	5	160 mg/l	25 min cycle	10%	141.2
10 min	Coated with iron oxide	80g	100 ml	5	160 mg/l	25 min cycle	10%	142

Table 7-3. The concentrations of nickel before and after filtration with PolyHIPE beads coated with iron oxide at low concentration.

C. before filtration	C. after filtration mg/l	Time (hour)	amount of adsorbate
20	13.8	8	3 g
20	27.6	8	3 g
20	30.6	8	3 g
20	27.7	8	3 g
20	23.6	8	3 g
20	24.1	8	3 g

7.5. EDX Analysis

Figure 7-3 show the EDX spectra obtained from were performed for all PolyHIPE samples after filtrations for both the sulphonated sample and non sulphonated samples. From Table 7-3 and figures Figure 7-5 and Table 7-4we can clearly see that the nickel does not appear in the results because the concentration of the nickel was less than 1% but there is a measurable iron content from the iron oxide particles. The sodium may be from the NaOH which is used in the preparation step of the iron oxide to change the pH. The predominant elements present are carbon from the PolyHIPE and oxygen from the iron oxide and SO_3H groups. There is more oxygen measured than can be accounted and sulphur present which suggest that the PolyHIPE surface may also have oxidised or that there is significant water retention within the PolyHIPE.

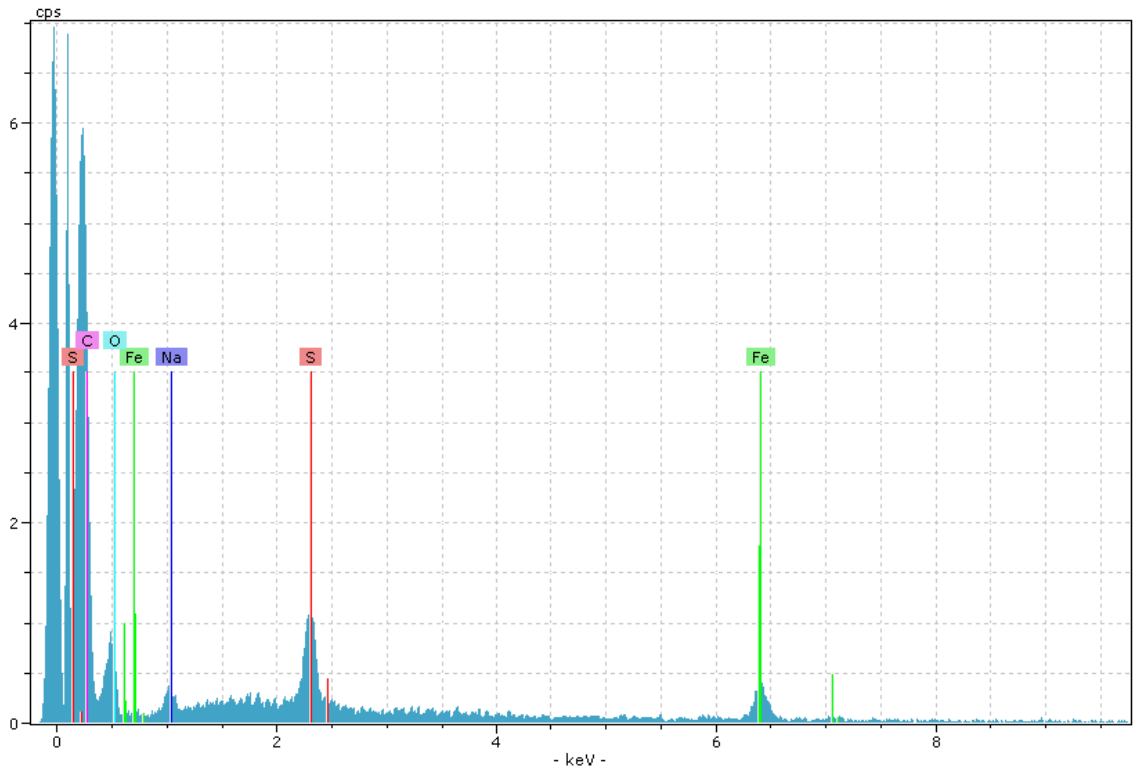

Figure 7-3. EDX for PHP sample with 10 min mixing time after sulphonation and coating.

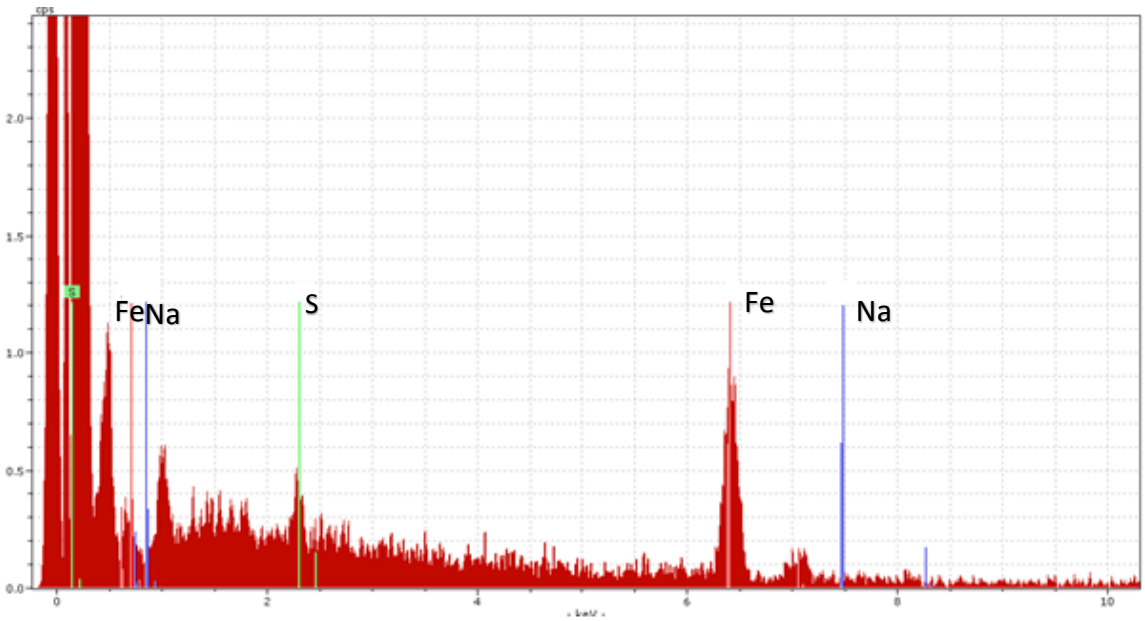

Figure 7-4. EDX analysis after sulphonation and coating for PHP sample with 10 min mixing time.

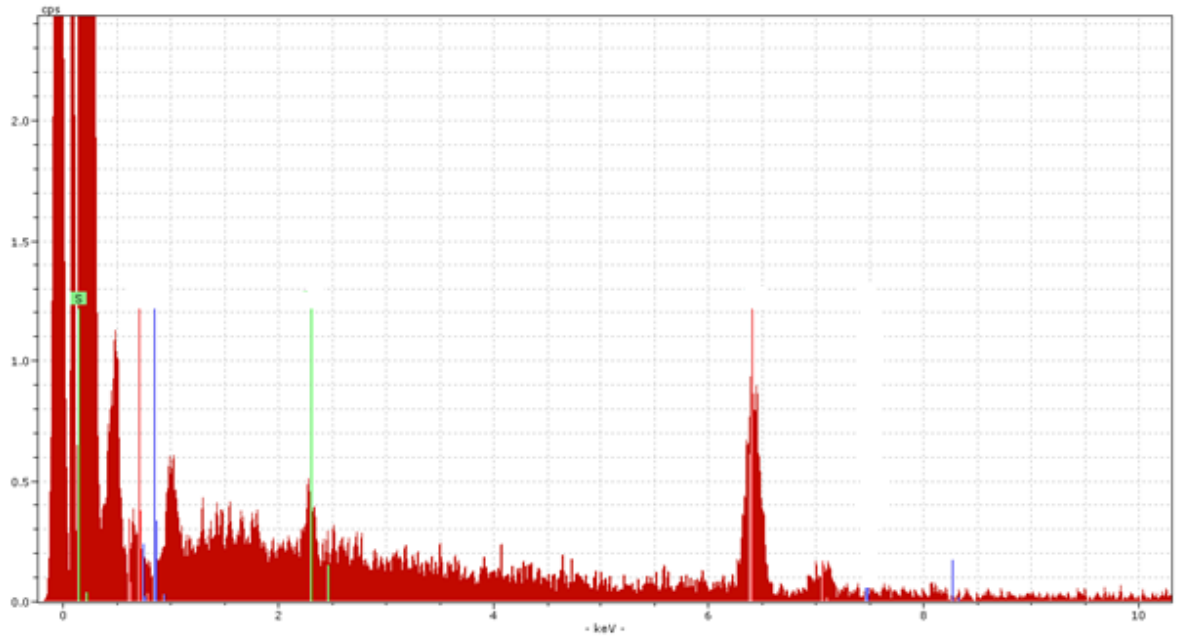

Figure 7-5. EDX analysis for PHP sample with 10 min mixing time. After coating and filtration but for the all surface.

Table 7-4. EDX results for the element concentration on the surface of PolyHIPE after coating with iron oxide.

Element	C .wt.%	C. At %
Sodium	0.56	0.33
Sulphur	2.93	1.26
Iron	4.14	1.02
Oxygen	30.55	26.35
Carbon	61.82	71.03

7.6. Zero point of Charge

Different solutions with pH between 5 and 11 were prepared after shaking iron oxide powder with deionised water and adjusting the pH with HCl and NaOH solutions added in a dropwise fashion. The iron oxide powder was taken from the coating layer on a PolyHIPE sample. The test was repeated three times for each sample assess experimental scatter. The zeta potential was then measured with the Malvern Zetasizer. The results show the iron oxide zero point charge was at pH 8.6 as shown in Figure 7-6 (b), and this result agrees with many studies that reported that iron oxide with crystalline or amorphous structure has zero point of charge between pH7 and 9 (Wilkie and Hering, 1996, Benjamin et al., 1996). At higher pH than this value, iron oxides become anionic [Fe $(OH)_4^-$] and can be used for adsorbing cationic metals such as nickel. While below that value it is cationic ($Fe(OH)_2^+$). It was found by previous research that, the highest adsorption for the nickel by iron oxide was at pH 7 (Malandrino et al., 2006).This probably reflects an ion exchange reaction between Fe and Ni In addition to that, the physicochemical properties of iron oxides such as point of zero charge are not affected by the coating process (Katsoyiannis and Zouboulis, 2002).

The fact that the filtration studies undertaken in this work were at a pH lower than 7 will thus clearly contribute to the low removal efficiency for cationic species. This is difficult to change since the sulphonation processes creates acidic conditions within the PolyHIPE during filtration studies and a different method of functionalisation would be necessary to support the iron oxide nanoparticles if PolyHIPE is to operate at neutral pH.

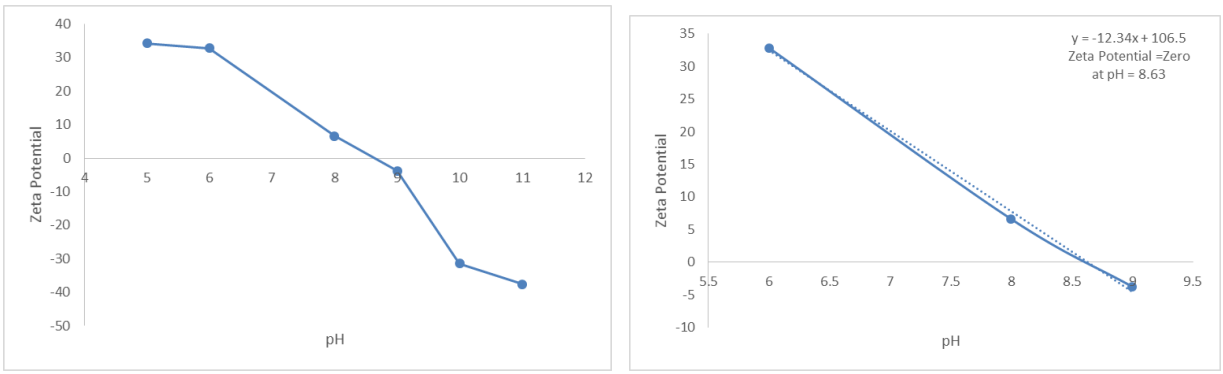

(a) (b)

Figure 7-6. The value of the zero of point charge

7.7. Summary

Iron oxide coating can be done both on both in situ and post sulphonation PolyHIPE. However, the iron oxide can only be used to remove nickel from high concentration solutions. The Zero point of charge at the expected value and a higher pH is expected for the adsorption reaction which cannot be achieved using sulphonated PolyHIPE as a support material. When we compare the removal efficiency for the PolyHIPE in this case with removal efficiency with PolyHIPE after sulphonation the results show that the sulphonation of PolyHIPE alone is a better filter medium for the ion exchange process. But it remains to be seen if a regeneration to recover the metals from the PolyHIPE beads is possible to make it more economically favourable as investigated in the next chapter.

8. Regeneration

Regeneration experiments have been done for the PolyHIPE beads after the post sulphonation and filtration processes with different heavy metals like nickel and copper and the binary system. Many regeneration solutions with different pH values are used during this process. ICP is used to measure the concentration of the heavy metals in solution after regeneration. The IC test is used to determine the concentrations of anions in the solution after the regeneration as well.

8.1 Nickel Regeneration

Three different solutions containing distilled water with different pH were used to regenerate the PolyHIPE beads from nickel after the filtration process using different pH (1, 5, and 11). Anion concentrations were measured by the ICS-1000 (Ion Chromatography System) in the solution after regeneration. The results show that the anion concentration is below the assessable limit specified by the World Health Organization Guideline as shown in Table 8-1 and figures Figure 8-2. The measured peaks contain contribution from a number of anions which are quantified by fitting the results from standard pure solution. The sulphate which came from unreacted sulphuric acid during the sulphonation process and nitrate came from nickel nitrate which was used to prepare nickel standard solution. Both remain the same after regeneration. However, Figure 8-1 shows that, with solution pH 5 the highest amount of nickel was recovered from the PolyHIPE which was about 0.5 mg/l but it is still a low value compare with the estimated value if all nickel in the bead is removed which is approximately 16.46 mg/l.

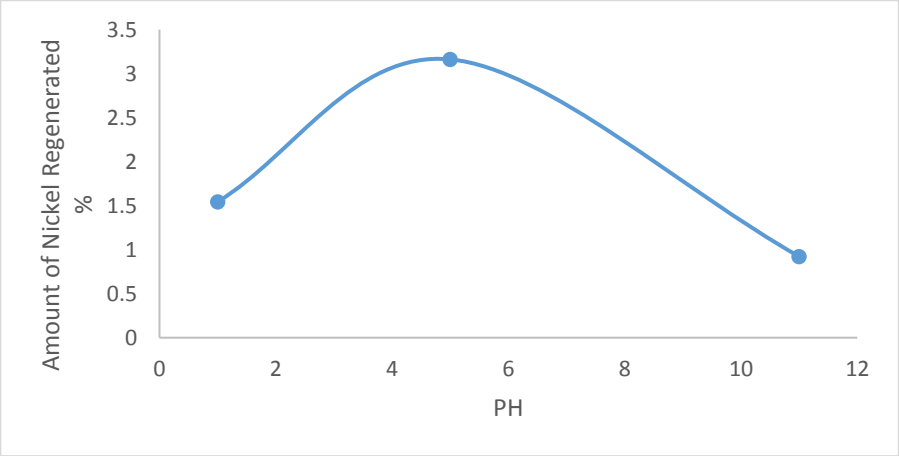

Figure 8-1. The ratio of nickel which is removed during regeneration compared to the initial nickel concentration for PolyHIPE beads at different pH. The figure plotted from single data

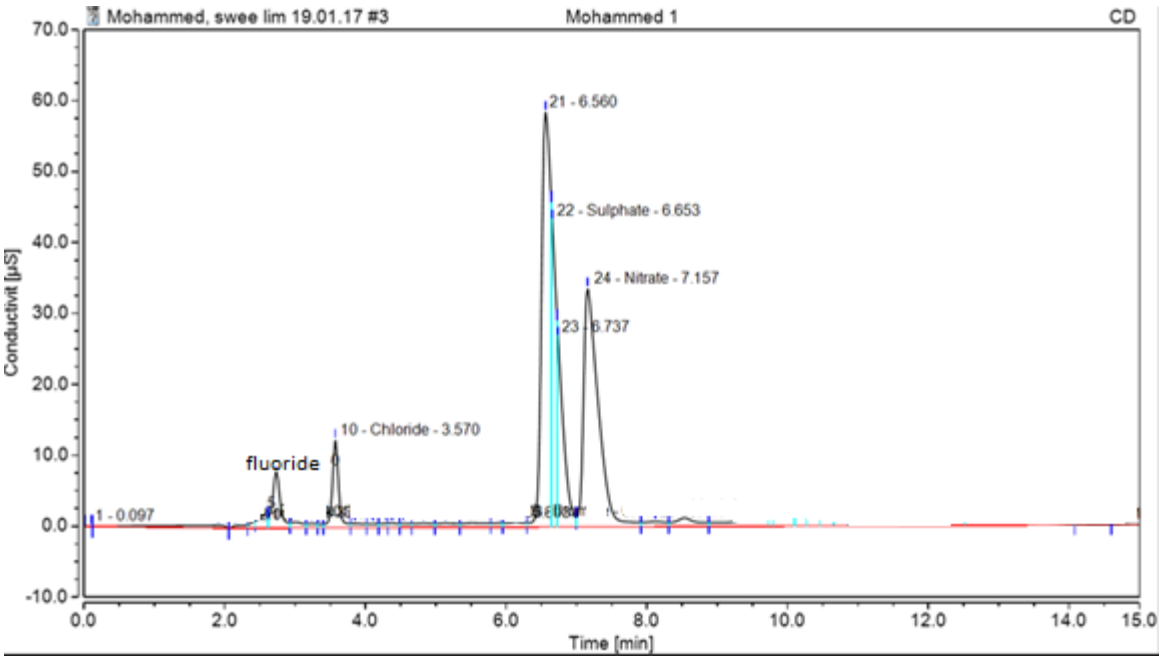

Figure 8-2. IC for anions which give the concentration of anions in the solution after regeneration process with different pH 5.

Table 8-1. The concentration of anions in the solution after regeneration process with different pH

Peak Name	Amount ppm at pH 11	Amount ppm at pH 5	Amount ppm at pH 1
Fluoride	0.20	0.20	2.85
Chloride	5.58	3.97	1.85
Nitrite	0.67	0.64	0.39
Bromide	3.39	1400	411
Sulphate	24.64	0.00676	0.01
Nitrate	70.60	176	77.7
Phospate	7.98	1.49	0.45

It is unlikely that this filter can be regenerated and reused given any of these concentrations. The filters will be single use and another method to recover the nickel needs to be developed as most of it remains trapped in the PolyHIPE.

Figure 6-7 to Figure 8-4 show the peaks for many anions like Nitrate, chloride and sulphate etc. The peaks represent the anion concentrations in the water after the regeneration process. The results show that nitrate and sulphate have the highest concentration due using nickel nitrate in the preparation step for the nickel standard solution, while sulphate come from unreacted sulphuric acid with the PolyHIPE beads. Other anions as show in Table 7-3 come from the deionized water.

8.2 Copper Regeneration

Regeneration experiments for copper were done by solutions with different pH values (3 and 11) than was used to recover the nickel from PolyHIPE beads after filtration. From Table 8-2, the amount of copper in solution regenerated at high pH is higher than at low pH but it is still very low compared with an estimation for the copper inside PolyHIPE beads which if it were all to be removed would be about 16.50 mg/l when the initial concentration for the copper before filtration was 20 mg/l.

Table 8-2. The concentrations of copper in (mg/l) after regeneration with high and low pH solution.

pH	C.Cu before filtration	C.Cu after regeneration at pH 11	C.Cu after regeneration at pH 3
6	20	0.653	0.818
7	20	0.227	2.641
8	20	0.142	0.568
9	20	0.131	0.249

As with Nickel there is not much copper removal from the PolyHIPE during regeneration so this would suggest it is only suitable for a single use filter. An alternative method to extract copper from the PolyHIPE needs to be developed.

8.3. Binary System (Nickel and Copper) Regeneration

The regeneration process for the PolyHIPE beads after filtration was done by using solutions with different pH values (11 and 3), and because the initial concentration for both metals was less than single system which is (10 mg/l) so the amount of nickel and copper which is recovered from the beads was less as well as shown in Table 8-1,Table 8-2 and Table 8-3, and is still a low value compared with the initial concentration of the metals.

Table 8-3. The concentrations of nickel and copper in (mg/l) after regeneration with high and low pH solution for the binary system.

Sample number	C. before filtration	C.After regeneration for nickel	C.After regeneration for copper (ppm)	pH
1	20	0.15	0.01	3
2	20	0.14	0.004	3
3	20	0.10	0.02	3
4	20	0.24	0.01	3
5	20	0.12	0.01	11
6	20	0.14	0.01	11
7	20	0.26	0.05	11
8	20	0.14	0.02	11

Although nickel is preferentially removed from the PolyHIPE the amount removed is small so this method of recovery is not suitable to extract the metal from the PolyHIPE and the filter would be single use as stated previously

8.4. X-ray fluorescence

X-ray fluorescence analysis has been done for the PolyHIPE beads after filtration with the solution containing binary system nickel-copper 10mg/l each and subsequent regeneration. The results show after simple calculation for 0.772 g of the sample a content of 0.82 g of nickel and 1.37g of copper which shows the regeneration efficiency is greater for nickel than copper process as mentioned in last section. In addition to that there is many elements in the solution which come from deionized water such as chlorine and calcium or the other metals which come from the tools which used in our experiment such as titanium and iron etc.as shown in Table 8-4.

Table 8-4. X-ray fluorescence test to measure the concentration of metal in polyHIPE beads after total washing with distilled water

N	Symbol.	Name	C.ppm
15	P	Phosphorus	537.2
16	S	Sulphur	76891.4
17	Cl	Chlorine	75
19	K	Potassium	204.4
20	Ca	Calcium	152.7
24	Cr	Chromium	6.8
25	Mn	Manganese	7.9
26	Fe	Iron	208.5
28	Ni	Nickel	272.1
29	Cu	Copper	1413.6

8.5. Summary

In summary the regeneration process was done by using many solution with different pH values to recover the heavy metals from the PolyHIPE structure after the sulphonation and filtration to remove heavy metals. The results show that the amount of the heavy metals recovered was low compared with the initial concentration which was used for the filtration process. Therefore further study is needed to improve the regeneration process.

9. Conclusions and Further Work

9.1. Conclusions

- PolyHIPE materials produced at low mixing times contain larger and more interconnected pores that have higher water uptake and are most suitable for filtration media trials. After sulphonation there is much less difference in morphology between the samples with different mixing times.

- The water uptake measurements show differences for the samples with instu sulphonation and post sulphonation due an increase in the amount of sulphur groups introduced during the post sulphonation process. The post-sulphonated material is more effective as an ion exchanger to remove nickel and copper from a solution. This may be because it has a high concentration of benzenesulphonic groups which are the active sites for heavy metal removal.

- Compression tests show that the samples have sufficient stiffness to washstand the solution flow rate and sufficient strength to not break during the filtration process.

- BET measurements show that PolyHIPE samples with 10 min mixing time have the best combination of surface area, pore size and pore volume to use for the filtration process.

- Small differences in pore size, water uptake, surface area, and pore volume do not show any major influence on removal efficiency which is controlled by surface chemistry.

- Post-sulphonation is the best surface chemistry treatment developed so far since filtration trials show both Ni and Cu can be removed from solution with high efficiency. In contrast, PolyHIPE samples coated with iron oxide show only 11% removal efficiency for nickel at high concentration, and did not show any change in removal efficiency at low concentration.

- Regeneration studies using these materials were less successful; the amount of nickel and copper in the solution after regeneration is less than its concentration before filtration and the majority of the metals remain attached to the polyHIPE surface. Further studies are needed to improve the regeneration process to make this method for removing heavy metals more viable.

- Thus PolyHIPEs are a good substrate for ion exchange water filtration and can be functionalised to aid metal ion removal.

9.2 Future work

Only basic filtration studies were undertaken in this project and the long term performance of these materials in the filtration environment has yet to be assessed. A more controlled filtration rig with in situ analysis of metal concentration in required to quantitatively assess the ability of different PolyHIPE structures to remove dissolved metal ions and organic particles from more realistic wastewater compositions. In addition, PolyHIPE samples with higher mechanical stiffness could be produced by increasing the oil content of the emulsion and the effect of sulphonation on their physical properties and filtration performance should be assessed. The aim is to optimise the PolyHIPE composition and processing for filtration.

Furthermore, the effect of different PolyHIPE structures where water is forced to flow through the PolyHIPE could be assessed to determine the effect of morphology on the filtration process, and the study could done at different temperatures. Changing the functionalisation to increase the amount of different adsorbants, and the use of different standard solutions could help to determine optimum surfaces for different contaminant metals. In addition to that, many factors could be changed to get better degree of sulphonation for the sulphonated samples such as, using sulphuric acid with different concentration or soaking the samples inside the sulphuric acid for different times. As a result, the number of active sites in the samples could be increased which would mean increasing the removal efficiency for the metal ions from the waste water and better life of the filter.

Finally, other methods for filter regeneration, such as different acids used in the regeneration solution should be studies further as, at present, there is no good way to regenerate the filter and they would be single use and relatively high cost.

9.2. Summary and Future Outlook

PolyHIPE can be made with different pore size controlled by mixing time. Additionally PolyHIPE can be made hydrophilic by sulphonation; in situ does not introduce as much sulphur functionality as post sulphonation. High water uptake and ion exchange capability have been demonstrated for removal of heavy metals at low ion concentration. Coating with iron oxide nanoparticles does not improve filtration performance probably because the acidic conditions generated by sulphonated polyHIPE do not give the best pH conditions for nickel removal by adsorption on iron oxide. The Filtration efficiency depends basically on pH in all cases.

It remains a distinct possibility that the functionalisation of polyHIPE can be optimised to improve adsorption of heavy metals. This should be a focus of future projects.

References

ADAMS, C., WANG, Y., LOFTIN, K. & MEYER, M. 2002. Removal of antibiotics from surface and distilled water in conventional water treatment processes. *Journal of environmental engineering,* 128**,** 253-260.

ADAMS, L. B., HALL, C. R., HOLMES, R. J. & NEWTON, R. A. 1988. An examination of how exposure to humid air can result in changes in the adsorption properties of activated carbons. *Carbon,* 26**,** 451-459.

ADELI, M., YAMINI, Y. & FARAJI, M. 2012. Removal of copper, nickel and zinc by sodium dodecyl sulphate coated magnetite nanoparticles from water and wastewater samples. *Arabian Journal of Chemistry*.

AFKHAMI, A., MADRAKIAN, T., KARIMI, Z. & AMINI, A. 2007. Effect of treatment of carbon cloth with sodium hydroxide solution on its adsorption capacity for the adsorption of some cations. *Colloids and Surfaces A: Physicochemical and Engineering Aspects,* 304**,** 36-40.

AGATEMOR, C. & BEAUCHEMIN, D. 2011. Matrix effects in inductively coupled plasma mass spectrometry: A review. *Analytica Chimica Acta,* 706**,** 66-83.

AHMED, M., MALIK, M. A., PERVEZ, S. & RAFFIQ, M. 2004. *Eur. Polym. J.,* 40**,** 1609.

AHN, C. K., PARK, D., WOO, S. H. & PARK, J. M. 2009. Removal of cationic heavy metal from aqueous solution by activated carbon impregnated with anionic surfactants. *Journal of hazardous materials,* 164**,** 1130-1136.

AKAY, G., BOKHARI, M. A., BYRON, V. J. & DOGRU, M. 2005a. Development of nano-structured micro-porous materials and their application in bioprocess–chemical process intensification and tissue engineering. *Chemical engineering: Trends and developments. John Wiley & Sons, New York***,** 171-197.

AKAY, G., ERHAN, E. & KESKINLER, B. 2005b. Bioprocess intensification in flow-through monolithic microbioreactors with immobilized bacteria. *Biotechnol Bioeng,* 90**,** 180-90.

AKLIL, A., MOUFLIH, M. & SEBTI, S. 2004. Removal of heavy metal ions from water by using calcined phosphate as a new adsorbent. *Journal of Hazardous Materials,* 112**,** 183-190.

ALEXANDRATOS, S. D. 2009. Ion-Exchange Resins: A Retrospective from Industrial and Engineering Chemistry Research. *Industrial & Engineering Chemistry Research,* 48**,** 388-398.

ALIKHANI, M. & MOGHBELI, M. R. 2014. Ion-exchange polyHIPE type membrane for removing nitrate ions: Preparation, characterization, kinetics and adsorption studies. *Chemical Engineering Journal,* 239**,** 93-104.

ALIVISATOS, A. P. 1996. Perspectives on the physical chemistry of semiconductor nanocrystals. *The Journal of Physical Chemistry,* 100**,** 13226-13239.

ALYÜZ, B. & VELI, S. 2009. Kinetics and equilibrium studies for the removal of nickel and zinc from aqueous solutions by ion exchange resins. *Journal of Hazardous Materials,* 167**,** 482-488.

AMAN, T., KAZI, A. A., SABRI, M. U. & BANO, Q. 2008. Potato peels as solid waste for the removal of heavy metal copper(II) from waste water/industrial effluent. *Colloids and Surfaces B: Biointerfaces,* 63**,** 116-121.

AMIN, M. T., ALAZBA, A. A. & MANZOOR, U. 2014. A review of removal of pollutants from water/wastewater using different types of nanomaterials. *Advances in Materials Science and Engineering,* 2014.

ANDERSEN, A., BERGE, S. R., ENGELAND, A. & NORSETH, T. 1996. Exposure to nickel compounds and smoking in relation to incidence of lung and nasal cancer among nickel refinery workers. *Occupational and environmental medicine,* 53**,** 708-713.

ARAI, Y. 2008. Spectroscopic evidence for Ni (II) surface speciation at the iron oxyhydroxides− water interface. *Environmental science & technology,* 42**,** 1151-1156.

ASHBOLT, N. J. 2004. Microbial contamination of drinking water and disease outcomes in developing regions. *Toxicology,* 198**,** 229-238.

AZIZ, H. A., ADLAN, M. N. & ARIFFIN, K. S. 2008. Heavy metals (Cd, Pb, Zn, Ni, Cu and Cr (III)) removal from water in Malaysia: Post treatment by high quality limestone. *Bioresource technology,* 99**,** 1578-1583.

BADRUDDOZA, A. Z. M., TAY, A. S. H., TAN, P. Y., HIDAJAT, K. & UDDIN, M. S. 2011. Carboxymethyl-β-cyclodextrin conjugated magnetic nanoparticles as nano-adsorbents for removal of copper ions: synthesis and adsorption studies. *Journal of hazardous materials,* 185**,** 1177-1186.

BAILEY, S. E., OLIN, T. J., BRICKA, R. M. & ADRIAN, D. D. 1999. A review of potentially low-cost sorbents for heavy metals. *Water research,* 33**,** 2469-2479.

BANERJEE, K., RAMESH, S. T., GANDHIMATHI, R., NIDHEESH, P. V. & BHARATHI, K. S. 2012. A novel agricultural waste adsorbent, watermelon shell for the removal of copper from aqueous solutions. *Iran. J. Energy Environ,* 3**,** 143-156.

BARAKAT, M. A. 2008. Adsorption of heavy metals from aqueous solutions on synthetic zeolite. *Research Journal of Environmental Sciences,* 2**,** 13-22.

BARAKAT, M. A. 2011. New trends in removing heavy metals from industrial wastewater. *Arabian Journal of Chemistry,* 4**,** 361-377.

BARBETTA, A., CAMERON, N. R. & COOPER, S. J. 2000. High internal phase emulsions (HIPEs) containing divinylbenzene and 4-vinylbenzyl chloride and the morphology of the resulting PolyHIPE materials. *Chemical Communications***,** 221-222.

BASALDELLA, E. I., VÁZQUEZ, P. G., IUCOLANO, F. & CAPUTO, D. 2007. Chromium removal from water using LTA zeolites: Effect of pH. *Journal of Colloid and Interface Science,* 313**,** 574-578.

BENJAMIN, M. M., SLETTEN, R. S., BAILEY, R. P. & BENNETT, T. 1996. Sorption and filtration of metals using iron-oxide-coated sand. *Water Research,* 30**,** 2609-2620.

BERTHOMIEU, C. & HIENERWADEL, R. 2009. Fourier transform infrared (FTIR) spectroscopy. *Photosynthesis Research,* 101**,** 157-170.

BEUKES, J. P., GIESEKKE, E. W. & ELLIOTT, W. 2000. Nickel retention by goethite and hematite. *Minerals engineering,* 13**,** 1573-1579.

BHATTACHARYYA, K. G. & GUPTA, S. S. 2008. Adsorption of a few heavy metals on natural and modified kaolinite and montmorillonite: a review. *Advances in colloid and interface science,* 140**,** 114-131.

BHUMGARA, Z. 1995. Polyhipe foam materials as filtration media. *Filtration & separation,* 32**,** 245-251.

BILAL, M., SHAH, J. A., ASHFAQ, T., GARDAZI, S. M. H., TAHIR, A. A., PERVEZ, A., HAROON, H. & MAHMOOD, Q. 2013. Waste biomass adsorbents for copper removal from industrial wastewater—a review. *Journal of Hazardous Materials,* 263**,** 322-333.

BODZEK, M., KORUS, I. & LOSKA, K. 1999. Application of the hybrid complexation-ultrafiltration process for removal of metal ions from galvanic wastewater. *Desalination,* 121**,** 117-121.

BOOTA, R., BHATTI, H. N. & HANIF, M. A. 2009. Removal of Cu(II) and Zn(II) Using Lignocellulosic Fiber Derived from Citrus reticulata (Kinnow) Waste Biomass. *Separation Science and Technology,* 44**,** 4000-4022.

BOUJELBEN, N., BOUZID, J. & ELOUEAR, Z. 2009. Adsorption of nickel and copper onto natural iron oxide-coated sand from aqueous solutions: Study in single and binary systems. *Journal of Hazardous Materials,* 163**,** 376-382.

BOUZID, J., ELOUEAR, Z., KSIBI, M., FEKI, M. & MONTIEL, A. 2008. A study on removal characteristics of copper from aqueous solution by sewage sludge and pomace ashes. *Journal of hazardous materials,* 152**,** 838-845.

BRAEKEN, L., BETTENS, B., BOUSSU, K., VAN DER MEEREN, P., COCQUYT, J., VERMANT, J. & VAN DER BRUGGEN, B. 2006. Transport mechanisms of dissolved organic compounds in aqueous solution during nanofiltration. *Journal of membrane science,* 279**,** 311-319.

BRIX, H. 1993. Wastewater treatment in constructed wetlands: system design, removal processes, and treatment performance. *Constructed wetlands for water quality improvement***,** 9-22.

BROWN, P. A., GILL, S. A. & ALLEN, S. J. 2000. Metal removal from wastewater using peat. *Water research,* 34**,** 3907-3916.

BRUNAUER, S., DEMING, L. S., DEMING, W. E. & TELLER, E. 1940. On a theory of the van der Waals adsorption of gases. *Journal of the American Chemical society,* 62**,** 1723-1732.

BURROWS, A., HOLMAN, J., PARSONS, A., PILLING, G. & PRICE, G. 2013. *Chemistry³: Introducing Inorganic, Organic and Physical Chemistry*, Oxford University Press.

BUSBY, W., CAMERON, N. R. & JAHODA, C. A. B. 2001. Emulsion-Derived Foams (PolyHIPEs) Containing Poly(ε-caprolactone) as Matrixes for Tissue Engineering. *Biomacromolecules,* 2**,** 154-164.

BUSBY, W., CAMERON, N. R. & JAHODA, C. A. B. 2002. Tissue engineering matrixes by emulsion templating. *Polymer International,* 51**,** 871-881.

BYRON, V. J. 2000. *The development of microcellular polymers as a support for tissue engineering.* University of Newcastle.

CALKAN, B. 2007. *Preparation of novel nano-structured macro-and meso-porous metal foams for process intensification and miniaturization.* University of Newcastle Upon Tyne.

CAMERON, N. R. 2005a. *Polymer,* 46**,** 1439.

CAMERON, N. R. 2005b. High internal phase emulsion templating as a route to well-defined porous polymers. *Polymer,* 46**,** 1439-1449.

CAMERON, N. R. & SHERRINGTON, D. C. 1997. Synthesis and Characterization of Poly(aryl ether sulfone) PolyHIPE Materials. *Macromolecules,* 30**,** 5860-5869.

CAMERON, N. R., SHERRINGTON, D. C., ANDO, I. & KUROSU, H. 1996. Chemical modification of monolithic poly(styrene-divinylbenzene) polyHIPE[registered sign] materials. *Journal of Materials Chemistry,* 6**,** 719-726.

CASTELBLANQUE, J. & SALIMBENI, F. 2004. NF and RO membranes for the recovery and reuse of water and concentrated metallic salts from waste water produced in the electroplating process. *Desalination,* 167**,** 65-73.

CAVALLO, D., URSINI, C. L., SETINI, A., CHIANESE, C., PIEGARI, P., PERNICONI, B. & IAVICOLI, S. 2003. Evaluation of oxidative damage and inhibition of DNA repair in an in vitro study of nickel exposure. *Toxicology in vitro,* 17**,** 603-607.

CERVERA, M. L., ARNAL, M. C. & DE LA GUARDIA, M. 2003. Removal of heavy metals by using adsorption on alumina or chitosan. *Analytical and bioanalytical chemistry,* 375**,** 820-825.

CHEN, Y.-H. & LI, F.-A. 2010. Kinetic study on removal of copper (II) using goethite and hematite nano-photocatalysts. *Journal of Colloid and Interface Science,* 347**,** 277-281.

CHEREMISINOFF, N. P. 2001. *Handbook of water and wastewater treatment technologies*, Butterworth-Heinemann.

CHEREMISINOFF, N. P. 2002a. Chapter 1 - An Overview of Water and Waste- Water Treatment. *In:* CHEREMISINOFF, N. P. (ed.) *Handbook of Water and Wastewater Treatment Technologies.* Woburn: Butterworth-Heinemann.

CHEREMISINOFF, N. P. 2002b. Chapter 3 - Chemical Additives that Enhance Filtration. *In:* CHEREMISINOFF, N. P. (ed.) *Handbook of Water and Wastewater Treatment Technologies.* Woburn: Butterworth-Heinemann.

CHEREMISINOFF, N. P. 2002c. Chapter 7 - What Sand Filtration is All About. *In:* CHEREMISINOFF, N. P. (ed.) *Handbook of Water and Wastewater Treatment Technologies.* Woburn: Butterworth-Heinemann.

CHONG, A. M. Y., WONG, Y. S. & TAM, N. F. Y. 2000. Performance of different microalgal species in removing nickel and zinc from industrial wastewater. *Chemosphere,* 41**,** 251-257.

CRINI, G. 2005. Recent developments in polysaccharide-based materials used as adsorbents in wastewater treatment. *Progress in polymer science,* 30**,** 38-70.

CUMBAL, L. & SENGUPTA, A. K. 2005. Arsenic removal using polymer-supported hydrated iron (III) oxide nanoparticles: role of Donnan membrane effect. *Environmental science & technology,* 39**,** 6508-6515.

DABROWSKI, A. & CURIE, S. 1999. *Adsorption and its applications in industry and environmental protection*, elsevier The Netherlands.

DAVIDSON, J. 2010. *REMOVAL OF NICKEL (II) FROM AQUEOUS SOLUTIONS BY POLYMER-ENHANCED ULTRAFILTRATION.* SHANGHAI JIAO TONG UNIVERSITY.

DEAN, J. G., BOSQUI, F. L. & LANOUETTE, K. H. 1972. Removing heavy metals from waste water. *Environmental Science & Technology,* 6**,** 518-522.

DELIYANNI, E. A., LAZARIDIS, N. K., PELEKA, E. N. & MATIS, K. A. 2004. Metals removal from aqueous solution by iron-based bonding agents. *Environmental Science and Pollution Research,* 11**,** 18-21.

DELIYANNI, E. A., PELEKA, E. N. & MATIS, K. A. 2009. Modeling the sorption of metal ions from aqueous solution by iron-based adsorbents. *Journal of hazardous materials,* 172**,** 550-558.

DERMENTZIS, K., CHRISTOFORIDIS, A. & VALSAMIDOU, E. 2011. Removal of nickel, copper, zinc and chromium from synthetic and industrial wastewater by electrocoagulation. *International Journal of Environmental Sciences,* 1**,** 697.

DIMIRKOU, A. & DOULA, M. K. 2008. Use of clinoptilolite and an Fe-overexchanged clinoptilolite in Zn2+ and Mn2+ removal from drinking water. *Desalination,* 224**,** 280-292.

DIZ, H. R. & NOVAK, J. T. 1999. Modeling biooxidation of iron in packed-bed reactor. *Journal of environmental engineering,* 125**,** 109-116.

DOULA, M. K. 2009. Simultaneous removal of Cu, Mn and Zn from drinking water with the use of clinoptilolite and its Fe-modified form. *Water Research,* 43**,** 3659-3672.

DZOMBAK, D. A. & MOREL, F. M. M. 1990. *Surface complexation modeling: hydrous ferric oxide*, John Wiley & Sons.

EDITION, F. 2011. Guidelines for drinking-water quality. *WHO chronicle,* 38**,** 104-108.

EDWARDS, M. 1994. Chemistry of arsenic removal during coagulation and Fe-Mn oxidation. *Journal of the American Water Works Association;(United States),* 86.

EICK, M. J. & FENDORF, S. E. 1998. Reaction sequence of nickel (II) with kaolinite: mineral dissolution and surface complexation and precipitation. *Soil Science Society of America Journal,* 62**,** 1257-1267.

EL-DESSOUKY, H. & ETTOUNEY, H. 2002. Teaching desalination-A multidiscipline engineering science. *Heat Transfer Engineering,* 23**,** 1-3.

FAN, M., BOONFUENG, T., XU, Y., AXE, L. & TYSON, T. A. 2005. Modeling Pb sorption to microporous amorphous oxides as discrete particles and coatings. *Journal of colloid and interface science,* 281**,** 39-48.

FENG, N.-C. & GUO, X.-Y. 2012. Characterization of adsorptive capacity and mechanisms on adsorption of copper, lead and zinc by modified orange peel. *Transactions of Nonferrous Metals Society of China,* 22**,** 1224-1231.

FENG, N., GUO, X., LIANG, S., ZHU, Y. & LIU, J. 2011. Biosorption of heavy metals from aqueous solutions by chemically modified orange peel. *Journal of Hazardous Materials,* 185**,** 49-54.

FEUERABENDT, F., JINDACHARIN, S., PAKEYANGKOON, P. & NITHITANAKUL, M. The Effect of Void Size and Level of Interconnectivity of Poly (S/DVB) HIPEs on Water Adsorption and Holding Capacities.

FIERRO, C., BENET, G. E., ZALLEN, A., HICKS, T. & FETCENKO, M. A. 2008. Process for converting nickel to nickel sulfate. Google Patents.

FU, F. & WANG, Q. 2011. Removal of heavy metal ions from wastewaters: a review. *Journal of environmental management,* 92**,** 407-418.

FURSE, M., HERING, D., MOOG, O., VERDONSCHOT, P., JOHNSON, R. K., BRABEC, K., GRITZALIS, K., BUFFAGNI, A., PINTO, P. & FRIBERG, N. 2006. The STAR project: context, objectives and approaches. *The Ecological Status of European Rivers: Evaluation and Intercalibration of Assessment Methods.* Springer.

GARCÍA-ROSALES, G. & COLÍN-CRUZ, A. 2010. Biosorption of lead by maize (Zea mays) stalk sponge. *Journal of Environmental Management,* 91**,** 2079-2086.

GECKELER, K. E. & VOLCHEK, K. 1996. Removal of hazardous substances from water using ultrafiltration in conjunction with soluble polymers. *Environmental science & technology,* 30**,** 725-734.

GODE, F. & PEHLIVAN, E. 2006. Removal of chromium (III) from aqueous solutions using Lewatit S 100: the effect of pH, time, metal concentration and temperature. *Journal of hazardous materials,* 136**,** 330-337.

GROSSL, P. R., SPARKS, D. L. & AINSWORTH, C. C. 1994. Rapid kinetics of Cu (II) adsorption/desorption on geothite. *Environmental Science and Technology;(United States),* 28.

GUAN, X. H., QIN, Y. C., WANG, L. W., YIN, R., LU, M. & YANG, Y. J. 2007. Study on the disposal process for removing heavy metal ions from wastewater by composite biosorbent of nano Fe3O4/Sphaerotilus natans. *Huan jing ke xue= Huanjing kexue/[bian ji, Zhongguo ke xue yuan huan jing ke xue wei yuan hui" Huan jing ke xue" bian ji wei yuan hui.],* 28**,** 436-440.

GUPTA, V. K. & ALI, I. 2000. Utilisation of bagasse fly ash (a sugar industry waste) for the removal of copper and zinc from wastewater. *Separation and purification technology,* 18**,** 131-140.

GUPTA, V. K., CARROTT, P. J. M., RIBEIRO CARROTT, M. M. L. & SUHAS 2009. Low-cost adsorbents: growing approach to wastewater treatment—a review. *Critical Reviews in Environmental Science and Technology,* 39**,** 783-842.

GUPTA, V. K., JAIN, C. K., ALI, I., SHARMA, M. & SAINI, V. K. 2003. Removal of cadmium and nickel from wastewater using bagasse fly ash—a sugar industry waste. *Water Research,* 37**,** 4038-4044.

GUPTA, V. K., MOHAN, D. & SHARMA, S. 1998a. > Removal of Lead from Wastewater Using Bagasse Fly Ash—A Sugar Industry Waste Material. *Separation Science and Technology,* 33**,** 1331-1343.

GUPTA, V. K., RASTOGI, A., DWIVEDI, M. K. & MOHAN, D. 1997a. Process development for the removal of zinc and cadmium from wastewater using slag—a blast furnace waste material. *Separation Science and Technology,* 32**,** 2883-2912.

GUPTA, V. K., SHARMA, S., YADAV, I. S. & MOHAN, D. 1998b. Utilization of bagasse fly ash generated in the sugar industry for the removal and recovery of phenol and p ‐ nitrophenol from wastewater. *Journal of Chemical Technology and biotechnology,* 71**,** 180-186.

GUPTA, V. K., SRIVASTAVA, S. K. & MOHAN, D. 1997b. Equilibrium uptake, sorption dynamics, process optimization, and column operations for the removal and recovery of malachite green from wastewater using activated carbon and activated slag. *Industrial & engineering chemistry research,* 36**,** 2207-2218.

GUTHA, Y., MUNAGAPATI, V. S., ALLA, S. R. & ABBURI, K. 2011. Biosorptive Removal of Ni(II) from Aqueous Solution by Caesalpinia bonducella Seed Powder. *Separation Science and Technology,* 46**,** 2291-2297.

HAIBACH, K., MENNER, A., POWELL, R. & BISMARCK, A. 2006. Tailoring mechanical properties of highly porous polymer foams: Silica particle reinforced polymer foams via emulsion templating. *Polymer,* 47**,** 4513-4519.

HAINEY, P., HUXHAM, I. M., ROWATT, B., SHERRINGTON, D. C. & TETLEY, L. 1991. Synthesis and ultrastructural studies of styrene-divinylbenzene Polyhipe polymers. *Macromolecules,* 24**,** 117-121.

HASAN, H. 2013. Preparation of novel composite polyHIPE polymers and their applications in intensified removal of tars from syngas.

HAUDRECH, P., FOUSSEREAU, J., MANTOUT, B. & BAROUX, B. 1994. Nickel release from nickel ‐ plated metals and stainless steels. *Contact dermatitis,* 31**,** 249-255.

HAUTHAL, H. G. 1990. Myers, D.: Surfactant science and technology. 331 S., 78 Abb., 44 Tab., 16 × 24 cm. Weinheim, Basel, Cambridge, New York: VCH Verlagsgesellschaft 1988. Kart., 58,– DM. *Journal für Praktische Chemie,* 332**,** 587-588.

HAYMAN, M. W., SMITH, K. H., CAMERON, N. R. & PRZYBORSKI, S. A. 2004. Enhanced neurite outgrowth by human neurons grown on solid three-dimensional scaffolds. *Biochemical and biophysical research communications,* 314**,** 483-488.

HAYWARD, A. S., EISSA, A. M., MALTMAN, D. J., SANO, N., PRZYBORSKI, S. A. & CAMERON, N. R. 2013. Galactose-Functionalized PolyHIPE Scaffolds for Use in Routine Three Dimensional Culture of Mammalian Hepatocytes. *Biomacromolecules,* 14**,** 4271-4277.

HERING, J. G., CHEN, P.-Y., WILKIE, J. A. & ELIMELECH, M. 1997. Arsenic removal from drinking water during coagulation. *Journal of Environmental Engineering,* 123**,** 800-807.

HU, J., CHEN, G. & LO, I. M. C. 2006. Selective removal of heavy metals from industrial wastewater using maghemite nanoparticle: performance and mechanisms. *Journal of environmental engineering,* 132**,** 709-715.

HUA, M., ZHANG, S., PAN, B., ZHANG, W., LV, L. & ZHANG, Q. 2012. Heavy metal removal from water/wastewater by nanosized metal oxides: a review. *Journal of Hazardous Materials,* 211**,** 317-331.

HUANG, J. G. & LIU, J. C. 1997. Enhanced removal of As (V) from water with iron-coated spent catalyst. *Separation science and technology,* 32**,** 1557-1569.

HUTTON, G., HALLER, L. & BARTRAM, J. 2007. Economic and health effects of increasing coverage of low cost household drinking-water supply and sanitation interventions to countries off-track to meet MDG target 10. *Economic and health effects of increasing coverage of low cost household drinking-water supply and sanitation interventions to countries off-track to meet MDG target 10.* OMS.

IIJIMA, S. 1991. Helical microtubules of graphitic carbon. *nature,* 354**,** 56.

INGLEZAKIS, V. J., LOIZIDOU, M. D. & GRIGOROPOULOU, H. P. 2003. Ion exchange of Pb 2+, Cu 2+, Fe 3+, and Cr 3+ on natural clinoptilolite: selectivity determination and influence of acidity on metal uptake. *Journal of Colloid and Interface Science,* 261**,** 49-54.

INSTRUMENTS, M. 2004. Zetasizer nano series user manual. *Worcestershire: Malvern Instruments Ltd*.

ISMAIL, I., SOLIMAN, A., ABDEL-MONEM, N., AHMED, H. S. & SOROUR, M. H. 2014. Nickel removal from electroplating waste water using stand-alone and electrically assisted ion exchange processes. *International Journal of Environmental Science and Technology,* 11**,** 199-206.

ISMAIL, M. H. S., ZHANG, X. T. & ADNAN, S. N. 2012. Application of Clinotptilolite in Removal Ofnickel (II) in Plating Wastewater. *World Applied Sciences Journal,* 18**,** 659-664.

JÄRUP, L. 2003. Hazards of heavy metal contamination. *British medical bulletin,* 68**,** 167-182.

JENKINS, R. 2000. X‐Ray Techniques: Overview. *Encyclopedia of analytical chemistry*.

JERÁBEK, K., PULKO, I., SOUKUPOVA, K., ŠTEFANEC, D. & KRAJNC, P. 2008. Porogenic solvents influence on morphology of 4-vinylbenzyl chloride based polyHIPEs. *Macromolecules,* 41**,** 3543-3546.

JIMAT, D. N. 2011. Bioprocess intensification: production of a-amylase by immobilised Bacillus subtilis in porous polymeric polyHIPE.

JUSOH, A., SHIUNG, L. S. & NOOR, M. 2007. A simulation study of the removal efficiency of granular activated carbon on cadmium and lead. *Desalination,* 206**,** 9-16.

KABBASHI, N. A., ATIEH, M. A., AL-MAMUN, A., MIRGHAMI, M. E. S., ALAM, M. D. Z. & YAHYA, N. 2009. Kinetic adsorption of application of carbon nanotubes for Pb (II) removal from aqueous solution. *Journal of Environmental Sciences,* 21**,** 539-544.

KADIRVELU, K., THAMARAISELVI, K. & NAMASIVAYAM, C. 2001a. Adsorption of nickel (II) from aqueous solution onto activated carbon prepared from coirpith. *Separation and purification Technology,* 24**,** 497-505.

KADIRVELU, K., THAMARAISELVI, K. & NAMASIVAYAM, C. 2001b. Removal of heavy metals from industrial wastewaters by adsorption onto activated carbon prepared from an agricultural solid waste. *Bioresource Technology,* 76**,** 63-65.

KANDAH, M. I. & MEUNIER, J.-L. 2007. Removal of nickel ions from water by multi-walled carbon nanotubes. *Journal of hazardous materials,* 146**,** 283-288.

KANG, S.-Y., LEE, J.-U., MOON, S.-H. & KIM, K.-W. 2004. Competitive adsorption characteristics of Co 2+, Ni 2+, and Cr 3+ by IRN-77 cation exchange resin in synthesized wastewater. *Chemosphere,* 56**,** 141-147.

KARVELAS, M., KATSOYIANNIS, A. & SAMARA, C. 2003. Occurrence and fate of heavy metals in the wastewater treatment process. *Chemosphere,* 53**,** 1201-1210.

KATSOYIANNIS, I. A. & ZOUBOULIS, A. I. 2002. Removal of arsenic from contaminated water sources by sorption onto iron-oxide-coated polymeric materials. *Water research,* 36**,** 5141-5155.

KEARNEY, M. & REARICK, D. E. Weak cation exchange softening: long term experience and recent developments. Proceedings from the 32nd Biennial ASSBT Meeting, TX, USA, 2003.

KRAJNC, P., LEBER, N., ŠTEFANEC, D., KONTREC, S. & PODGORNIK, A. 2005a. Preparation and characterisation of poly(high internal phase emulsion) methacrylate monoliths and their application as separation media. *Journal of Chromatography A,* 1065**,** 69-73.

KRAJNC, P., ŠTEFANEC, D., BROWN, J. F. & CAMERON, N. R. 2005b. Aryl acrylate based high-internal-phase emulsions as precursors for reactive monolithic polymer supports. *Journal of Polymer Science Part A: Polymer Chemistry,* 43**,** 296-303.

KRATOCHVIL, D. & VOLESKY, B. 1998. Advances in the biosorption of heavy metals. *Trends in biotechnology,* 16**,** 291-300.

KUMAR, P. S., RAMALINGAM, S., SATHYASELVABALA, V., KIRUPHA, S. D., MURUGESAN, A. & SIVANESAN, S. 2012. Removal of cadmium(II) from aqueous solution by agricultural waste cashew nut shell. *Korean Journal of Chemical Engineering,* 29**,** 756-768.

KUO, C.-Y. & LIN, H.-Y. 2009. Adsorption of aqueous cadmium (II) onto modified multi-walled carbon nanotubes following microwave/chemical treatment. *Desalination,* 249**,** 792-796.

KURNIAWAN, T. A., CHAN, G. Y. S., LO, W.-H. & BABEL, S. 2006. Physico–chemical treatment techniques for wastewater laden with heavy metals. *Chemical engineering journal,* 118**,** 83-98.

LASHEEN, M. R., AMMAR, N. S. & IBRAHIM, H. S. 2012. Adsorption/desorption of Cd(II), Cu(II) and Pb(II) using chemically modified orange peel: Equilibrium and kinetic studies. *Solid State Sciences,* 14**,** 202-210.

LEE, J., AHN, W.-Y. & LEE, C.-H. 2001. Comparison of the filtration characteristics between attached and suspended growth microorganisms in submerged membrane bioreactor. *Water Research,* 35**,** 2435-2445.

LETTINGA, G. 1995. Anaerobic digestion and wastewater treatment systems. *Antonie van leeuwenhoek,* 67**,** 3-28.

LETTINGA, G., VAN VELSEN, A. F. M., HOBMA, S. W., DE ZEEUW, W. & KLAPWIJK, A. 1980. Use of the upflow sludge blanket (USB) reactor concept for biological wastewater treatment, especially for anaerobic treatment. *Biotechnology and bioengineering,* 22**,** 699-734.

LI, L., FAN, M., BROWN, R. C., VAN LEEUWEN, J., WANG, J., WANG, W., SONG, Y. & ZHANG, P. 2006. Synthesis, properties, and environmental applications of nanoscale iron-based materials: a review. *Critical Reviews in Environmental Science and Technology,* 36**,** 405-431.

LI, Y.-H., XU, C., WEI, B., ZHANG, X., ZHENG, M., WU, D. & AJAYAN, P. M. 2002. Self-organized ribbons of aligned carbon nanotubes. *Chemistry of materials,* 14**,** 483-485.

LI, Y., LIU, F., XIA, B., DU, Q., ZHANG, P., WANG, D., WANG, Z. & XIA, Y. 2010. Removal of copper from aqueous solution by carbon nanotube/calcium alginate composites. *Journal of Hazardous Materials,* 177**,** 876-880.

LO, S.-L. & CHEN, T.-Y. 1997. Adsorption of Se (IV) and Se (VI) on an iron-coated sand from water. *Chemosphere,* 35**,** 919-930.

LO, S.-L., JENG, H.-T. & LAI, C.-H. 1997. Characteristics and adsorption properties of iron-coated sand. *Water science and technology,* 35**,** 63-70.

LOUKIDOU, M. X. & ZOUBOULIS, A. I. 2001. Comparison of two biological treatment processes using attached-growth biomass for sanitary landfill leachate treatment. *Environmental Pollution,* 111**,** 273-281.

MACDONALD, J. E. & VEINOT, J. G. C. 2008. Removal of residual metal catalysts with iron/iron oxide nanoparticles from coordinating environments. *Langmuir,* 24**,** 7169-7177.

MAHDAVIAN, A. R. & MIRRAHIMI, M. A.-S. 2010. Efficient separation of heavy metal cations by anchoring polyacrylic acid on superparamagnetic magnetite nanoparticles through surface modification. *Chemical engineering journal,* 159**,** 264-271.

MALANDRINO, M., ABOLLINO, O., GIACOMINO, A., ACETO, M. & MENTASTI, E. 2006. Adsorption of heavy metals on vermiculite: influence of pH and organic ligands. *Journal of Colloid and Interface Science,* 299**,** 537-546.

MALIK, M. A., ALI, S. W. & AHMED, I. 2010. Sulfonated Styrene−Divinybenzene Resins: Optimizing Synthesis and Estimating Characteristics of the Base Copolymers and the Resins. *Industrial & Engineering Chemistry Research,* 49**,** 2608-2612.

MEENA, A. K., MISHRA, G. K., RAI, P. K., RAJAGOPAL, C. & NAGAR, P. N. 2005. Removal of heavy metal ions from aqueous solutions using carbon aerogel as an adsorbent. *Journal of hazardous materials,* 122**,** 161-170.

MENG, X., KORFIATIS, G. P., CHRISTODOULATOS, C. & BANG, S. 2001. Treatment of arsenic in Bangladesh well water using a household co-precipitation and filtration system. *Water Research,* 35**,** 2805-2810.

MENNER, A. & BISMARCK, A. 2006. New Evidence for the Mechanism of the Pore Formation in Polymerising High Internal Phase Emulsions or Why polyHIPEs Have an Interconnected Pore Network Structure. *Macromolecular Symposia,* 242**,** 19-24.

MENNER, A., HAIBACH, K., POWELL, R. & BISMARCK, A. 2006. Tough reinforced open porous polymer foams via concentrated emulsion templating. *Polymer,* 47**,** 7628-7635.

MOINE, L., DELEUZE, H. & MAILLARD, B. 2003. Preparation of high loading PolyHIPE monoliths as scavengers for organic chemistry. *Tetrahedron letters,* 44**,** 7813-7816.

MOLINARI, R., GALLO, S. & ARGURIO, P. 2004. Metal ions removal from wastewater or washing water from contaminated soil by ultrafiltration–complexation. *Water research,* 38**,** 593-600.

MOLINARI, R., POERIO, T. & ARGURIO, P. 2008. Selective separation of copper (II) and nickel (II) from aqueous media using the complexation–ultrafiltration process. *Chemosphere,* 70**,** 341-348.

MORGAN, L. G. & FLINT, G. N. 1989. Nickel alloys and coatings: release of nickel. *Nickel and the skin: immunology and toxicology. CRC, Boca Raton***,** 45-54.

MOTSI, T., ROWSON, N. A. & SIMMONS, M. J. H. 2009. Adsorption of heavy metals from acid mine drainage by natural zeolite. *International Journal of Mineral Processing,* 92**,** 42-48.

NAH, I. W., HWANG, K.-Y., JEON, C. & CHOI, H. B. 2006. Removal of Pb ion from water by magnetically modified zeolite. *Minerals Engineering,* 19**,** 1452-1455.

NGAH, W. S. W., ENDUD, C. S. & MAYANAR, R. 2002. Removal of copper (II) ions from aqueous solution onto chitosan and cross-linked chitosan beads. *Reactive and Functional Polymers,* 50**,** 181-190.

NGUYEN, T. A. H., NGO, H. H., GUO, W. S., ZHANG, J., LIANG, S., YUE, Q. Y., LI, Q. & NGUYEN, T. V. 2013. Applicability of agricultural waste and by-products for adsorptive removal of heavy metals from wastewater. *Bioresource technology,* 148**,** 574-585.

NIEBOER, E., FLETCHER, G. G. & THOMASSEN, Y. 1999. Relevance of reactivity determinants to exposure assessment and biological monitoring of the elements. *Journal of Environmental Monitoring,* 1**,** 1-14.

NORMATOV, J. & SILVERSTEIN, M. S. 2007a. Porous interpenetrating network hybrids synthesized within high internal phase emulsions. *Polymer,* 48**,** 6648-6655.

NORMATOV, J. & SILVERSTEIN, M. S. 2007b. Silsesquioxane-Cross-Linked Porous Nanocomposites Synthesized within High Internal Phase Emulsions. *Macromolecules,* 40**,** 8329-8335.

O'CONNELL, D. W., BIRKINSHAW, C. & O'DWYER, T. F. 2008. Removal of copper, nickel and lead from wastewater using a modified cellulose material: a comparison. *WIT Transactions on Ecology and the Environment,* 109**,** 809-818.

O'CONNELL, D. W., BIRKINSHAW, C. & O'DWYER, T. F. 2008. Heavy metal adsorbents prepared from the modification of cellulose: A review. *Bioresource Technology,* 99**,** 6709-6724.

ODOM, T. W., HUANG, J.-L., KIM, P. & LIEBER, C. M. 1998. Atomic structure and electronic properties of single-walled carbon nanotubes. *Nature,* 391**,** 62-64.

OFOMAJA, A. E., NAIDOO, E. B. & MODISE, S. J. 2010. Biosorption of copper(II) and lead(II) onto potassium hydroxide treated pine cone powder. *Journal of Environmental Management,* 91**,** 1674-1685.

ORDOMSKY, V. V., SCHOUTEN, J. C., VAN DER SCHAAF, J. & NIJHUIS, T. A. 2012. Foam supported sulfonated polystyrene as a new acidic material for catalytic reactions. *Chemical Engineering Journal,* 207–208**,** 218-225.

OSTROSKI, I. C., BARROS, M. A. S. D., SILVA, E. A., DANTAS, J. H., ARROYO, P. A. & LIMA, O. C. M. 2009. A comparative study for the ion exchange of Fe (III) and Zn (II) on zeolite NaY. *Journal of Hazardous Materials,* 161**,** 1404-1412.

OZAKI, H. Rejection of micropollutants by membrane filtration. Proceedings of the Regional Symposium on Membrane Science and Technology, 2004. Citeseer.

PAN, B., PAN, B., ZHANG, W., LV, L., ZHANG, Q. & ZHENG, S. 2009a. Development of polymeric and polymer-based hybrid adsorbents for pollutants removal from waters. *Chemical Engineering Journal,* 151**,** 19-29.

PAN, B., QIU, H., PAN, B., NIE, G., XIAO, L., LV, L., ZHANG, W., ZHANG, Q. & ZHENG, S. 2010. Highly efficient removal of heavy metals by polymer-supported nanosized hydrated Fe (III) oxides: behavior and XPS study. *Water Research,* 44**,** 815-824.

PAN, B., WU, J., PAN, B., LV, L., ZHANG, W., XIAO, L., WANG, X., TAO, X. & ZHENG, S. 2009b. Development of polymer-based nanosized hydrated ferric oxides (HFOs) for enhanced phosphate removal from waste effluents. *Water Research,* 43**,** 4421-4429.

PANDA, G. C., DAS, S. K. & GUHA, A. K. 2008. Biosorption of cadmium and nickel by functionalized husk of Lathyrus sativus. *Colloids and Surfaces B: Biointerfaces,* 62**,** 173-179.

PANDEY, P. K., CHOUBEY, S., VERMA, Y., PANDEY, M., KAMAL, S. S. & CHANDRASHEKHAR, K. 2007. Biosorptive removal of Ni (II) from wastewater and industrial effluent. *International journal of environmental research and public health,* 4**,** 332-339.

PARK, D., YUN, Y.-S. & PARK, J. M. 2010. The past, present, and future trends of biosorption. *Biotechnology and Bioprocess Engineering,* 15**,** 86-102.

PARK, H. G., KIM, T. W., CHAE, M. Y. & YOO, I.-K. 2007. Activated carbon-containing alginate adsorbent for the simultaneous removal of heavy metals and toxic organics. *Process Biochemistry,* 42**,** 1371-1377.

PENDLETON, P., WONG, S. H., SCHUMANN, R., LEVAY, G., DENOYEL, R. & ROUQUERO, J. 1997. Properties of activated carbon controlling 2-methylisoborneol adsorption. *Carbon,* 35**,** 1141-1149.

PERGOLIZZI, J., BÖGER, R. H., BUDD, K., DAHAN, A., ERDINE, S., HANS, G., KRESS, H. G., LANGFORD, R., LIKAR, R. & RAFFA, R. B. 2008. Opioids and the management of chronic severe pain in the elderly: consensus statement of an International Expert Panel with focus on the six clinically most often used World Health Organization Step III opioids (buprenorphine, fentanyl, hydromorphone, methadone, morphine, oxycodone). *Pain Practice,* 8**,** 287-313.

PERIASAMY, K. & NAMASIVAYAM, C. 1995. Removal of nickel (II) from aqueous solution and nickel plating industry wastewater using an agricultural waste: peanut hulls. *Waste management,* 15**,** 63-68.

PETE, P. 2010. Introduction to energy-dispersive x-ray fluorescence (XRF)–an analytical chemistry perspective. *Department of Chemistry & Biochemistry San Francisco State University. Creative Commons Attribution-ShareAlike,* 3.

PIRNIE, M. 1999. Technologies and costs for removal of arsenic from drinking water. *Technologies and costs for removal of arsenic from drinking water.* EPA.

PRADEEP, T. 2009. Noble metal nanoparticles for water purification: a critical review. *Thin solid films,* 517**,** 6441-6478.

PRETSCH, E., BÜHLMANN, P., AFFOLTER, C., PRETSCH, E., BHUHLMANN, P. & AFFOLTER, C. 2009. *Structure determination of organic compounds*, Springer.

PROWS, D. R., MCDOWELL, S. A., ARONOW, B. J. & LEIKAUF, G. D. 2003. Genetic susceptibility to nickel-induced acute lung injury. *Chemosphere,* 51**,** 1139-1148.

PULKO, I., KOLAR, M. & KRAJNC, P. 2007. Atrazine removal by covalent bonding to piperazine functionalized PolyHIPEs. *Science of the total environment,* 386**,** 114-123.

QU, X., ALVAREZ, P. J. J. & LI, Q. 2013. Applications of nanotechnology in water and wastewater treatment. *Water research,* 47**,** 3931-3946.

RAJAPAKSHA, A. U., VITHANAGE, M., WEERASOORIYA, R. & DISSANAYAKE, C. B. 2012. Surface complexation of nickel on iron and aluminum oxides: A comparative study with single and dual site clays. *Colloids and Surfaces A: Physicochemical and Engineering Aspects,* 405**,** 79-87.

RAJIC, N., STOJAKOVIC, D., JOVANOVIC, M., LOGAR, N. Z., MAZAJ, M. & KAUCIC, V. 2010. Removal of nickel (II) ions from aqueous solutions using the natural clinoptilolite and preparation of nano-NiO on the exhausted clinoptilolite. *Applied Surface Science,* 257**,** 1524-1532.

RAO, G. P., LU, C. & SU, F. 2007. Sorption of divalent metal ions from aqueous solution by carbon nanotubes: a review. *Separation and Purification Technology,* 58**,** 224-231.

RICKERBY, D. G. & MORRISON, M. 2007. Nanotechnology and the environment: A European perspective. *Science and Technology of Advanced Materials,* 8**,** 19-24.

RIVAS, B. L., PEREIRA, E. D. & MORENO-VILLOSLADA, I. 2003. Water-soluble polymer–metal ion interactions. *Progress in Polymer Science,* 28**,** 173-208.

ROSENTHAL, S. J. 2001. Bar-coding biomolecules with fluorescent nanocrystals. *Nature biotechnology,* 19**,** 621-623.

ROY, D., GREENLAW, P. N. & SHANE, B. S. 1993. Adsorption of heavy metals by green algae and ground rice hulls. *Journal of Environmental Science & Health Part A,* 28**,** 37-50.

RUHRBERG, M. 2006. Assessing the recycling efficiency of copper from end-of-life products in Western Europe. *Resources, Conservation and Recycling,* 48**,** 141-165.

RULE, K. L., COMBER, S. D. W., ROSS, D., THORNTON, A., MAKROPOULOS, C. K. & RAUTIU, R. 2006. Diffuse sources of heavy metals entering an urban wastewater catchment. *Chemosphere,* 63**,** 64-72.

SAHMOUNE, M. N., LOUHAB, K. & BOUKHIAR, A. 2011. Advanced biosorbents materials for removal of chromium from water and wastewaters. *Environmental Progress & Sustainable Energy,* 30**,** 284-293.

SAROJAM, P. 2010. Analysis of Wastewater for Metals using ICP-OES. *Shelton, USA: PerkinElmer, Inc*.

SEILER, H. G., SIGEL, H. & SIGEL, A. 1988. Handbook on toxicity of inorganic compounds.

SHAKORFOW, A. M. 2012. Process intensification in the demulsification of water-in-crude oil emulsions via crossflow microfiltration through a hydrophilic polyHIPE polymer (PHP).

SHAWABKEH, R., AL-HARAHSHEH, A. & AL-OTOOM, A. 2004. Copper and zinc sorption by treated oil shale ash. *Separation and Purification Technology,* 40**,** 251-257.

SING, K. S. W. 1985. Reporting physisorption data for gas/solid systems with special reference to the determination of surface area and porosity (Recommendations 1984). *Pure and applied chemistry,* 57**,** 603-619.

SING, K. S. W. 1994. Physisorption of gases by carbon blacks. *Carbon,* 32**,** 1311-1317.

SOMASUNDARAN, P. & AGAR, G. E. 1967. The zero point of charge of calcite. *Journal of Colloid and Interface Science,* 24**,** 433-440.

SRIVASTAVA, N. K. & MAJUMDER, C. B. 2008. Novel biofiltration methods for the treatment of heavy metals from industrial wastewater. *Journal of hazardous materials,* 151**,** 1-8.

STAFIEJ, A. & PYRZYNSKA, K. 2007. Adsorption of heavy metal ions with carbon nanotubes. *Separation and Purification Technology,* 58**,** 49-52.

STUART, B. 2005. *Infrared spectroscopy*, Wiley Online Library.

STUMM, W. & MORGAN, J. J. 1981. Aquatic chemistry: an introduction emphasizing chemical equilibria in natural waters. *Aquatic chemistry: An introduction emphasizing chemical equilibria in natural waters.*

SU, Q., PAN, B., PAN, B., ZHANG, Q., ZHANG, W., LV, L., WANG, X., WU, J. & ZHANG, Q. 2009. Fabrication of polymer-supported nanosized hydrous manganese dioxide (HMO) for enhanced lead removal from waters. *Science of the Total Environment,* 407**,** 5471-5477.

SUD, D., MAHAJAN, G. & KAUR, M. P. 2008. Agricultural waste material as potential adsorbent for sequestering heavy metal ions from aqueous solutions–A review. *Bioresource technology,* 99**,** 6017-6027.

TAFFAREL, S. R. & RUBIO, J. 2009. On the removal of Mn 2+ ions by adsorption onto natural and activated Chilean zeolites. *Minerals Engineering,* 22**,** 336-343.

TAHA, G., ARIFIEN, A. & EL-NAHAS, S. 2011. Removal efficiency of potato peels as a new biosorbent material for uptake of Pb (II) Cd (II) and Zn (II) from their aqueous solutions. *The Journal of Solid Waste Technology and Management,* 37**,** 128-140.

TAHA, G. M. 2006. Utilization of Low‐Cost Waste Material Bagasse Fly Ash in Removing of Cu2+, Ni2+, Zn2+, and Cr3+ from Industrial Waste Water. *Groundwater Monitoring & Remediation,* 26**,** 137-141.

TAI, H., SERGIENKO, A. & SILVERSTEIN, M. S. 2001. Organic–inorganic networks in foams from high internal phase emulsion polymerizations. *Polymer,* 42**,** 4473-4482.

TALLKVIST, J., WING, A. M. & TJÄLVE, H. 1994. Enhanced Intestinal Nickel, Absorption in Iron‐Deficient Rats. *Basic & Clinical Pharmacology & Toxicology,* 75**,** 244-249.

TAN, T. C., CHIA, C. K. & TEO, C. K. 1985. Uptake of metal ions by chemically treated human hair. *Water Research,* 19**,** 157-162.

TAVARES, C. R., VIEIRA, M., PETRUS, J. C. C., BORTOLETTO, E. C. & CERAVOLLO, F. 2002. Ultrafiltration/complexation process for metal removal from pulp and paper industry wastewater. *Desalination,* 144**,** 261-265.

TCHOUNWOU, P. B., YEDJOU, C. G., PATLOLLA, A. K. & SUTTON, D. J. 2012. Heavy metal toxicity and the environment. *Molecular, clinical and environmental toxicology.* Springer.

ÜÇER, A., UYANIK, A. & AYGÜN, Ş. 2006. Adsorption of Cu (II), Cd (II), Zn (II), Mn (II) and Fe (III) ions by tannic acid immobilised activated carbon. *Separation and Purification Technology,* 47**,** 113-118.

UNICEF & WORLD HEALTH, O. 2014. *Progress on sanitation and drinking water: 2014 update*, World Health Organization.

URASE, T. & KIKUTA, T. 2005. Separate estimation of adsorption and degradation of pharmaceutical substances and estrogens in the activated sludge process. *Water Research,* 39**,** 1289-1300.

VARMA, S., SARODE, D., WAKALE, S., BHANVASE, B. A. & DEOSARKAR, M. P. 2013. Removal of nickel from waste water using graphene nanocomposite. *International Journal of Chemical and Physical Sciences,* 2**,** 132-139.

VASEASHTA, A., VACLAVIKOVA, M., VASEASHTA, S., GALLIOS, G., ROY, P. & PUMMAKARNCHANA, O. 2007. Nanostructures in environmental pollution detection, monitoring, and remediation. *Science and Technology of Advanced Materials,* 8**,** 47-59.

VEGLIO, F., QUARESIMA, R., FORNARI, P. & UBALDINI, S. 2003. Recovery of valuable metals from electronic and galvanic industrial wastes by leaching and electrowinning. *Waste Management,* 23**,** 245-252.

VENGRIS, T., BINKIEN, R. & SVEIKAUSKAIT, A. 2001. Nickel, copper and zinc removal from waste water by a modified clay sorbent. *Applied Clay Science,* 18**,** 183-190.

VIEIRA, M. G. A., NETO, A. F. A., GIMENES, M. L. & DA SILVA, M. G. C. 2010. Removal of nickel on Bofe bentonite calcined clay in porous bed. *Journal of Hazardous Materials,* 176**,** 109-118.

VILLAESCUSA, I., FIOL, N., MARTíNEZ, M. A., MIRALLES, N., POCH, J. & SERAROLS, J. 2004. Removal of copper and nickel ions from aqueous solutions by grape stalks wastes. *Water Research,* 38**,** 992-1002.

VON GUNTEN, U. 2003. Ozonation of drinking water: Part I. Oxidation kinetics and product formation. *Water Research,* 37**,** 1443-1467.

VÖRÖSMARTY, C. J., GREEN, P., SALISBURY, J. & LAMMERS, R. B. 2000. Global water resources: vulnerability from climate change and population growth. *science,* 289**,** 284-288.

WAKEMAN, R. J., BHUMGARA, Z. G. & AKAY, G. 1998. Ion exchange modules formed from polyhipe foam precursors. *Chemical Engineering Journal,* 70**,** 133-141.

WALSH, D. C., STENHOUSE, J. I. T., KINGSBURY, L. P. & WEBSTER, E. J. 1996. PolyHIPE foams: Production, characterisation, and performance as aerosol filtration materials. *Journal of Aerosol Science,* 27, Supplement 1**,** S629-S630.

WANG, H., ZHOU, A., PENG, F., YU, H. & YANG, J. 2007. Mechanism study on adsorption of acidified multiwalled carbon nanotubes to Pb (II). *Journal of Colloid and Interface Science,* 316**,** 277-283.

WANG, J., ZHENG, S., SHAO, Y., LIU, J., XU, Z. & ZHU, D. 2010. Amino-functionalized Fe 3 O 4@ SiO 2 core–shell magnetic nanomaterial as a novel adsorbent for aqueous heavy metals removal. *Journal of Colloid and Interface Science,* 349**,** 293-299.

WILKIE, J. A. & HERING, J. G. 1996. Adsorption of arsenic onto hydrous ferric oxide: effects of adsorbate/adsorbent ratios and co-occurring solutes. *Colloids and Surfaces A: Physicochemical and Engineering Aspects,* 107**,** 97-110.

WILLIAMS, J. M., GRAY, A. J. & WILKERSON, M. H. 1990. Emulsion stability and rigid foams from styrene or divinylbenzene water-in-oil emulsions. *Langmuir,* 6**,** 437-444.

WILLIAMS, J. M. & WROBLESKI, D. A. 1988. Spatial distribution of the phases in water-in-oil emulsions. Open and closed microcellular foams from cross-linked polystyrene. *Langmuir,* 4**,** 656-662.

WORLD HEALTH, O. 2005. Nickel in drinking-water. *Background document for development of WHO guidelines for drinking-water quality. Geneva: World Health Organization*.

WU, R., MENNER, A. & BISMARCK, A. 2013. Macroporous polymers made from medium internal phase emulsion templates: Effect of emulsion formulation on the pore structure of polyMIPEs. *Polymer,* 54**,** 5511-5517.

YABE, M. J. S. & DE OLIVEIRA, E. 2003. Heavy metals removal in industrial effluents by sequential adsorbent treatment. *Advances in Environmental Research,* 7**,** 263-272.

YANAGISAWA, H., MATSUMOTO, Y. & MACHIDA, M. 2010. Adsorption of Zn (II) and Cd (II) ions onto magnesium and activated carbon composite in aqueous solution. *Applied Surface Science,* 256**,** 1619-1623.

YEE, R. S. L., ZHANG, K. & LADEWIG, B. P. 2013. The effects of sulfonated poly (ether ether ketone) ion exchange preparation conditions on membrane properties. *Membranes,* 3**,** 182-195.

ZHANG, L.-M. & CHEN, D.-Q. 2002. An investigation of adsorption of lead (II) and copper (II) ions by water-insoluble starch graft copolymers. *Colloids and surfaces A: physicochemical and engineering aspects,* 205**,** 231-236.

ZHANG, Q., JIANG, P., PAN, B., ZHANG, W. & LV, L. 2009. Impregnating zirconium phosphate onto porous polymers for lead removal from waters: effect of nanosized particles and polymer chemistry. *Industrial & Engineering Chemistry Research,* 48**,** 4495-4499.

ZHENG, X., ZHANG, Y., WANG, H. & DU, Q. 2014. Interconnected Macroporous Polymers Synthesized from Silica Particle Stabilized High Internal Phase Emulsions. *Macromolecules,* 47**,** 6847-6855.

ZHOU, W.-Q., GU, T.-Y., SU, Z.-G. & MA, G.-H. 2007. Synthesis of macroporous poly(styrene-divinyl benzene) microspheres by surfactant reverse micelles swelling method. *Polymer,* 48**,** 1981-1988.

ZHOU, W., APKARIAN, R., WANG, Z. L. & JOY, D. 2006. Fundamentals of scanning electron microscopy (SEM). *Scanning microscopy for nanotechnology.* Springer.

Arif Malik. M, (2010), Sulfonated Styrene- Divinybenzene Resins: Optimizing Synthesis and Estimating Characteristics of the Base Copolymers and the Resins., Ind. Eng. Chem. Res., 49, 2608–2612

Barbetta, Andrea, (2002), Emulsion-derived (PolyHIPE) foams: optimization of properties and morphology for fluid low applications.Department of Chemistry University of Durham